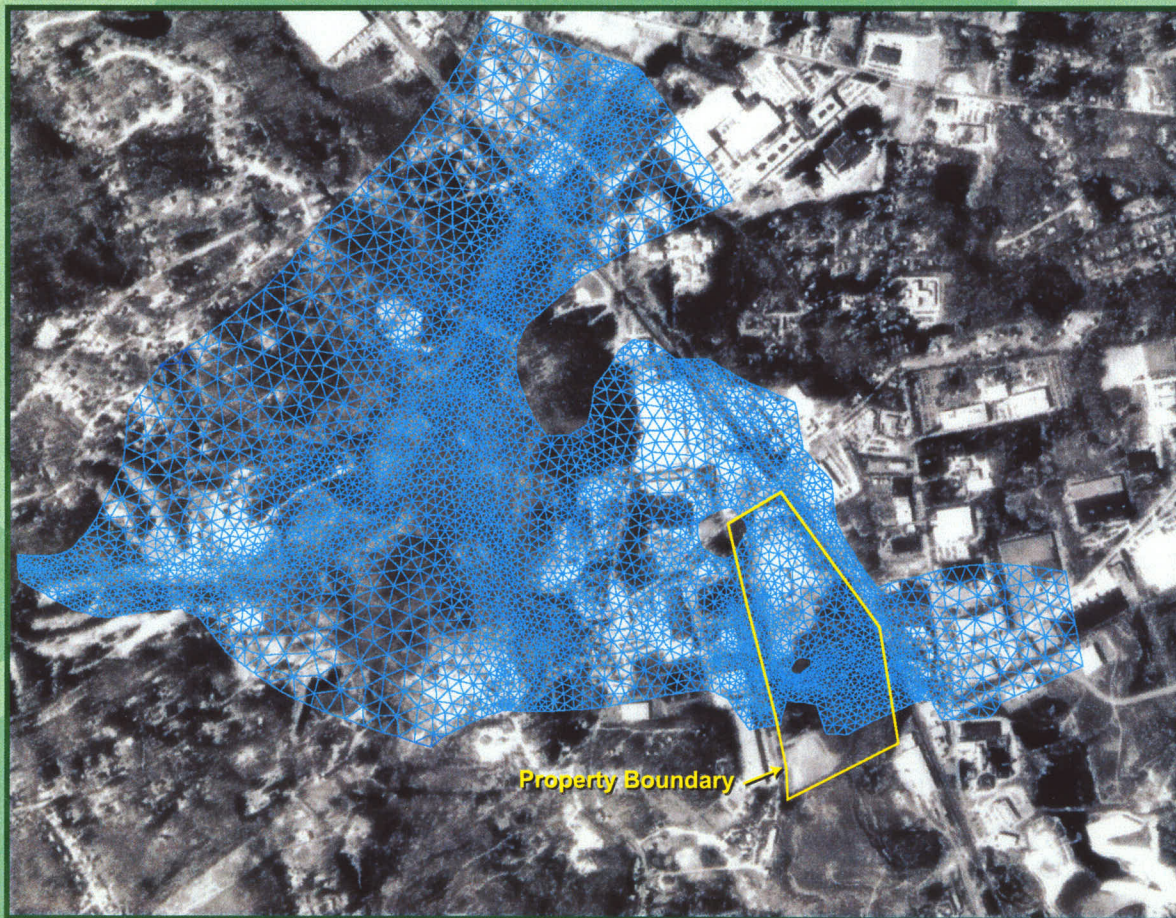


# Olin Wilmington Technical Series

## XIV. A Groundwater Flow and Solute Transport Model for the Olin Corporation Site (RTN: 3-0471) in Wilmington, Massachusetts



Prepared for:

Olin Corporation  
Wilmington, MA Facility

April 27, 2001



*geomega*  
good science • hard work • creative thinking

**A GROUNDWATER FLOW AND SOLUTE TRANSPORT MODEL  
FOR THE OLIN CORPORATION SITE (RTN: 3-0471)  
IN WILMINGTON, MASSACHUSETTS**

April 27, 2001

Prepared for:

**Olin Environmental Management, Inc.  
1186 Lower River Road, NW  
Charleston, Tennessee 37310-0248**

Prepared by:

**Geomega, Inc.  
2995 Baseline Road, Suite 202  
Boulder, Colorado 80303  
(303) 938-8115**



## ***EXECUTIVE SUMMARY***

A numerical groundwater flow and solute transport model has been constructed for the Olin Corporation Site (RTN: 3-0471) in Wilmington, Massachusetts. The model simulates groundwater flow conditions and solute transport at the 51 Eames Street property and further west in the Maple Meadow Brook aquifer. The model is intended to be used to improve understanding of wellhead capture zones, the locations of groundwater divides, and the effects of pumping at the water-supply wells, as well as assist in the evaluation of potential remediation design alternatives. This report describes the development of that model.

The hydrogeologic setting of the site is summarized and used as the basis for developing a conceptual model of the groundwater system. The information and framework of the conceptual model were translated into a numerical model, which was implemented with the finite-element code FEFLOW. The FEFLOW model covers essentially the same area and uses the same inputs as the steady-state MODFLOW model that was previously developed for the site. However, the FEFLOW model is more robust for simulating fluctuating water-table conditions and has additional capabilities that increase its usefulness for the Olin Corporation site.

The flow component of the model was first calibrated under the assumption of steady-state conditions, then subsequently calibrated to transient conditions simulating cyclic, seasonal fluctuations in the groundwater system. The seasonal fluctuations were represented by average conditions derived from recorded precipitation, stream flow, and pumping data. Finally, the transient flow model was adapted and configured for solute transport simulations.

Scatter plot results together with the calibration statistics indicate that an excellent calibration was achieved for the steady-state flow model. The generally greater challenge of calibrating a transient model is magnified at the Wilmington site by the extensive size of the aquifer, the heterogeneous distribution of till and stratified drift, the variability of pumping withdrawals, and the poorly constrained quantification of unsteady groundwater

recharge. Despite these difficulties, the calibrated transient flow model appears to be reasonably accurate in simulating regional groundwater flow patterns.

The calibrated transient flow model was used to evaluate capture areas of pumping wells and the seasonal movement of the groundwater divide between the Aberjona and Ipswich watersheds. Model results were examined at two different times during the year, during the wet season (April) and during the dry season (October). Particle tracking was used to delimit capture areas and flow zones within the groundwater system. Results of the analysis indicate that the Chestnut Street wells capture area does not extend to the area of existing DAPL at any time of the year. The Butters Row flow zone includes all of the upstream reach of Maple Meadow Brook, and its eastern boundary shifts to the east over areas of existing DAPL during dry periods. The Town Park capture area is limited to a relatively small part of the model domain northeast of the Butters Row 2 well. The groundwater divide between the Ipswich and Aberjona watersheds shifts to the west during wet periods, primarily due to increased groundwater heads on the northern and central parts of the Eames Street property. In October, the divide runs approximately through the center of the northern and central part of the Eames Street property, while in April it is located mostly west of the property.

The solute transport model is an extension of the transient flow model, and uses flow model velocities to calculate the advective component of transport. In addition to advection, the model is also capable of simulating the effects of diffusion, dispersion, retardation, and decay. The assignments of material properties and boundary and initial conditions pertaining to mass transport are described. Because the existing sources of solutes in the Maple Meadow Brook aquifer are currently poorly understood, a rigorous calibration of the transport component of the model cannot be performed. However, the collective effects of the sources have been measured (e.g., fluctuations in solute concentrations at the Town wells resulting from variable pumping rates), and these observations can be used to develop representations of “effective sources.” Identifying the potential locations of source areas and their relative contributions of solutes to the groundwater system by delineating effective sources is a task that can be investigated through additional modeling.

A detailed sensitivity analysis was performed to evaluate the sensitivity of the calibrated model with respect to various input parameters. The analysis was designed and conducted in accordance with established, industry-standard guidelines. Both calibration and prediction components of the model were evaluated for the purpose of identifying model sensitivities. Model input parameters that were varied during the sensitivity analysis include horizontal hydraulic conductivities, recharge rate, and specific yield. A total of 114 simulations were completed for the sensitivity analysis, including both steady-state and transient model runs. Results of the analysis show that, as a whole, the model is most sensitive to the recharge rate and two hydraulic conductivity units at depth in the area of Maple Meadow Brook. The model was relatively insensitive to the other hydraulic parameters tested.

**Table of Contents**

## Table of Contents

<b>1. INTRODUCTION.....</b>	<b>1</b>
1.1 SCOPE OF INVESTIGATION.....	1
1.2 PREVIOUS MODELING EFFORTS .....	1
1.3 MODELING OBJECTIVES AND APPROACH.....	2
<b>2. HYDROGEOLOGIC SETTING AND CONCEPTUAL MODEL .....</b>	<b>4</b>
2.1 TOPOGRAPHY AND SURFACE WATER FEATURES .....	4
2.2 GEOLOGIC SETTING .....	5
2.2.1 Overburden Geology .....	5
2.2.2 Bedrock Geology .....	6
2.3 HYDROGEOLOGIC CONCEPTUALIZATION .....	7
2.3.1 Hydrostratigraphic Units.....	7
2.3.2 Hydrogeologic Parameters.....	8
2.3.3 Sources and Sinks of Water .....	8
2.3.4 Directions of Groundwater Flow.....	11
2.4 DENSE AQUEOUS PHASE LIQUID (DAPL).....	12
2.5 CONCEPTUAL MODEL .....	13
2.5.1 Hydraulic and Physical Boundaries of the Flow System.....	13
2.5.2 Water Budget.....	13
2.5.3 Historical DAPL Intrusion and Migration .....	14
<b>3. MODEL DESIGN .....</b>	<b>15</b>
3.1 DESCRIPTION OF THE CODE.....	15
3.2 RELATIONSHIP BETWEEN CONCEPTUAL AND NUMERICAL MODELS .....	16
3.3 STEADY-STATE FLOW MODEL.....	17
3.3.1 Model Area and Discretization.....	17
3.3.2 Model Boundaries.....	18
3.3.3 Assignment of Parameter Values.....	18
3.3.4 Aquifer Stresses .....	19
3.3.5 Steady-State Calibration.....	19
3.4 TRANSIENT FLOW MODEL .....	21
3.4.1 Time-Varying Model Components .....	22
3.4.2 Transient Calibration .....	25
3.4.3 Seasonal Flow Zone Analysis .....	27
3.5 SOLUTE TRANSPORT MODEL .....	29
3.5.1 Model Boundaries.....	29
3.5.2 Assignment of Parameter Values.....	29
3.5.3 Initial Conditions and Representation of Solute Sources .....	30
<b>4. SENSITIVITY ANALYSIS.....</b>	<b>32</b>
<b>5. REFERENCES.....</b>	<b>36</b>
<b>TABLES</b>	
<b>FIGURES</b>	
<b>APPENDIX – SENSITIVITY SUMMARIES</b>	

## **List of Tables**

1. Details of municipal wellfield.
2. Calibration statistics for steady-state flow model.
3. Comparison of measured and simulated stream outflows at model boundary.
4. Results of stream gauging in Maple Meadow Brook, April 1998.
5. Temporal distribution of recharge based on model calibration.
6. Calibration statistics for transient flow model.
7. Sensitivity analysis results.

## **List of Figures**

1. Location of the Wilmington Property.
2. Topography, surface water, and site features.
3. Surficial geology map.
4. Bedrock elevation contour map.
5. Potentiometric surface map based on shallow wells, April 1998.
6. Potentiometric surface map based on deep wells, April 1998.
7. Thickness and extent of DAPL in 1998.
8. Schematic showing hydrological system.
9. Historical flooding of liquid waste.
10. Regional model domain.
11. Regional FEFLOW model mesh and MODFLOW model grid.
12. Regional model boundary conditions.
13. Bottom slice topographic elevations in regional model.
14. Regional model recharge distribution.
15. Hydraulic conductivity in Layer 1.
16. Hydraulic conductivity in Layer 2.
17. Hydraulic conductivity in Layer 3.
18. Hydraulic conductivity in Layer 4.
19. Contour map of simulated water table surface and calibration residuals.
20. Simulated vs. observed heads.
21. Generalized water budget for FEFLOW model domain.
22. Average monthly pumping rates at Town Wells, 1989-99.
23. Average monthly stream flows, 1962-74.
24. Maple Meadow Brook – Ipswich River regression results.
25. Average monthly stream flow in Maple Meadow Brook.
26. Locations of monitoring wells used in transient model calibration.
27. Comparison of simulated and observed average monthly heads in transient calibration target wells.
28. Transient calibration statistics by well.
29. Particle tracks showing capture areas and flow zones for average wet conditions (April).
30. Particle tracks showing capture areas and flow zones for average dry conditions (October).
31. Groundwater model RMSE response curve.



## **1 INTRODUCTION**

The 51 Eames Street property in Wilmington, Massachusetts is a former chemical manufacturing plant that has been owned and operated by various companies since the early 1950s. Manufacturing operations ceased there in 1986. The Wilmington property and surrounding area are shown on Figure 1.

Recent investigations of the Wilmington property have revealed the presence of a dense, aqueous-phase liquid (DAPL) containing more than 100,000 milligrams per liter (mg/L) of total dissolved solids (TDS). The dense liquid has migrated via density-dependent flow mechanisms through the groundwater flow system, down the Western Bedrock Valley, and toward the Maple Meadow Brook wetlands (CRA 1993; Smith 1997). The Town of Wilmington operates a municipal water-supply wellfield surrounding Maple Meadow Brook consisting of five production wells, which together typically pump over one million gallons of water per day.

### ***1.1 Scope of Investigation***

This investigation was undertaken to develop a numerical model for the Wilmington site that simulates groundwater flow conditions and solute transport at the Eames Street property and further west in the Maple Meadow Brook aquifer. The model is intended to be used to improve understanding of wellhead capture zones, the locations of groundwater divides, and the effects of pumping at the water-supply wells, as well as assist in the evaluation of potential remediation design alternatives. This report describes the development of that model.

### ***1.2 Previous Modeling Efforts***

Groundwater flow modeling was performed as part of the Supplemental Phase II Investigations (Smith 1997, Appendix P). That modeling effort consisted of the following activities.

- *Constant-density groundwater flow modeling of the aquifer system surrounding Maple Meadow Brook and including the Wilmington property:* The constant-density flow model was developed by using the U.S. Geological Survey's (USGS) finite-difference code MODFLOW (McDonald and Harbaugh 1988). That model was designed to simulate the interaction between surface water and groundwater, determine groundwater flow directions and velocities, and to simulate pumping at the municipal supply wells.
- *Determination of groundwater flow paths:* Groundwater flow paths were calculated by using the USGS code MODPATH, which uses the output flow terms from MODFLOW to determine particle tracks (Pollock 1994). The objective of this phase was to determine the capture zone of pumping wells by initiating particle tracks at certain receptors and then backtracking upgradient to identify the areas of groundwater contributing to water quality at the receptors.
- *Dual-density groundwater flow modeling at a scale encompassing the waste disposal areas and extending beyond the center of the buried bedrock valley beneath Maple Meadow Brook:* The dual-density flow model was developed by using the USGS finite-difference code SHARP, which simulates the movement of two non-mixing fluids having different densities (Essaid 1990). The objective of this model was to aid in understanding potential movement of the DAPL and to predict if and where the DAPL might move to in the future.

The MODFLOW model developed by Smith (1997) was modified by LAW (1999) to incorporate additional data collected since the Supplemental Phase II investigation and to refine the model's resolution and calibration. In the remainder of this report, the phrase "MODFLOW model" refers to the most recent model modified by LAW.

### *1.3 Modeling Objectives and Approach*

The objective of the present study was to develop a flow and transport model that reliably simulates groundwater conditions in the vicinity of the Wilmington property and the

Maple Meadow Brook aquifer, as well as the movement of diffuse solutes in groundwater to key discharge points (e.g., ditch systems and pumping wells).

A regional-scale flow model was constructed with the finite-element code FEFLOW (Diersch 1998). The FEFLOW model covers essentially the same area and uses the same inputs as the MODFLOW model. However, the FEFLOW model has additional capabilities (e.g., seamless integration of flow and transport calculations) that increase its usefulness for the Wilmington site. The flow model was first calibrated under steady-state conditions, then subsequently calibrated to transient conditions simulating cyclic, seasonal fluctuations in the groundwater system. Finally, the transient flow model was adapted for solute transport simulations.

The model was developed and calibrated prior to recent (Fall 2000) redevelopment work at the Eames Street property, which included the installation of an underground containment wall and reconfiguration of the on-property ditch system. Consequently, those features are not reflected in this model development and calibration report, and the following text describes the property as it existed prior to redevelopment. The model was subsequently updated to incorporate the recent on-property modifications.



## **2 HYDROGEOLOGIC SETTING AND CONCEPTUAL MODEL**

The hydrogeology of the site and surrounding area is discussed in detail in the *Comprehensive Site Assessment Phase II Field Investigation Report* (CRA 1993), and in the *Supplemental Phase II Report* (Smith 1997). Those reports include detailed discussions of collected data, data analyses, and conclusions. For the purpose of this report, many of the previous conclusions are restated below, but most of the specific data are not repeated.

### **2.1 Topography and Surface Water Features**

The Wilmington property lies in an area of low relief with a few isolated hills (Figure 2). The plant operating areas are located in the northern part of the site, which is bordered by Eames Street and relatively higher ground. From there, the ground surface slopes gently to a lower marshy area to the south and west. The southern part of the property is wooded. Drainage ditches border the site on the eastern and western edges; a third drainage complex crosses the center of the property from west to east, running through the marshy area and adjacent to a small pond. The Calcium Sulfate Landfill is located at the southernmost end of the property on a topographic high.

The ditch system that borders two sides and crosses the center of the property is an interconnected, man-made surface water drainage system (Figure 2) consisting of the West Ditch, South Ditch, Ephemeral Ditch, and East Ditch. The West Ditch is divided into two segments, the On-Property West Ditch and the Off-Property West Ditch. Both segments of the West Ditch flow to the south and join at the upstream end of the South Ditch. The South Ditch and the Ephemeral Ditch flow to the east and merge where they cross the eastern property boundary, just before joining the East Ditch.

Maple Meadow Brook flows through an extensive wetland area west of the Wilmington property (Figure 2). The Town of Wilmington operates five municipal water-supply wells around the sides of the wetland: Butters Row 1 and 2 and Chestnut Street 1 and 1A/2

wells are located on the western edge of the wetland, while the Town Park well is located to the north.

## *2.2 Geologic Setting*

The two major geologic units in the study area are unconsolidated glacial deposits and the underlying crystalline metamorphic and igneous bedrock. Figure 3 shows the surficial geology in the vicinity of the Wilmington property.

### *2.2.1 Overburden geology*

Regionally, the unconsolidated overburden deposits can be divided into four general units:

- Peat and organic sediment;
- Sands and silts;
- Sand, gravel, cobbles, and boulders; and
- Clayey to silty sand and gravel (till).

The peat and organic sediment ranges from a dark brown, dense, highly-fibrous material rich in organics to an olive gray-green, plastic, organic, silty material. Peat and organic sediment thickness varies throughout the site, with the majority of the peat and organic sediment located in the Maple Meadow Brook wetlands. The material ranges in thickness from zero to approximately 30 feet, with the greatest thickness near the center of the wetlands.

Below the muck or surface soil, the overburden material consists of layers of fine, clean sand and a mixture of sand, gravel, and cobbles. The sand is typically yellow-orange, light brown, tan, or gray in color. The material is interpreted as glacial outwash deposits, which were laid down by proglacial streams as the glaciers melted.

Below the sand the overburden materials are less well sorted, and consist of a mixture of light brown, sorted to poorly sorted, coarse sand, gravel, and cobbles. The materials are poorly stratified, and layers are discontinuous, variably dipping, and can be highly

irregular. These deposits of gravel and cobbles are interpreted as ice contact deposits, which were deposited by glacial meltwater along the margins of the glaciers.

Till exists at the base of the overburden materials at various isolated locations throughout the region. The till in areas on or near the Wilmington property is described as a gray, poorly-sorted, unstratified, sand and gravel with a clayey to silty matrix. The till is variable in thickness and is absent in some areas. Borings in the upper part of the Western Bedrock Valley indicate approximately 10 to 20 feet of till on top of bedrock in that area.

### *2.2.2 Bedrock geology*

The bedrock in the study area mainly consists of late Proterozoic and early Paleozoic quartzitic sediments, volcanoclastics, and intrusive rocks. These rocks were formed approximately 600 million years ago and have a long and active history of tectonic deformation. A period of deformation over 500 million years ago produced fine-grained rocks from coarser-grained rocks, without significant chemical alteration of the granulated materials. Present day bedrock in the study area is mostly dark gray amphibolite gneiss, with minor amounts of biotite gneiss, felsic mylonite, and some granodiorite.

The composition and texture of the bedrock units in the study area reflects their original rock type and the history of tectonic deformation. These, in turn, control the relative hardness of the rock and its susceptibility to weathering and erosion. The harder bedrock with less fracturing is exposed as rounded and knobby hills throughout the region, while the more weathered and fractured rock within fault zones has been further eroded and covered by glacial deposits, and is therefore poorly exposed.

The present bedrock surface within the study area is highly irregular, with a maximum relief of approximately 120 feet. The top of bedrock surface has been determined from outcrops, borings, seismic refraction profiles, and seismic reflection profiles. A contour map of the bedrock surface is shown on Figure 4.

## *2.3 Hydrogeologic Conceptualization*

### *2.3.1 Hydrostratigraphic units*

Groundwater in the area surrounding the Wilmington property occurs in the two primary geologic units: the unconsolidated sand and gravel deposits, and the underlying crystalline bedrock. The sand and gravel deposits form the significant water-bearing unit in this area. Hence, the term “aquifer,” as it is used in this report, refers to these sand and gravel deposits. Bedrock outcrops locally interrupt the aquifer, while bedrock valleys allow the aquifer to attain an appreciable thickness in some areas.

The unconsolidated sand and gravel deposits typically have a high porosity and permeability, and are thus able to transmit large quantities of water, providing a highly productive aquifer. Locally, the unconsolidated deposits are heterogeneous, as evidenced from the detailed well logs generated during the installation of monitoring wells on the Wilmington property and in the Western Bedrock Valley. However, outside of the local scale the sand and gravel deposits exhibit fairly uniform hydrologic properties.

In general, the aquifer is unconfined with the exception of the area beneath the Maple Meadow Brook wetland. That area is overlain by extensive swamp deposits (peat and muck), up to 30 feet thick, which restrict vertical groundwater flow and are likely to locally confine the underlying sand and gravel aquifer.

In contrast to the high permeability of the overburden material, the underlying bedrock has a much lower permeability. Because of its low primary porosity, the majority of the groundwater flow takes place through fractures in the crystalline rock. These fractures occupy only a small percentage of the bedrock formation, and so the bedrock typically contains only a very small amount of water compared to the overlying sand and gravel. The poor yielding nature of the bedrock is demonstrated during purging of bedrock wells prior to sampling, when they are easily pumped dry. In contrast, wells in the sand and gravel aquifer show little drawdown, even at significantly higher purging rates. Consequently, the bedrock formation constitutes an insignificant part of the overall groundwater flow system in the area.

### *2.3.2 Hydrogeologic parameters*

Hydraulic properties of the sand and gravel aquifer were evaluated for the Supplemental Phase II Investigation (Smith 1997). Slug tests were performed in selected monitoring wells around the site and data from those tests were evaluated. Data from four pumping tests previously conducted at the Town Wells were also reevaluated by Smith (1997) to estimate aquifer properties in the vicinity of those wells.

As part of the Supplemental Phase II Investigation, slug tests were performed on 18 wells screened in the sand and gravel aquifer. Analysis of the test data by the Bouwer and Rice (1976) method indicate that horizontal hydraulic conductivities within the aquifer range between 2 and 3,000 ft/d, reflecting the degree of heterogeneity of the sand and gravel aquifer. Results from the four pumping tests at the Town Wells indicate transmissivities between 2,000 and 13,000 ft<sup>2</sup>/d, with horizontal hydraulic conductivities ranging from 20 to 250 ft/d (Smith 1997). Pumping tests conducted at former municipal water-supply wells in the adjacent town of Woburn, Massachusetts, which borders the Wilmington property on the south, indicate that the transmissivity of the glacial sand and gravel deposits in that area is between 11,500 and 14,000 ft<sup>2</sup>/d (Lima and Olimpio 1989).

Laboratory tests on samples of the unconsolidated deposits in the Wilmington–Reading area indicate that porosity and specific yield are approximately 30% for both sand and gravel deposits and till, while peat and muck has a much higher value of up to 70% (Baker et al. 1964).

### *2.3.3 Sources and Sinks of Water*

Sources and sinks of water to the system include precipitation, evapotranspiration, groundwater pumpage, and recharge and discharge relationships with surface water bodies.

#### *2.3.3.1 Recharge to groundwater*

The most significant source of water within the study area is precipitation. Northeastern Massachusetts receives an average of 41 inches of precipitation per year (Baker et

al. 1964). A relatively large percentage (47 percent for 1930 through 1959) of that amount is lost to evapotranspiration, which primarily occurs during the growing season. Of the remaining precipitation, most is received as groundwater recharge. Runoff occurs in areas covered by buildings, roads, and other pavement, but much of this water infiltrates into the subsurface near the edges of the pavement. Surface runoff also occurs on the slopes of bedrock hills. However, a large percentage of this water also infiltrates into the sand and gravel aquifer near the base of hills.

Because of the relatively high permeability of the shallow sandy soils, surface water bodies are hydraulically connected to the aquifer. Stream water enters the groundwater system where the potentiometric surface is lower than the surface water level. This occurs in parts of Maple Meadow Brook and at a few places along the on-property ditches.

Minor and local sources of water include Olin's NPDES outfall to the On-Property West Ditch and septic leachfields at certain residential properties along Main Street. Olin operates a groundwater interceptor system at Plant B in the northeast part of its property. This recovery system removes oil from the groundwater in the vicinity of a former chemical production area and then discharges the treated water via a NPDES-permitted outfall located at the head of the On-Property West Ditch. Additionally, there are 15 residential properties along Main Street that use septic leachfields, but obtain water from the municipal distribution system. The septic discharge from these properties constitutes a minor local recharge to groundwater.

#### *2.3.3.2 Groundwater discharge*

The dominant mechanisms of water loss from the sand and gravel aquifer are pumpage for municipal and industrial supply, and discharge to surface water bodies.

Evapotranspiration is excluded from this discussion because it is considered to intercept recharge.

There are currently five public and two major industrial water-supply wells that withdraw groundwater in the vicinity of the Wilmington property. The locations of these wells relative to the Wilmington property are shown on Figure 2.

The municipal water-supply wellfield was developed over the 30-year period from 1961 to 1991. Table 1 lists the dates when individual wells were installed and their maximum design yield. Usage of the wellfield has been variable since its initial development, and there is only limited information available about pumping rates at individual wells for earlier time periods. For 1984 through 1989, pumping rates for the wellfield as a whole are available. From 1989 to 2000, pumping rates at individual wells are summarized in the annual *Groundwater Monitoring Report: Western Bedrock Valley and Sentinel Well Groundwater Monitoring Programs* (BCM 1998; LAW 1998, 2000). Historically, total pumping from the five Town Wells has generally exceeded one million gallons per day.

The former Altron (now Sanmina) facility operates two pumping wells to supply process water to their plant. The first well, B1, began operating in October 1977, and the second well, B3, began operating in 1985. Both wells are screened at shallow depths (approximately 20 to 30 feet below ground surface). Since 1981, the average annual pumping rate from the Altron wells has ranged from approximately 38,000 to 146,000 gallons per day, with an average annual daily discharge volume of 90,000 gallons (Anthony Cigliano, written communication to MADEP, 1998).

A minor amount of groundwater discharge occurs due to the operation of the groundwater interceptor system at Plant B. The recovery system has been operating since 1981 and presently consists of three pumping wells (IW-11, IW-12, and IW-13) that collectively pump a total of about 12,400 gallons per day (LAW 1999).

Groundwater also discharges to surface water bodies whenever the potentiometric surface is higher than the stage of the stream. This occurs along portions of Maple Meadow Brook and the associated wetlands away from the influence of the Town Wells. This also occurs along parts of the ditch systems and at some of the ponds in the study area.

Finally, groundwater discharges by subsurface flow away from the study area within the aquifer. This occurs southeast of the Wilmington property and east of the East Ditch, and also northward within the bedrock valley beneath Maple Meadow Brook.

### 2.3.4 Directions of Groundwater Flow

Complete rounds of groundwater and surface water levels were collected in October 1995 and April/May 1996. Data from those sampling events are presented in Section 2 of the *Supplemental Phase II Report* (Smith 1997). The most recent and comprehensive set of groundwater and surface water measurements occurred in April 1998 and are reported in the *Groundwater Monitoring Report: Western Bedrock Valley and Sentinel Well Groundwater Monitoring Programs* (LAW 1998). Potentiometric contour maps prepared from the April 1998 data (Figures 5 and 6) form the basis for the following discussion of groundwater flow patterns.

The Wilmington property is located on a groundwater divide, with flow from much of the property to the southeast within the Aberjona River watershed. Flow from part of the property and most of the area to the west of the property is toward the west within the Ipswich River watershed. The divide crosses a groundwater mound located on the northern part of the Wilmington property and continues to the bedrock high beneath Cook Avenue, west of the Calcium Sulfate Landfill. East of the divide, groundwater flows locally toward the ditch system and to the East Ditch. To the west of the divide, flow is westward toward the Maple Meadow Brook wetlands and the water supply wells. Groundwater flow patterns observed in shallow and deep wells are similar.

Local groundwater flow patterns are slightly different than originally identified in the Comprehensive Site Assessment (CRA 1993) because of the presence of the weir at the upstream end of the South Ditch. The weir was installed in 1994 and, since that time, has slightly modified local groundwater interactions with the South Ditch and the On- and Off-Property West Ditch system.

As previously mentioned, in contrast to the highly permeable sand and gravel aquifer, the bedrock formation is much less permeable. Rain that falls onto bedrock outcrops cannot infiltrate as readily because of the lower permeability and steeper slopes. Consequently, excess water runs off into the surrounding sand and gravel aquifer. This creates increased hydraulic heads and steeper gradients in the aquifer adjacent to bedrock exposures.

In general, vertical hydraulic gradients are small, with head differences between shallow and deep wells typically on the order of tenths of a foot. Upward vertical gradients generally occur immediately adjacent to surface water bodies (e.g., Maple Meadow Brook and the ditches). Downward vertical gradients generally occur in the remainder of the area, although there are some locations with no significant head difference between shallow and deep wells.

Due to local heterogeneities within the sand and gravel aquifer and the change in local gradients, groundwater velocities are highly variable. Reported values of average linear groundwater velocities range from 100 to 325 ft/yr on the Wilmington property and 10 to 425 ft/yr west of the property (CRA 1993). Borehole flow rates were measured in 21 wells on the Wilmington property and west of the property as part of the Supplemental Phase II Investigation. The measured velocities in shallow wells were between 0.5 and 3.0 ft/d, with an average velocity of 1.7 ft/d (Smith 1997).

#### *2.4 Dense Aqueous Phase Liquid (DAPL)*

The present-day DAPL resides in localized depressions on top of the low-permeability bedrock surface at the base of the sand and gravel aquifer. The DAPL is characterized by a specific gravity substantially greater than water (due to solute concentrations exceeding 100,000 mg/l) and a low pH (< 3.9). The major DAPL constituents are ammonia, chloride, sodium, and sulfate. Of the inorganic constituents present within the DAPL, sulfate is detected at the highest concentrations. Recent groundwater samples of the existing DAPL indicate maximum concentrations of approximately 125,000 milligrams per liter for the combination of the four major DAPL constituents. Maximum concentrations of other DAPL constituents, such as chromium, are typically two or three orders of magnitude lower than this range (cf. Geomega 1999, Table 1).

The distribution of the DAPL and its estimated vertical extent in 1998 are shown on Figure 7. Discrimination of the DAPL, as opposed to more diffuse solute concentrations and ambient groundwater conditions, is based on a variety of field data—including multilevel piezometers, down-hole inductance logging, specific conductivity profiling,

and water quality sampling—and detailed statistical analyses of those data (Geomega 1999).

## *2.5 Conceptual Model*

### *2.5.1 Hydraulic and physical boundaries of the flow system*

Natural hydrogeologic boundaries define the extent of the sand and gravel aquifer within the study area (Figure 8). These boundaries include:

- contacts between the unconsolidated deposits and bedrock at valley walls and along hills that crop out within the aquifer;
- the top of the aquifer as defined by the water table, which moves up and down depending upon the balance of hydrologic stresses acting on the system; and
- the bottom of the aquifer as defined by the contact between the sand and gravel deposits and the underlying bedrock.

### *2.5.2 Water budget*

The steady state water budget for the groundwater basin consists of inflowing and outflowing components. Groundwater enters the sand and gravel aquifer by several mechanisms, including:

- subsurface flow from upgradient locations in the aquifer;
- infiltration from surface water bodies;
- infiltration of runoff from adjacent upland areas;
- infiltration of precipitation that falls directly on the aquifer; and
- discharge from septic leachfields.

Groundwater leaves the aquifer by:

- pumping at municipal and industrial supply wells;
- discharge to Maple Meadow Brook and the ditches;
- subsurface flow within the aquifer; and

- evapotranspiration.

Many of these components are interrelated. For example, groundwater discharges to Maple Meadow Brook, but also is recharged by the brook as it passes through the study area. The relative proportion of discharge to recharge is also influenced by pumping at the Town Wells. Additionally, infiltration of precipitation is generally limited by evapotranspiration, especially during the growing season.

### *2.5.3 Historical DAPL intrusion and migration*

Liquid wastes with high concentrations of dissolved solids and low pH were historically discharged to unlined pits and ponds on the Wilmington property. Because these pits and ponds were unlined and the underlying soil was reasonably permeable, much of the liquid waste infiltrated into the subsurface. Because the bottoms of the pits and ponds were either in direct contact with the water table or within a few feet of the groundwater surface, liquid wastes discharged into the unlined pits and ponds rapidly entered the groundwater system.

Owing to its high density compared with ambient groundwater, the liquid wastes tended to sink through the groundwater until they reached the low permeability bedrock surface. At that point, the bulk movement of the DAPL was controlled primarily by the shape of the bedrock surface and local permeability contrasts within the unconsolidated glacial deposits, rather than by regional hydraulic gradients. Once the DAPL reached the bedrock, it continued to flow down-slope along the top of the bedrock under the influence of gravity. When bedrock depressions filled, DAPL overtopped the downgradient bedrock barriers and continued to flow to other areas and bedrock depressions. This process led to the creation of the DAPL plume at the base of the aquifer in the vicinity of the Wilmington property (Figure 9).



### **3 MODEL DESIGN**

It is necessary to synthesize a variety of factors related to the hydrogeologic conditions in the vicinity of the Wilmington property to determine groundwater flow patterns and where and how solute transport occurs in the groundwater system. Mathematical models are thought to be the best tool available for analyzing complex groundwater problems (Friedman et al. 1984). As an example of their widespread and accepted usage, the U.S. Environmental Protection Agency routinely uses mathematical models describing the transport and transformation of contaminants in subsurface systems to make regulatory assessments and environmental decisions (EPA 1989, 1991). Consequently, a mathematical groundwater flow and transport model was developed for the Wilmington property and adjacent Maple Meadow Brook aquifer.

#### **3.1 *Description of the Code***

The code used to simulate groundwater flow and mass transport in this study is the finite-element code FEFLOW (Diersch 1998). The FEFLOW code has undergone extensive testing against a series of well-known benchmarks and has been rigorously verified by comparing its results to analytical and other numerical model predictions. It has been selected for use in practical applications at numerous groundwater contamination sites by public service and state agencies, private companies, and research institutes in Europe, North America, Australia, Africa, and Japan (WASY 1999). FEFLOW is the most sophisticated groundwater modeling software that is presently available.

FEFLOW is far superior for the objectives of this modeling study compared to other popular codes that could have been used, in part because it seamlessly integrates groundwater flow and solute transport. If desired, it can also simulate unsaturated flow and the variable density conditions associated with diffuse and dense components in groundwater at the Wilmington site. FEFLOW is also more physically realistic and numerically stable than MODFLOW when simulating wetting and drying conditions associated with a transient, fluctuating water table.

### *3.2 Relationship Between Conceptual and Numerical Models*

The information and framework of the conceptual model (Section 2) was translated into a numerical model, which was implemented with the FEFLOW code. The numerical model represents all of the components of the conceptual model, including:

- the three-dimensional geometry of the aquifer and its hydrogeologic boundaries;
- variations in hydraulic properties of aquifer materials;
- recharge from precipitation and runoff from bedrock outcrops;
- sources and sinks of water, including artificial recharge (e.g., septic systems) and pumping wells;
- groundwater interactions with streams, ditches, and ponds;
- directions of groundwater flow; and
- solute transport from remnant DAPL or other non-DAPL related source areas.

In the finite-element approach employed by FEFLOW, the model area is subdivided into subareas called elements. Triangular elements with linear interpolation were used in the present study. The finite-element nodes, where the unknown heads and concentrations are calculated, are located at the corners of each element. The three-dimensional geometry of the model domain is constructed on the basis of slices and layers. Slices are surfaces on which the finite-element nodes lie and represent the topography and discontinuities between stratigraphic units, or just subdivide layers to refine the vertical discretization. Layers are bounded on the top and bottom by slices and represent the material properties of the system. Initial conditions and boundary conditions for the model are assigned at nodes on slices, whereas material parameters (e.g., hydraulic conductivity, porosity) are assigned to elements in layers.

Depending on which parts of the code are activated, the model will perform either a flow-only or a combined flow and transport simulation under either steady-state or transient conditions. The following sections, 3.3 through 3.5, describe the different configurations of the model: steady-state flow, transient flow, and transient flow and solute transport, respectively.

### *3.3 Steady-State Flow Model*

The steady-state FEFLOW model is essentially the same as the MODFLOW model. Minor differences between the two steady-state models are discussed in the following paragraphs.

#### *3.3.1 Model area and discretization*

The regional extent of the FEFLOW model domain is shown on Figure 10. The FEFLOW model domain is essentially that of the MODFLOW model domain, with the following exceptions (cf. Figure 11):

- The region south of the Calcium Sulfate Landfill, which includes part of the Woburn Landfill, is not included in the FEFLOW model.
- The upstream extent of the FEFLOW model boundaries along Maple Meadow Brook and Sawmill Brook are slightly reduced in comparison to the MODFLOW model.
- The extent of the northern part of the model, where Maple Meadow Brook exits the model, is reduced in size compared to the MODFLOW model.

The remaining model boundaries generally coincide with the MODFLOW model boundaries. The criterion for the location of model boundaries near bedrock outcrop was to place the boundary out from the intersection of the outcrop and soil surface where soil depth was estimated at five feet. The effect of this criterion is that edges of the aquifer where the saturated thickness is less than approximately 1.5 feet are not simulated in the model. Along bedrock outcrops, aquifer thicknesses less than this amount are potential areas of numerical instability, especially under conditions of low recharge.

The model domain was discretized by using triangular finite elements with linear interpolation across the elements (Figure 11). Node spacing varies from approximately 25 to 200 feet, with finer resolution along streams and ditches and around wells. Vertically, the model was divided into four layers and five slices. The four layers represent the three layers of the MODFLOW model, with the top MODFLOW layer being divided into two layers. The extra layer is a one-meter (3.28 ft) thick layer at the top of the model that was

included to facilitate the representation of streams and ditches. In FEFLOW, the horizontal limits of all layers extend to the model boundaries shown on Figure 10. As such, regions that are represented by only one layer in the MODFLOW model are represented by all four layers in the FEFLOW model. Nevertheless, the overall aquifer thicknesses are the same in the two models because the FEFLOW model layers have varying thicknesses and thin out along the edges of the aquifer.

### *3.3.2 Model boundaries*

Model boundary conditions are shown on Figure 12 and include:

- vertical recharge on the upper surface of the model;
- lateral recharge, no-flow, or prescribed head boundary conditions along the model perimeter;
- no-flow boundary conditions at the base of the aquifer, which corresponds to the top of bedrock; and
- extraction and recharge wells within the model domain.

Lateral recharge boundaries account for accumulated runoff from upland areas adjacent to the model domain. Prescribed head boundaries are located where the downstream reaches of Maple Meadow Brook and the East Ditch intersect the model boundary, and where the model boundary borders the surface water body east of the downstream end of East Ditch (Figure 2). For the steady-state calibration simulation, well extraction and recharge rates, including the septic systems along Main Street, are the same as those used in the MODFLOW model (LAW 1999).

The modeled bedrock surface is shown on Figure 13, and is represented by fixed nodal elevations on the bottom slice of the model.

### *3.3.3 Assignment of parameter values.*

Steady-state recharge rates assigned to the model are shown on Figure 14. Vertical recharge was applied at a uniform rate of 20 inches per year over the model domain.

Lateral recharge rates were determined for the model boundary segments shown on Figure 14. Lateral recharge segments represent two types of groundwater inflows. One type represents the stream inflows into the model at Sawmill Brook, Maple Meadow Brook and East Ditch. The remaining segments represent those parts of the model boundary for which runoff estimates were made for adjacent catchments, as described by LAW (1999). Prescribed head boundaries represent water elevations of the respective surface water bodies.

Hydraulic conductivity distributions for layers 1-4 are shown on Figures 15 through 18. Hydraulic conductivity ranges from 1 ft/d in regions consisting of till to 300 ft/d near the Town Wells. A vertical to horizontal hydraulic conductivity ratio of 1/10 was used throughout the entire model domain. This ratio is within the range used for other models in the region (e.g., Guswa and LeBlanc 1985; Lima and Olimpio 1989), and is consistent with reported hydrologic characteristics of unconsolidated deposits in the Wilmington–Reading area of Massachusetts (Baker et al. 1964).

#### *3.3.4 Aquifer stresses*

Pumping was simulated at the Town Wells, Altron wells and Plant B groundwater interceptor wells by using 4<sup>th</sup>-type boundary conditions. The boundary conditions were applied at nodes having elevations that correspond to the screened intervals of the wells. Rates of discharge used for the steady-state calibration were those reported for April 1998, which is when the calibration-target data were collected.

#### *3.3.5 Steady-state calibration*

Calibration consists of adjusting model parameters within reasonable bounds so that the model results replicate observed field conditions. In the case of the regional flow model, the observed field conditions used for model calibration consist of measured water levels in wells, vertical hydraulic gradients at nested well pairs, and measured flows in streams and ditches within the model domain. The model was calibrated by minimizing the difference between observed and simulated values for the following variables:

- Hydraulic head – 89 observation points were available within the regional model area for comparing heads.
- Vertical hydraulic gradient – 21 pairs of observation points provided vertical hydraulic gradient measurements with which the simulated vertical gradients were compared. The vertical location of an observation point was taken as the midpoint of the well-screen interval.
- Stream flows – flow measurements at locations where streams and ditches enter and exit the model domain provide a check on the overall model flow budget.

The data used for model calibration were collected in April 1998. As previously mentioned, this data set represents the most recent and comprehensive set of groundwater and surface water measurements available for the study area.

#### *3.3.5.1 Assessment of the calibration*

Figure 19 shows the simulated water table and calibration residuals for the steady-state model. The maximum difference between observed and simulated heads was 1.2 feet at well GW-29S. Calibration statistics for the difference between observed and simulated heads are shown on Table 2. Key statistics that were computed include the root-mean-squared error (RMSE), mean absolute error (MAE), and the residual mean error (ME).

The RMSE and the MAE are the best measures, in an average sense, of how closely the simulation represents observed conditions. These statistics, which by definition are greater than or equal to zero, should be minimized. The RMSE of the calibrated model was calculated to be 0.45 feet, and the MAE was calculated to be 0.34 feet. The ME measures the bias in the model (i.e., whether, on average, the simulated heads are higher or lower than the observed heads). Thus, the ME should be as close to zero as possible. The ME of the calibrated model was –0.025 feet, indicating virtually no bias.

Additionally, to determine the degree of model error that is acceptable, it is necessary to consider the magnitude in the change in observed heads over the model domain. If the ratio of the RMSE to the total head loss over the system is small (e.g., less than 10%), the

errors are considered to be a negligible part of the overall model response (Anderson and Woessner 1992). For the calibrated steady-state model, the ratio of the RMSE to the head range is 0.037, indicating that any residual errors are an insignificant part of the model's behavior.

Figure 20 shows a scatter-plot of simulated versus measured heads, with values falling close to the 1-to-1 line indicating a satisfactory model fit to the observed data. The results shown on Figure 20, together with the calibration statistics, indicate that an excellent calibration was achieved for the steady-state flow model.

Sensitivity tests with the FEFLOW model and similar analyses with the MODFLOW model (LAW 1999) indicate that both models are generally insensitive to the ratio of vertical to horizontal conductivity ( $K_v/K_h$ ). This is consistent with the findings of other modeling studies of glacial-drift aquifers in the region (e.g., Tiedeman et al. 1998). Decreasing the vertical to horizontal conductivity ratio in the FEFLOW model to 1/50 (the value used in the MODFLOW model) only marginally improved the vertical gradient residuals, while producing a less satisfactory fit of simulated-to-observed heads. The best model fit for heads was achieved with  $K_v/K_h = 1/10$ .

#### *3.3.5.2 Simulated water balance*

There are two locations where measured stream flows can be compared to model outflows as a check on the overall water balance of the model. These locations are Maple Meadow Brook at Route 38 and East Ditch at the culvert south of South Ditch. In each case the simulated flows are comparable to the measured flows (Table 3). The simulated steady-state water budget for the FEFLOW model domain is shown on Figure 21.

### *3.4 Transient Flow Model*

The transient flow model requires the same inputs as the steady-state model, but also requires additional information about aquifer storage parameters and how certain model parameters and boundary conditions vary with time. For storage in the unconfined aquifer, a uniform specific yield value of 0.3 was used throughout the model domain.

This is the value that was used for sand, silt, and clay deposits forming the stratified-drift aquifer in the nearby Woburn, Massachusetts, groundwater modeling study (Lima and Olimpio 1989), and it is also consistent with the specific yields measured in laboratory tests of unconsolidated deposits in the Wilmington–Reading area of Massachusetts (Baker et al. 1964). The handling of time-varying elements in the transient flow model is described in the following paragraphs.

#### *3.4.1 Time-varying model components*

Elements of the groundwater system that vary with time and cause changes in groundwater heads within the aquifer include withdrawal rates at pumping wells, stream discharges, and vertical and lateral recharge rates. Within the model domain, only the municipal water supply wells (Town Wells) were simulated as having time-varying characteristics; it was assumed that the Altron industrial wells were operated at a constant average pumping rate throughout the year. Also, inflows to the model from the East Ditch were assumed to be constant because flows in the ditch are a relatively minor component of the site-wide surface water discharge, and because currently there is no information on seasonal flow variability in the East Ditch. The substantially greater flows in Sawmill Brook and Maple Meadow Brook, however, were simulated as having time-varying discharges where they enter the model domain.

Vertical recharge was simulated as a time-varying material parameter on the upper most slice of the model. Lateral recharge, pumping rates, and stream inflows were treated as time-varying boundary conditions. FEFLOW has the capability of handling temporal variations in any and all material parameters and boundary conditions without restrictions on the timing of the changes (i.e., vertical recharge rates can fluctuate over different time intervals than pumping rates). Thus it is possible to specify variations in vertical and lateral recharge on a seasonal basis, while prescribing pumping rates and stream flows on monthly time intervals, which is how the time-varying components of the model were developed.

#### *3.4.1.1 Pumping rates*

Pumping rates at the Town Wells were assigned on the basis of historical data. Records of monthly withdrawals are available for each well from January 1989 through the present. The time period January 1989 through December 1999 was used to compute average monthly pumping rates for each of the Town Wells (Figure 22). The calculated average monthly rates were used as model inputs.

#### *3.4.1.2 Stream flows*

The USGS operated a gauging station on Maple Meadow Brook where it crosses Route 38 from October 1962 through September 1974. Only a few, sporadic flow measurements have been made in Maple Meadow Brook and its tributaries since that time. However, a USGS gauging station has been continuously operated on the Ipswich River at South Middleton (downstream of the Maple Meadow Brook confluence) since June 1938. Consequently, stream inflows at Maple Meadow Brook and Sawmill Brook were developed on the basis of a correlation between historical flows in Maple Meadow Brook at Route 38 and the Ipswich River at South Middleton, and more recent (1989-1999) data from the Ipswich River station.

A close relationship between flows in Maple Meadow Brook and the Ipswich River is evident during the 1962-74 period when both streams were concurrently monitored (Figure 23). A regression of average monthly flow data from the streams during that time period resulted in a coefficient of determination ( $r^2$ ) value of 0.92, indicating that Ipswich River data could be used to estimate flows in Maple Meadow Brook (Figure 24). The regression relationship was applied to Ipswich River data from the years 1989 through 1999 to calculate average monthly values of flow in Maple Meadow Brook at Route 38 in more recent times (Figure 25).

Maple Meadow Brook at Route 38 is located just outside of the model domain, at the downstream end of the brook. However, the model requires inputs of stream flows at the upstream reaches of Sawmill Brook and Maple Meadow Brook, where the brooks enter the model domain. (Sawmill Brook merges with Maple Meadow Brook within the model

domain.) Stream discharge measurements made in Sawmill Brook and at two locations in Maple Meadow Brook on April 11, 1998 were used to calculate the required inputs at the upstream ends of the brooks where they cross the model boundary.

Discharge data were collected in Maple Meadow Brook at Route 38 and also upstream where it flows through the gravel pit, and in Sawmill Brook where it crosses Chestnut Street. The gravel pit and Chestnut Street correspond to upstream locations proximal to the model boundary. Data collected on April 11, 1998 (Table 4) indicate that 56% of the discharge in Maple Meadow Brook at Route 38 was accounted for by flow in Sawmill Brook at Chestnut Street, while 29% of the discharge was attributable to flow in Maple Meadow Brook at the gravel pit. Small tributaries to Maple Meadow Brook provided approximately 5% of the flow at Route 38, and the remaining 10% was derived from groundwater discharge to the brook as it passed through the model domain. These percentages were used to calculate the model inflow rates at the upstream ends of Sawmill and Maple Meadow Brooks on the basis of previously determined average monthly flows in Maple Meadow Brook at Route 38.

#### *3.4.1.3 Recharge rates*

Temporal variations in vertical and lateral recharge rates are understood conceptually for the regional area encompassing the model domain (e.g., most of the annual recharge occurs from about the middle of October to April and there is little, if any, recharge that occurs during the growing season; Baker et al. 1964). However, there is insufficient information available to quantify actual recharge rates throughout the year. Groundwater recharge does not correlate with precipitation in the study area because some of the precipitation occurs as snow and does not infiltrate until it melts and the ground thaws in the spring. Also, the effects of evapotranspiration limit the potential for precipitation to reach the water table during the growing season. Thus, even though precipitation is distributed fairly uniformly throughout the year, groundwater recharge is not.

Because temporal variations in recharge can not be quantified from available data, vertical and lateral recharge rates were treated as model calibration parameters (as discussed below in Section 3.4.2). The resulting temporal breakdown of recharge that

was ultimately used in the transient flow model is listed on Table 5. Lateral recharge rates were specified over the same time intervals and scaled consistently with vertical recharge.

### *3.4.2 Transient calibration*

The transient calibration involved adjusting only the temporal distribution of recharge (vertical and lateral), while keeping all other model parameters and boundary conditions constant or set at their prescribed time-varying values. Based on a conceptual understanding of recharge characteristics, the calendar year was subdivided into several time intervals, each with a different prescribed recharge rate. The steady-state vertical recharge rate of 20 inches per year (Section 3.3.3) was used as a constraint on the overall recharge amount, and the temporal distribution of recharge—in terms of timing and percentages of the annual total recharge—was varied until an acceptable fit to the transient groundwater head data was achieved. Many different combinations of time intervals and prescribed recharge rates were evaluated before an acceptable fit to transient groundwater head data was achieved. Table 5 shows the temporal distribution of recharge that resulted from this procedure, expressed as a percentage of the total annual recharge.

Thirty-five monitoring wells were selected for use as transient calibration targets (Figure 26). The wells were selected on the basis of location, as well as quantity and monthly distribution of available data. Wells that have been used once or only a few times for water-level measurements were deemed to have insufficient data for transient model calibration purposes. The selected calibration targets represent a broad spatial distribution of control points within the model domain and include both shallow and deep wells. For comparison purposes, observation points were assigned in the model at nodes corresponding to the locations and mid-screen elevations of the selected target wells.

Because the simulated stresses in the model were based on average values (e.g., average monthly pumping rates and stream flows, average annual recharge amount, etc.), the calibration target data were also developed to represent average heads. For each calibration well, all of the available data for a particular month were averaged to obtain a single target value for that month and well. Some of the calibration wells do not have

data for all 12 months of the year, and in some cases there is only one data point available for a particular month. Thus, the transient calibration targets are associated with various levels of uncertainty.

#### *3.4.2.1 Assessment of the calibration*

Results of the transient calibration are shown graphically in a series of hydrographs comparing simulated heads with average monthly values for each target well (Figure 27a-i). Error bars associated with average observed head values in Figure 27 represent one standard deviation of the monthly measurements; where no error bar is shown, there is only a single data point available for that month. Considering the uncertainty in average observed conditions, as indicated by the error bars, in most cases the calibrated model produced a reasonable match to the target data. The largest discrepancies between simulated and average observed head values were for wells GW-84D, GW-85D, GW-86S, and GW-87D, and for all of these wells the discrepancies were associated with monthly values represented by single data points, which are probably not indicative of average conditions. Specifically, the observed values were lower than the simulated average conditions for these wells during the summer months, but the target data were collected in 1997 and 1999 and both of those years experienced exceptionally low precipitation during the spring and/or summer months.

Calibration statistics reported for the steady-state model (Section 3.3.5.1) were also computed for the transient model (Table 6). Considering all of the available target data, the RMSE of the calibrated transient model was calculated to be 1.40 feet, and the MAE was calculated to be 1.01 feet. These results indicate that the transient model generally represents average observed heads to within about 1.5 feet or less. The ME of the calibrated transient model was -0.26 feet, indicating that, on average, the model tended to slightly underpredict target head values. Also, the ratio of the RMSE to the head range for the calibrated transient model is 0.095, indicating that the model's behavior is not significantly influenced by any residual errors.

Figure 28 shows the ME, MAE, and RMSE for each well calculated by using the monthly residual values. The largest RMSE values were associated with wells GW-63S, GW-73S,

GW-84D and GW-85D. For the latter two of these wells, the relatively large RMSE values are interpreted as being the result of singular monthly data points that are unrepresentative of average conditions, as discussed above. Wells GW-63S and GW-73S are in close proximity to the Chestnut Street and Town Park water-supply wells, respectively, and their relatively large RMSE values are at least partly the result of slight underestimation of drawdown near the pumping wells due to the spatial discretization that is necessary for a regional model. (Note that wells GW-64S and GW-65S, which are located close to the Butters Row pumping wells, also shows this effect, although to a lesser degree.) Well GW-32S also has an elevated RMSE value, relative to most of the other wells, but one half of its calibration targets are based on singular monthly data points that could be unrepresentative of average conditions. Apart from these outliers, the remaining calibration target wells had RMSE values of approximately one foot or less.

The study area poses significant modeling challenges due to the extensive size of the aquifer, the heterogeneous distribution of till and stratified drift, the variability of pumping withdrawals, and the poorly constrained quantification of unsteady groundwater recharge. Despite these difficulties, the calibrated transient flow model appears to be reasonably accurate in simulating regional groundwater flow patterns.

### *3.4.3 Seasonal flow-zone analysis*

The calibrated transient flow model was used to evaluate general capture areas of pumping wells and the seasonal movement of the groundwater divide between the Aberjona and Ipswich watersheds. To account for uncertainty in initial conditions, the model simulation spanned a cyclic two-year period, and results from the second year were used for the analysis.

Model results were examined at two different times during the year, during the wet season (April) and during the dry season (October). Particle tracking was used to delimit capture areas and flow zones within the groundwater system. Particle tracks were initiated at a mid-level elevation in the model, rather than at the water table surface, to better represent the effects of pumping on flow conditions in the area of contaminant

concentrations. This is a better representation from a solute transport perspective because the shallow groundwater carries essentially no contaminant-related mass.

The capture areas and flow zones within the model domain can be categorized as follows:

- East Ditch (all flows in this zone ultimately end up in the Aberjona Watershed),
- Altron (Sanmina),
- Chestnut Street,
- Butters Row,
- Town Park,
- Maple Meadow Brook (all flows in this zone ultimately end up in the Ipswich Watershed).

These generalized areas are referred to in subsequent discussion of the simulation results.

#### *3.4.3.1 Results*

Results of the simulation are shown on Figures 29 and 30. The particle tracks clearly show the limited capture area of the Chestnut Street wells. At no time of the year does the capture zone extend to the area of existing DAPL, or even as far as Maple Meadow Brook and the general location of the Western Bedrock Valley. The Butters Row area includes all of the upstream reach of Maple Meadow Brook, and its eastern boundary with the Altron (Sanmina) area shifts to the east during dry periods. Although this flow zone is associated with the Butters Row wells, not all of the groundwater within this zone is captured by the wells because some of the groundwater discharges to Maple Meadow Brook and leaves the flow zone as surface water discharge. The Town Park capture area is limited to a relatively small part of the model domain northeast of the Butters Row 2 well. The simulation results also show that the Altron wells capture most of the shallow groundwater flow over the top of the existing DAPL under both wet and dry conditions.

The groundwater divide between the Ipswich and Aberjona watersheds shifts to the west during wet periods, primarily due to increased groundwater heads on the northern and central parts of the Eames Street property. In October, the divide runs approximately

through the center of the northern and central part of the Eames Street property, while in April it is located mostly west of the property. As a result of this seasonal shift in the groundwater divide, the model predicts that the direction of surface water flow in the Off-Property West Ditch should also change between wet and dry seasons. This is consistent with observations on several occasions of seasonally-reversed flow directions in the Off-Property West Ditch.

### *3.5 Solute Transport Model*

The solute transport model is an extension of the transient flow model, and uses flow model velocities to calculate the advective component of transport. In addition to advection, the model also simulates the effects of diffusion, dispersion, retardation, and, if necessary, decay. The transport model requires additional information about the initial distribution of solute concentrations in the system and material properties and boundary conditions pertaining to mass transport.

#### *3.5.1 Model boundaries*

Boundary conditions for the transport component of the modeling consist of prescribed concentration (1<sup>st</sup>-type) and prescribed flux (2<sup>nd</sup>-type). Along inflowing parts of the model boundary, “freshwater conditions” are prescribed for a particular analyte by specifying a small constant concentration that is consistent with ambient water quality data for the Ipswich and Mystic basins (Trombley 1992). Outflowing parts of the model boundary are left unspecified, resulting in the “natural” (2<sup>nd</sup>-type) boundary condition, which allows for the calculation of concentrations at nodes where outflow conditions occur.

#### *3.5.2 Assignment of parameter values*

Transport parameters include porosity, molecular diffusion, longitudinal and transverse dispersivities, and sorption and decay rates. The porosity of all units is set at 0.3, consistent with the specific yield. Reported values of the molecular diffusion coefficients for major DAPL-related ions (calcium, chromium, iron, and sulfate) in water range

between  $5.5 \times 10^{-4} \text{ ft}^2/\text{d}$  and  $1.0 \times 10^{-3} \text{ ft}^2/\text{d}$  (Spitz and Moreno 1996, Table D-1). A value of  $9.3 \times 10^{-4} \text{ ft}^2/\text{d}$  is specified in the present model. Longitudinal and transverse dispersivities are set at 98 and 33 feet (30 and 10 meters), respectively. These values are representative of many aquifers (cf. Neuman 1990), and are within the ranges reported for glaciofluvial sands and gravels and glacial till at comparable, regional migration distances (Spitz and Moreno 1996, Table D-3).

Sorption rates vary for the different DAPL-related constituents depending on ambient geochemical conditions. For example, column tests that were performed with aquifer materials and DAPL groundwater collected at the site (PTI 1997) showed that sulfate, ammonium, and chromium have minimal adsorption to the aquifer matrix within the low pH DAPL zone (retardation coefficients are close to one and the partition coefficients are close to zero). However, at the higher pH levels that are characteristic of shallow groundwater, chromium can readily sorb to aquifer materials (Bartlett and James 1988). Under the site-specific geochemical conditions associated with the DAPL constituents, chromium also precipitates out of solution, as evidenced by the occurrence of chromium oxyhydroxides in monitoring well GW-83D (Smith 1997). Therefore, the assignment of sorption values depends on the focus of the simulation (i.e., DAPL zone or shallow groundwater) and on the particular constituent under consideration. Decay rates are set to zero in the present model because there are no DAPL-related organic or radioactive constituents.

### *3.5.3 Initial Conditions and Representation of Solute Sources*

#### *3.5.3.1 Initial transport conditions*

Initial conditions for transport modeling are typically estimated on the basis of measured field concentrations. However, the robustness of the estimation depends strongly on the amount and spatial distribution of available data. Despite the substantial number of monitoring wells that have been installed at the Wilmington site, there are still large parts of the model domain for which no data are available. To account for the uncertainty in initial conditions due to data limitations, the solute transport model is presently run over a several-year period and the early-time results are ignored. In this case, initial conditions

are specified uniformly throughout the model domain on the basis of ambient background concentrations. Sensitivity tests with the model indicate that with this approach it takes the simulated system between one and five years to equilibrate and eliminate the effects of specified initial conditions.

#### *3.5.3.2 Representation of solute sources*

Sources of solutes within the model domain are thought to be at least partly associated with residual zones of DAPL-related constituents (Smith 1997). In general these zones coincide with known bedrock depressions in the vicinity of the Eames Street property and further west in the Western Bedrock Valley. However, the complex topology of the bedrock surface precludes full knowledge of the actual distribution of remnant reservoirs within the aquifer. Furthermore, recent investigations in the vicinity of the gravel pit near Maple Meadow Brook indicate that there could be additional separate sources of contaminant mass distinct from the historical DAPL.

Because the existing sources of solutes in the Maple Meadow Brook aquifer are currently poorly understood, a rigorous calibration of the transport component of the model cannot be performed. Nevertheless, the collective effects of the sources have been measured (e.g., fluctuations in solute concentrations at the Town wells resulting from variable pumping rates), and these observations can be used to develop representations of “effective sources.” Identifying the potential locations of source areas and their relative contributions of solutes to the groundwater system by delineating effective sources is a task that can be investigated through additional modeling. In this application, effective source areas are represented in the model by prescribed concentration boundary conditions, with constraints available for use to limit the chemical mass that can be mobilized.



#### **4 SENSITIVITY ANALYSIS**

An analysis was performed to evaluate the sensitivity of the calibrated model with respect to various model input parameters. The sensitivity of a model is indicated by differences in calibration residuals and/or model conclusions due to a change or perturbation of a model input parameter. Thus, a sensitivity analysis shows the importance of individual parameters to the simulation results. The sensitivity analysis described in this section was designed and conducted in accordance with guidelines established by the American Society for Testing and Materials (ASTM 1994).

Calibration residuals examined in this analysis included the mean error (ME), root-mean-squared-error (RMSE), maximum residual, and minimum residual. The model calibration component of the sensitivity analysis was evaluated under steady-state flow conditions for all parameters tested except specific yield, which was tested under transient flow conditions.

Simulated ammonia concentrations at the Chestnut Street 1 and Butters Row 1 municipal water-supply wells constituted the model conclusions that were used for the predictive component of the sensitivity analysis. A Base Case simulation, consisting of the transient calibrated model with historical average recharge and pumping conditions, was constructed to serve as a point of comparison for the predictive component of the analysis. All predictive simulations were run with steady-flow, transient-transport conditions for a period of one year. At the end of the one-year period, sensitivity simulation results were compared with the Base Case simulation. The standard deviation ( $\sigma$ ) of historical ammonia data from the Chestnut Street 1 and Butters Row 1 wells served as an indication of the variability of measured concentrations. A bound of  $\pm 1\sigma$  was applied to the Base Case simulation results to represent limits indicating a significant change in the model's conclusions (i.e., any sensitivity simulation result indicating a change greater than  $\pm 1\sigma$  of the Base Case value was considered to be significant).

Model parameters that were varied during the sensitivity analysis include horizontal hydraulic conductivities, recharge rate (both vertical and lateral), and specific yield. The

ratio of horizontal to vertical hydraulic conductivity was kept constant at 10:1 throughout the analysis. Hydraulic conductivities were varied by multipliers of 10, 2, 0.5, and 0.1 to evaluate uncertainty in the immediate vicinity (numerically speaking) of the calibrated model. All of the hydraulic conductivity units shown on Figures 15 through 18 were tested according to their prescribed value (i.e., all regions having the same value were varied simultaneously, regardless of where in the model they were located). Recharge was tested by uniformly varying recharge rates by approximately  $\pm 20\%$  and  $\pm 40\%$ . Specific yield was varied by  $\pm 1/3$  and  $\pm 2/3$  of the calibrated value.

A total of 114 simulations were completed for the sensitivity analysis, including both steady-state and transient model runs. After each steady-state simulation (transient simulation for specific yield), calculated hydraulic heads at well locations were compared with target wells and the ME, RMSE, and maximum and minimum residuals were calculated. Table 7 lists the calibration statistics for each simulation of the sensitivity analysis. The statistical results are compared to the Base Case simulation results, given at the top of Table 7, as a indication of how much the model's calibration changed due to the change in the input parameter. Graphical presentations of the statistical results are provided in the appendix.

For the calibration component of the sensitivity analysis, the statistical results show the trend of the RMSE in the vicinity of the calibrated model as a function of individual model parameter values (e.g., Figure 31). For a given model parameter, the slope of the model RMSE curve indicates the model's sensitivity, as a whole, to that parameter. The slope of the response curve should approach zero in the vicinity of an optimum calibration, corresponding to minimization of the RMSE. Thus, the results for recharge (Figure 31), for example, indicate that the model RMSE, as a function of recharge rate, has been minimized.

The predictive component of the sensitivity analysis is equally important as the calibration component. If variations in some model inputs result in insignificant changes in the degree of calibration but cause significantly different conclusions, then the mere fact of having used a calibrated model does not necessarily mean that the modeling

conclusions are valid. Thus, it was necessary to examine both calibration and prediction components in the sensitivity analysis. According to ASTM (1994), there are four types of sensitivity, Types I through IV, depending on whether the changes to the calibration residuals and model's conclusions are significant or insignificant. The four types of sensitivity are described as follows:

- *Type I Sensitivity*—When variation of an input causes insignificant changes in the calibration residuals as well as the model's conclusions, then that model has a Type I sensitivity to the input. Type I sensitivity is of no concern because regardless of the value of the input, the conclusion will remain the same.
- *Type II Sensitivity*—When variation of an input causes significant changes in the calibration residuals but insignificant changes in the model's conclusions, then that model has a Type II sensitivity to the input. Type II sensitivity is of no concern because regardless of the value of the input, the conclusion will remain the same.
- *Type III Sensitivity*—When variation of an input causes significant changes to both the calibration residuals and the model's conclusions, then that model has a Type III sensitivity to the input. Type III sensitivity is of no concern because, even though the model's conclusions change as a result of variation of the input, the parameters used in those simulations cause the model to become uncalibrated. Therefore, the calibration process eliminates those values from being considered to be realistic.
- *Type IV Sensitivity*—If, for some value of the input that is being varied, the model's conclusions are changed but the change in calibration residuals is insignificant, then the model has a Type IV sensitivity to that input. Type IV sensitivity calls model results into question because over the range of that parameter in which the model can be considered calibrated, the conclusions of the model change. A Type IV sensitivity generally indicates that additional data should be collected to decrease the range of possible values of the parameter.

Table 7 lists the identified sensitivity types for each of the parameters tested, and figures showing changes in the model's predictions as input parameters were varied are included in the appendix. Results of the analysis show that, as a whole, the model is most sensitive

to the recharge rate (Type III) and the  $K_h=150$  feet/day (Type IV) and  $K_h=300$  feet/day (Type III or IV) horizontal hydraulic conductivity units. The analysis also indicates slight sensitivity of the model, although only in terms of its calibration component, to the value of specific yield. The model was relatively insensitive to the other hydraulic parameters tested.



## 5 REFERENCES

- Anderson, M.P. and W.W. Woessner. 1992. *Applied Groundwater Modeling: Simulation of Flow and Advective Transport*. Academic Press, San Diego, CA.
- ASTM. 1994. Standard Guide for Conducting a Sensitivity Analysis for a Ground-Water Flow Model Application. D5611-94. October 1994. American Society for Testing and Materials, Philadelphia, PA.
- Baker, J.A., H.G. Healy, and O.M. Hackett. 1964. Geology and Ground-Water Conditions in the Wilmington-Reading Area, Massachusetts. U.S. Geological Survey Water-Supply Paper 1694.
- Bartlett, R.J. and B.R. James. 1988. Mobility and Bioavailability of Chromium in Soils. In: *Chromium in the Natural Environment*, J.O. Nriagu and E. Nieboer, eds. John Wiley & Sons, New York, NY.
- BCM. 1998. Groundwater Monitoring Report: Western Bedrock Valley and Sentinel Well Groundwater Monitoring Programs, July 1996 – June 1997. January 1998. BCM Engineers, Inc., Plymouth Meeting, PA.
- Bouwer, H. and R.C. Rice. 1976. A Slug Test for Determining Hydraulic Conductivity of Unconfined Aquifers with Completely or Partially Penetrating Wells. *Water Resources Research*, Vol. 12, p, 423-428.
- Castle, R.O. 1959. Surficial Geology of the Wilmington Quadrangle, Massachusetts. U.S. Geological Survey Map GQ-122.
- Cigliano, Anthony. 1998. Groundwater Withdrawal Permit Application, sent to Massachusetts Department of Environmental Protection. (Mr. Cigliano was Director of Environmental Services for Altron in October 1998.)
- CRA. 1993. Comprehensive Site Assessment: Phase II Field Investigation Report. June 1993. Conestoga-Rovers & Associates, Waterloo, Ontario, Canada.

- Diersch, H.-J.G. 1998. FEFLOW Reference Manual. WASY Institute for Water Resources Planning and Systems Research Ltd., Berlin, Germany.
- Essaid, H.I. 1990. The Computer Model SHARP, A Quasi-Three-Dimensional Finite-Difference Model to Simulate Freshwater and Saltwater Flow in Layered Coastal Aquifer Systems. U.S. Geological Survey Water-Resources Investigations Report 90-4130.
- EPA. 1989. Predicting Subsurface Contaminant Transport and Transformation: Considerations for Model Selection and Field Validation. U.S. Environmental Protection Agency, EPA/600/2-89/045.
- EPA. 1991. Handbook, Groundwater, Volume II: Methodology. U.S. Environmental Protection Agency, EPA/625/6-90/016b.
- Friedman, R., C. Ansell, S. Diamond, and Y.Y. Haimes. 1984. The Use of Models for Water Resource Management, Planning and Policy. *Water Resources Research*, Vol. 20, p. 793-802.
- Geomega. 1999. Olin Wilmington Technical Series: III. Results of the August 1998 Multilevel Piezometer Sampling Event and DAPL/Diffuse Layer Discrimination Analysis. January 1999. Geomega, Inc., Boulder, CO.
- Guswa, J.H. and D.R. LeBlanc. 1985. Digital Models of Ground-Water Flow in the Cape Cod Aquifer System, Massachusetts. U.S. Geological Survey Water-Supply Paper 2209.
- IEP. 1990. Aquifer Protection Study: Town of Wilmington. June 1990. IEP Inc., Sandwich, MA.
- LAW. 1998. Groundwater Monitoring Report: Western Bedrock Valley and Sentinel Well Groundwater Monitoring Programs, July 1997 – June 1998. September 1998. LAW Engineering and Environmental Services, Inc., Kennesaw, GA.

- LAW. 1999. Groundwater Flow Model Report for Olin Corporation, Wilmington, Massachusetts Facility. Draft, February 1999. LAW Engineering and Environmental Services, Inc., Kennesaw, GA.
- LAW. 2000. Groundwater Monitoring Report: Western Bedrock Valley Town Wells and Sentinel Wells Groundwater Monitoring Programs, July 1998 – May 2000. October 2000. LAW Engineering and Environmental Services, Inc., Kennesaw, GA.
- Lima, V. de. and J.C. Olimpio. 1989. Hydrogeology and Simulation of Ground-Water Flow at Superfund-Site Wells G and H, Woburn, Massachusetts. U.S. Geological Survey Water-Resources Investigations Report 89-4059.
- McDonald, M.G. and A.W. Harbaugh. 1988. A Modular Three-Dimensional Finite-Difference Ground-Water Flow Model: U.S. Geological Survey Techniques of Water-Resources Investigations, Book 6.
- Neuman, P.S. 1990. Universal Scaling of Hydraulic Conductivities and Dispersivities in Geologic Media. *Water Resources Research*, Vol. 26, p. 1749-1758.
- Pollock, D.W. 1994. User's Guide for MODPATH/MODPATH-PLOT, Version 3: A Particle Tracking Post-Processing Package for MODFLOW, the U.S. Geological Survey Finite-Difference Ground-Water Flow Model. U.S. Geological Survey Open-File Report 94-464.
- PTI. 1997. Evaluation of Reactive Barrier Effectiveness Batch and Column Tests at the Wilmington, Massachusetts Site. December 1997. PTI Environmental Services, Bellevue, WA.
- Smith. 1997. Supplemental Phase II Report, Olin Corporation, Wilmington, Massachusetts Site. June 1997. Smith Technology Corporation, Plymouth Meeting, PA.
- Spitz, K. and J. Moreno. 1996. *A Practical Guide to Groundwater and Solute Transport Modeling*. John Wiley & Sons, Inc., New York, NY.

Tiedeman, C.R., D.J. Goode, and P.A. Hsieh. 1998. Characterizing a Ground Water Basin in a New England Mountain and Valley Terrain. *Ground Water*, Vol. 36, p.611-620.

Trombley, T.J. 1992. Quality of Water From Public Supply Wells in Massachusetts, 1975-86. U.S. Geological Survey Water-Resources Investigations Report 91-4129.

WASY. 1999. Internet Site: <http://www.wasy.de> (FEFLOW References).



**Table 1. Details of Municipal Wellfield**

<b>Well</b>	<b>Date of Installation</b>	<b>Collar Elevation (ft amsl)</b>	<b>Screened Interval (ft bgs)</b>	<b>Maximum Design Yield (gpm)</b>
BR-1	Oct. 1971	87.81	39-51.5	900
BR-2	Mar. 1979	79.79	36-46	950
CS-1	Sept. 1961	84.81	40-55	950
CS-1A/2	Aug. 1991	81.51	45-55	500
TP	July 1964	81.33	29-39	350

Source: CRA 1993; IEP 1990

**Table 2. Calibration Statistics for Steady-State Flow Model**

Parameter	Value
Number of Observation Points	89
Residual Mean Error (ft)	-0.025
Mean Absolute Error (ft)	0.340
Root-Mean-Squared-Error (ft)	0.451
Minimum Residual (ft)	-1.018
Maximum Residual (ft)	1.206
RMSE/Head Range	0.037

**Table 3. Comparison of Measured and Simulated Stream Outflows  
at Model Boundary**

<b>Location</b>	<b>Measured Flow (ft<sup>3</sup>/d)</b>	<b>Simulated Flow (ft<sup>3</sup>/d)</b>	<b>Residual Flow (ft<sup>3</sup>/d)</b>
Maple Meadow Brook at Route 38	514,944	502,337	12,607
East Ditch below South Ditch	34,560	38,330	-3,770

**Table 4. Results of Stream Gauging in Maple Meadow Brook, April 1998**

Site	Flow (cfs)
Maple Meadow Brook at Route 38	5.96
Maple Meadow Brook at Gravel Pit	1.72
Sawmill Brook at Chestnut Street	3.32
Minor Tributaries to Maple Meadow Brook	0.28

Source: Dan Morrissey, written communication, May 1998

**Table 5. Temporal Distribution of Recharge Based on Model Calibration**

<b>Time Period</b>	<b>Duration (days)</b>	<b>Percentage of Annual Recharge</b>	<b>Vertical Recharge Rate (inches/day)</b>
October	31	20	0.1290
November	30	15	0.1000
December – March	121	40	0.0661
April	30	5	0.0333
May – July	92	0	0.0000
August	31	5	0.0323
September	30	15	0.1000

Annual recharge assumed to be 20 inches/year

**Table 6. Calibration Statistics for Transient Flow Model**

Parameter	Value
Number of Observation Points	357
Residual Mean Error (ft)	-0.259
Mean Absolute Error (ft)	1.006
Root-Mean-Squared-Error (ft)	1.401
Minimum Residual (ft)	-7.698
Maximum Residual (ft)	3.731
RMSE/Head Range	0.095

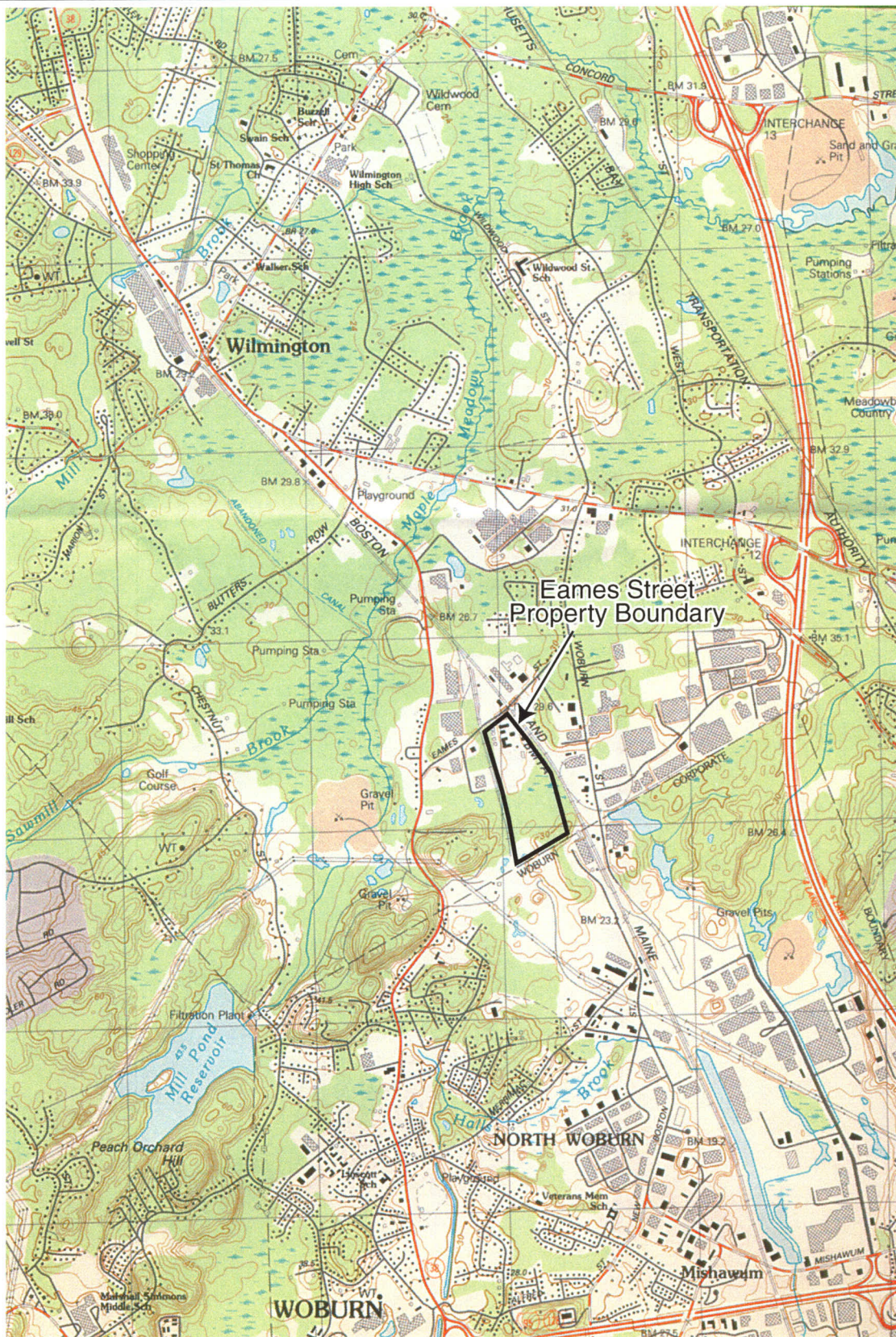
**Table 7. Sensitivity Analysis Results**

Parameter Tested	Multiplier	Value	ME (feet)	RMSE (feet)	Maximum Residual (feet)	Minimum Residual (feet)	Sensitivity Type
Calibrated Model (Base Case)	1		0.25	0.67	1.77	-1.17	
K <sub>h</sub> =1 (feet/day)	10	10	0.42	0.90	3.68	-1.07	II
	2	2	0.32	0.72	1.78	-1.14	
	0.5	0.5	0.11	0.84	1.74	-2.98	
	0.1	0.1	-0.70	3.93	1.74	-20.34	
K <sub>h</sub> =2 (feet/day)	10	20	0.25	0.67	1.79	-1.17	I
	2	4	0.24	0.67	1.75	-1.21	
	0.5	1	0.24	0.67	1.75	-1.21	
	0.1	0.2	0.24	0.67	1.74	-1.21	
K <sub>h</sub> =3 (feet/day)	10	30	0.27	0.66	1.76	-1.18	I or II
	2	6	0.26	0.66	1.76	-1.17	
	0.5	1.5	0.22	0.69	1.75	-1.98	
	0.1	0.3	0.15	1.17	1.76	-9.11	
K <sub>h</sub> =10 (feet/day)	10	100	0.24	0.67	1.75	-1.20	I
	2	20	0.24	0.67	1.75	-1.20	
	0.5	5	0.25	0.67	1.76	-1.18	
	0.1	1	0.24	0.67	1.75	-1.20	
K <sub>h</sub> =15 (feet/day)	10	150	0.25	0.67	1.77	-1.17	I
	2	30	0.25	0.67	1.76	-1.17	
	0.5	7.5	0.25	0.67	1.76	-1.17	
	0.1	1.5	0.25	0.66	1.76	-1.18	
K <sub>h</sub> =18 (feet/day)	10	180	0.67	0.98	2.61	-1.25	II
	2	36	0.37	0.70	1.93	-1.18	
	0.5	9	0.05	0.81	1.60	-2.40	
	0.1	1.8	-0.72	2.30	1.56	-9.20	
K <sub>h</sub> =30 (feet/day)	10	300	0.23	0.67	1.75	-1.28	I
	2	60	0.24	0.67	1.75	-1.14	
	0.5	15	0.25	0.67	1.75	-1.27	
	0.1	3	0.27	0.74	1.76	-2.23	
K <sub>h</sub> =70 (feet/day)	10	700	0.26	0.68	1.84	-1.17	I
	2	140	0.25	0.67	1.79	-1.18	
	0.5	35	0.24	0.68	1.95	-1.22	
	0.1	7	0.33	0.85	2.86	-1.18	
K <sub>h</sub> =75 (feet/day)	10	750	0.27	0.66	1.76	-1.20	I
	2	150	0.25	0.66	1.75	-1.20	
	0.5	37.5	0.22	0.67	1.74	-1.22	
	0.1	7.5	0.18	0.69	1.71	-1.26	
K <sub>h</sub> =150 (feet/day)	10	1500	0.75	0.96	2.49	-1.33	IV
	2	300	0.35	0.70	1.98	-1.04	
	0.5	75	0.16	0.67	1.64	-1.31	
	0.1	15	0.06	0.77	1.78	-2.05	
K <sub>h</sub> =250 (feet/day)	10	2500	0.36	0.68	2.07	-0.90	I
	2	500	0.28	0.66	1.86	-1.03	
	0.5	125	0.20	0.70	1.74	-1.42	
	0.1	25	0.25	0.92	3.29	-1.73	

**Table 7. Sensitivity Analysis Results**

Parameter Tested	Multiplier	Value	ME (feet)	RMSE (feet)	Maximum Residual (feet)	Minimum Residual (feet)	Sensitivity Type
$K_h=300$ (feet/day)	10	3000	0.18	0.68	1.79	-1.80	III or IV
	2	600	0.22	0.64	1.77	-1.17	
	0.5	150	0.28	0.78	3.10	-1.21	
	0.1	30	0.42	1.47	8.87	-1.21	
Recharge = 20 (inches/year)	1.38	27.6	-1.04	1.25	0.33	-2.83	III
	1.19	23.8	-0.41	0.74	1.00	-1.99	
	0.81	16.2	1.03	1.23	2.69	-0.55	
	0.63	12.6	1.97	2.12	3.78	0.00	
$S_y = 0.3$ (dimensionless)	0.33	0.1	0.17	5.52	8.01	-9.04	II
	0.67	0.2	-0.17	2.64	4.94	-8.15	
	1.33	0.4	-0.26	1.74	2.98	-7.46	
	1.67	0.5	-0.23	1.65	2.45	-7.35	

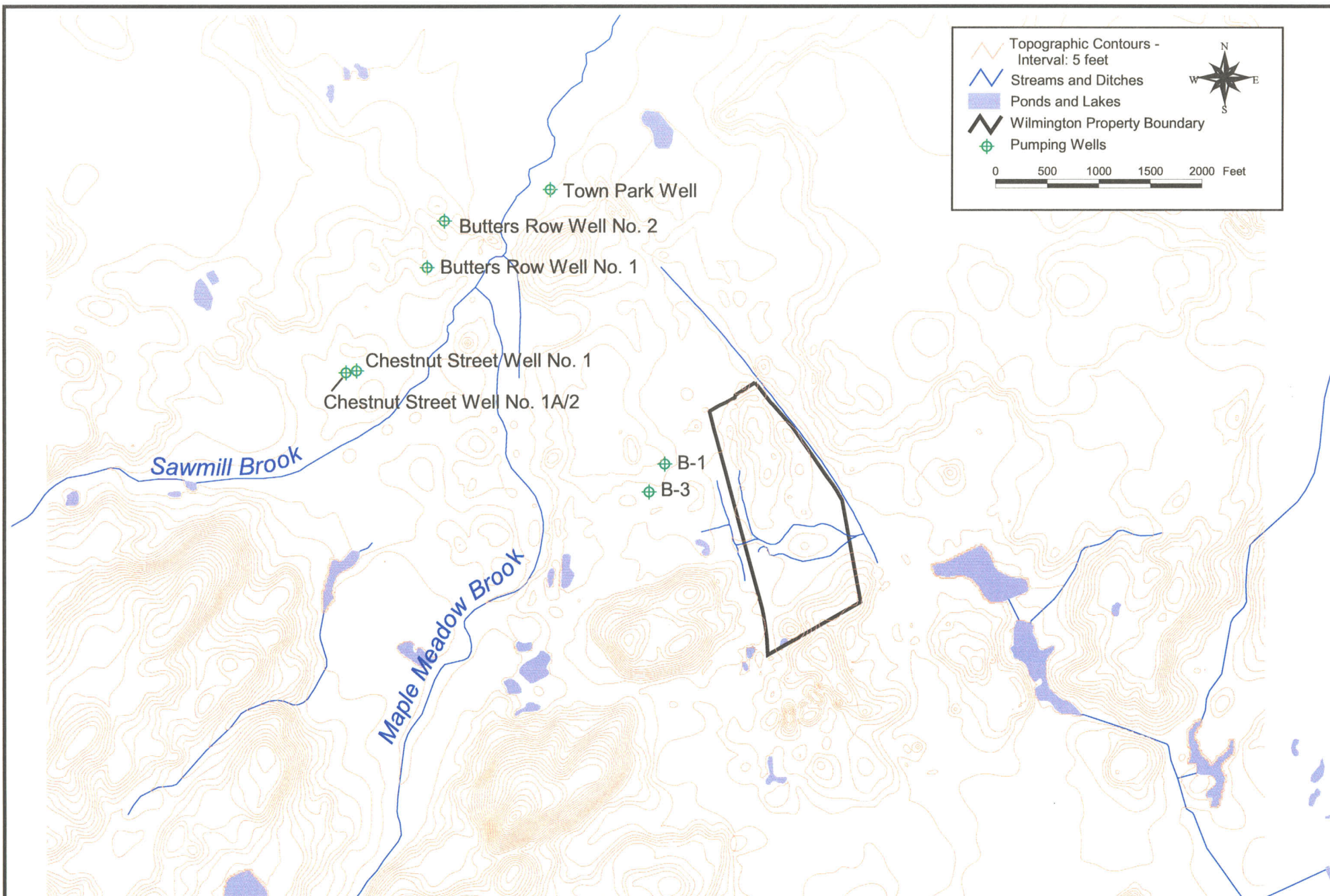




Generation  
Date:  
4/18/01

Figure 1. Location of the Wilmington Property.

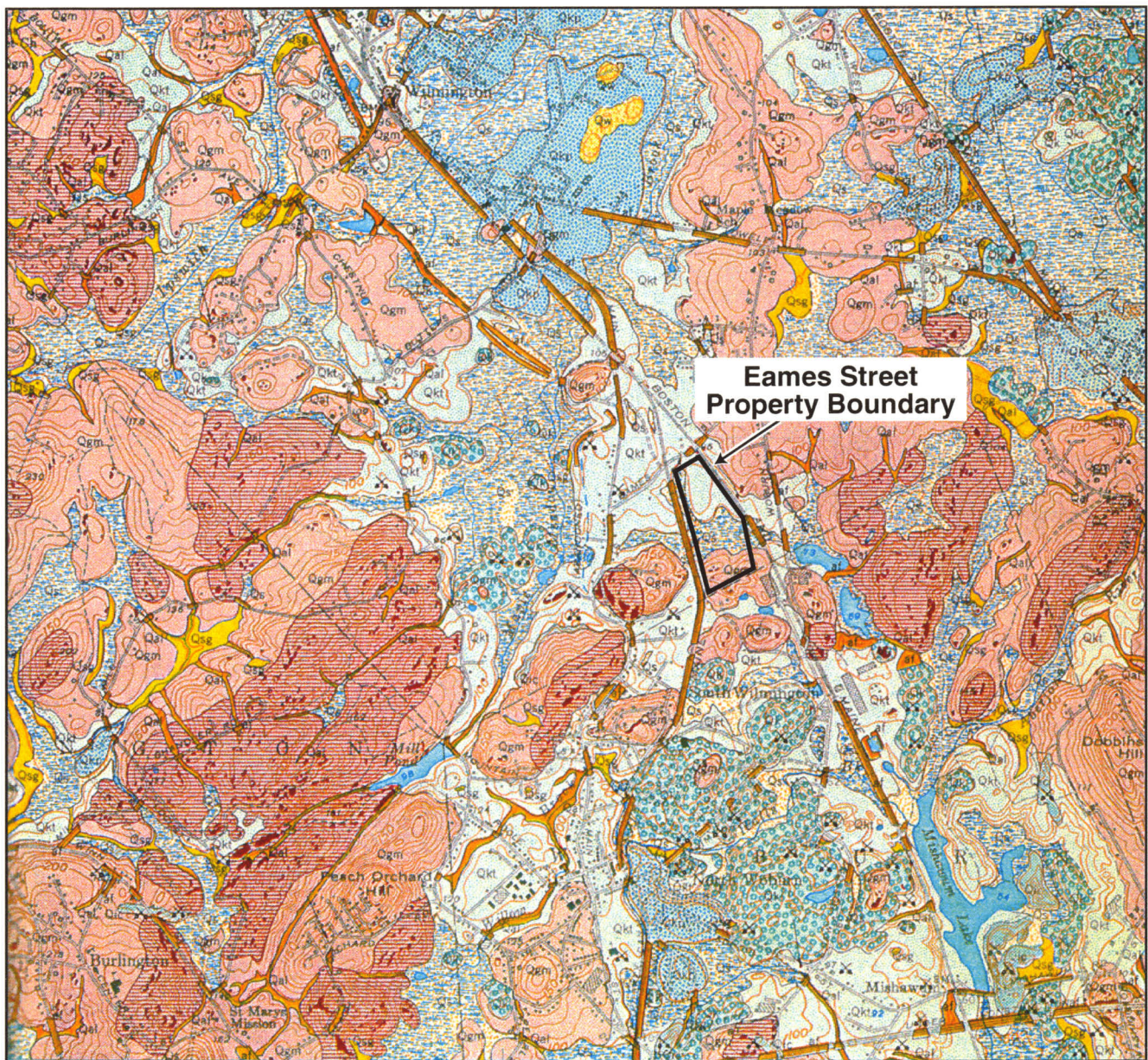




Generation  
Date:  
4/2701

Figure 2. Topography, surface water, and site features.





### Legend



Swamp Deposits



River terrace/flood plain deposits



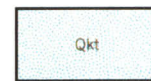
Local alluvial deposits



Wind deposits



Sand/gravel, undifferentiated



Kame terrace deposits



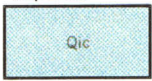
Kame plain deposits



Kame delta deposits



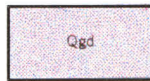
Kame deposits



Ice-channel fillings



Ground moraine deposits



Drumlin deposits



Igneous & metamorphic rocks



Artificial fill

Generation  
Date:  
4/18/01

Figure 3. Surficial geology map.  
(Source: Castle, 1959)

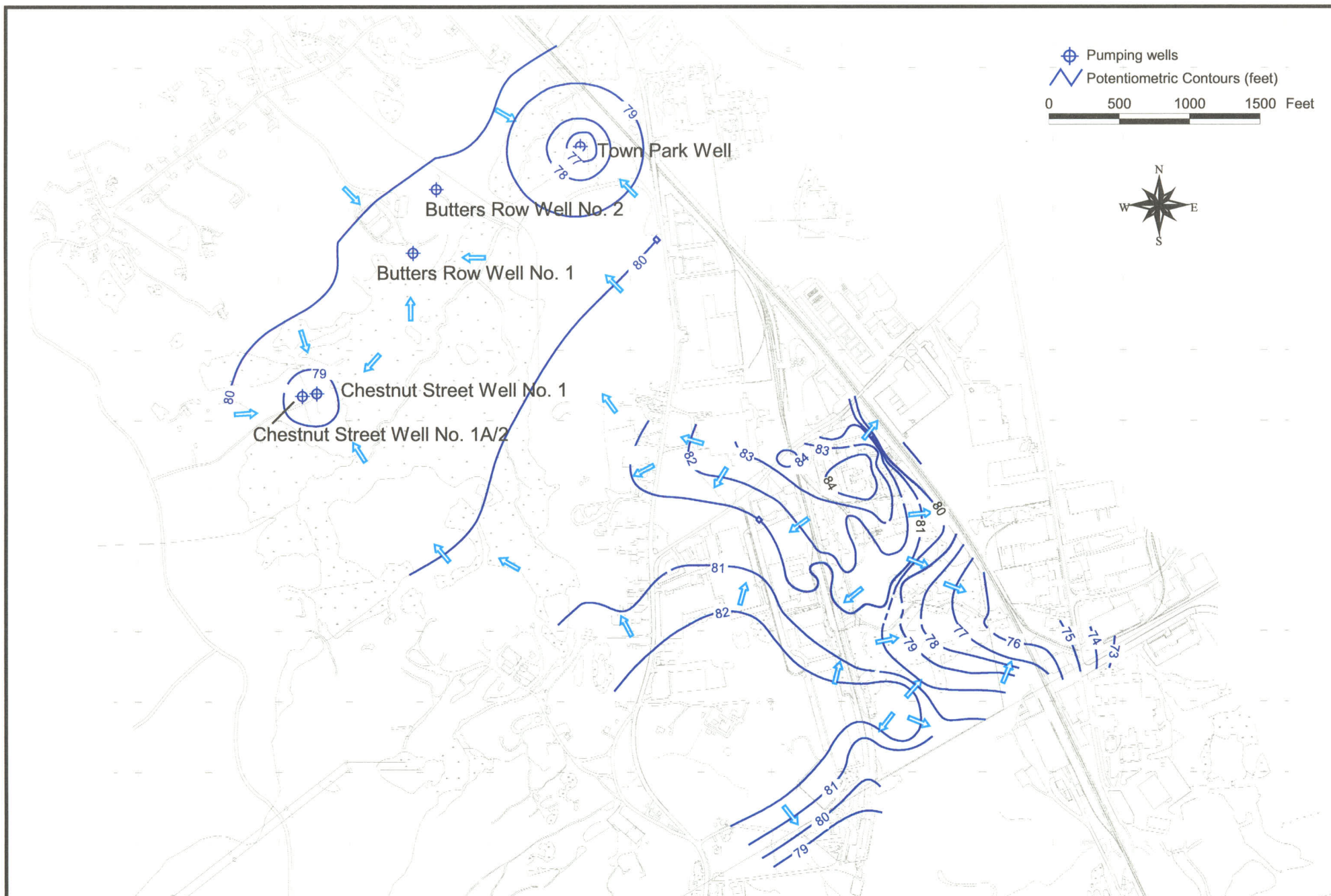
  
**Geomega**



Generation  
Date:  
4/27/01

Figure 4. Bedrock elevation contour map.

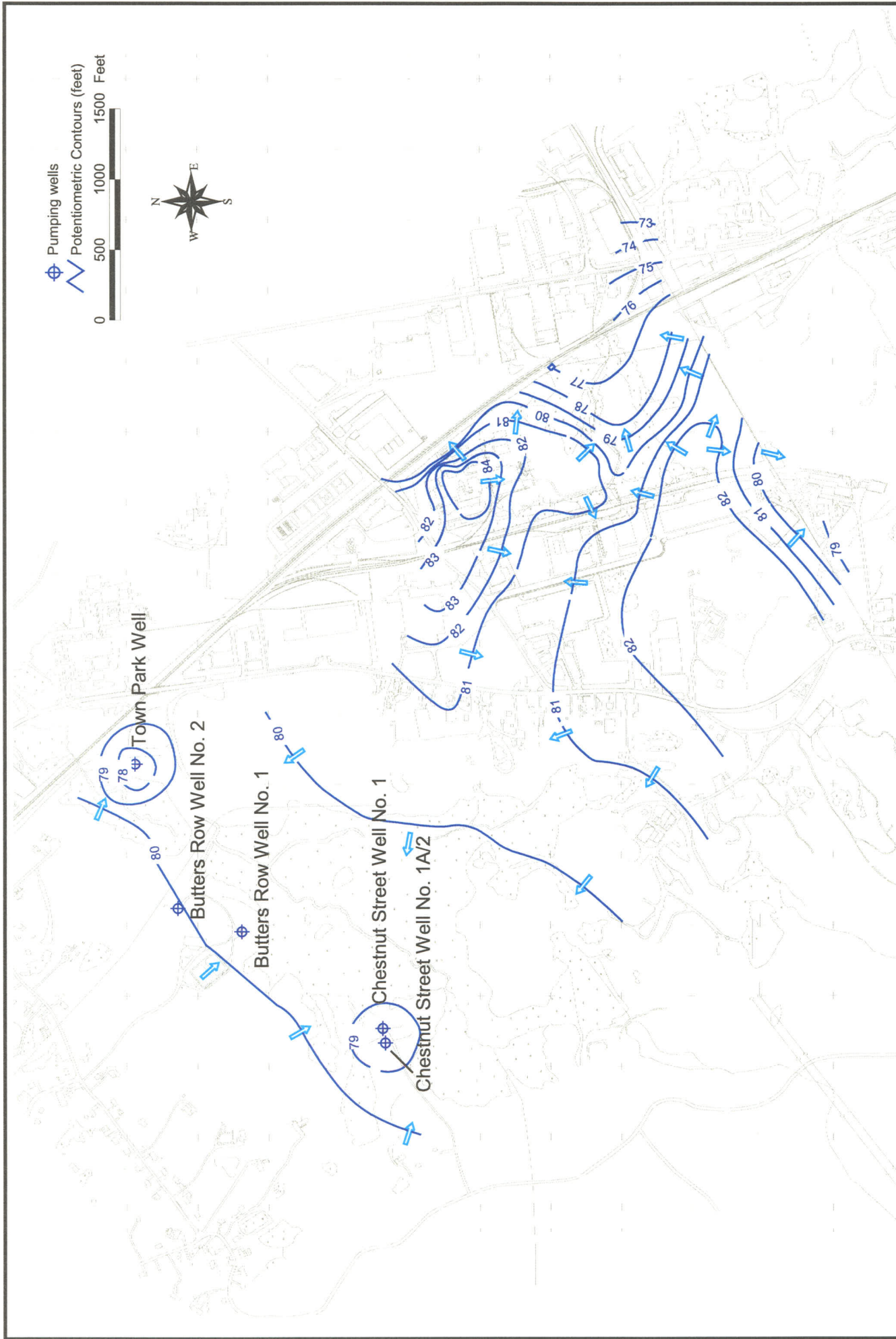




Generation  
 Date:  
 4/27/01

Figure 5. Potentiometric surface map based on shallow wells, April 1998.



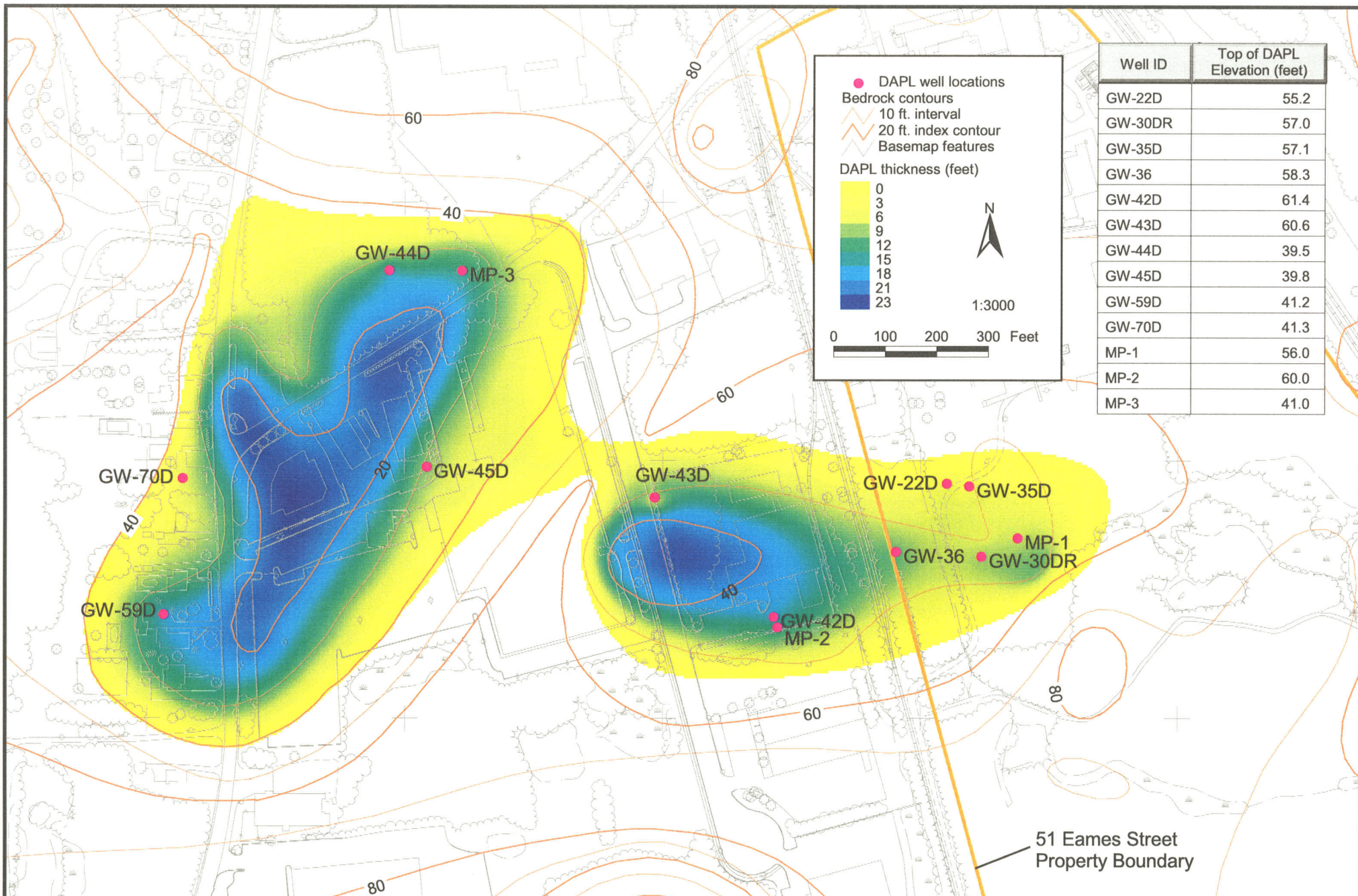


Generation

Date:

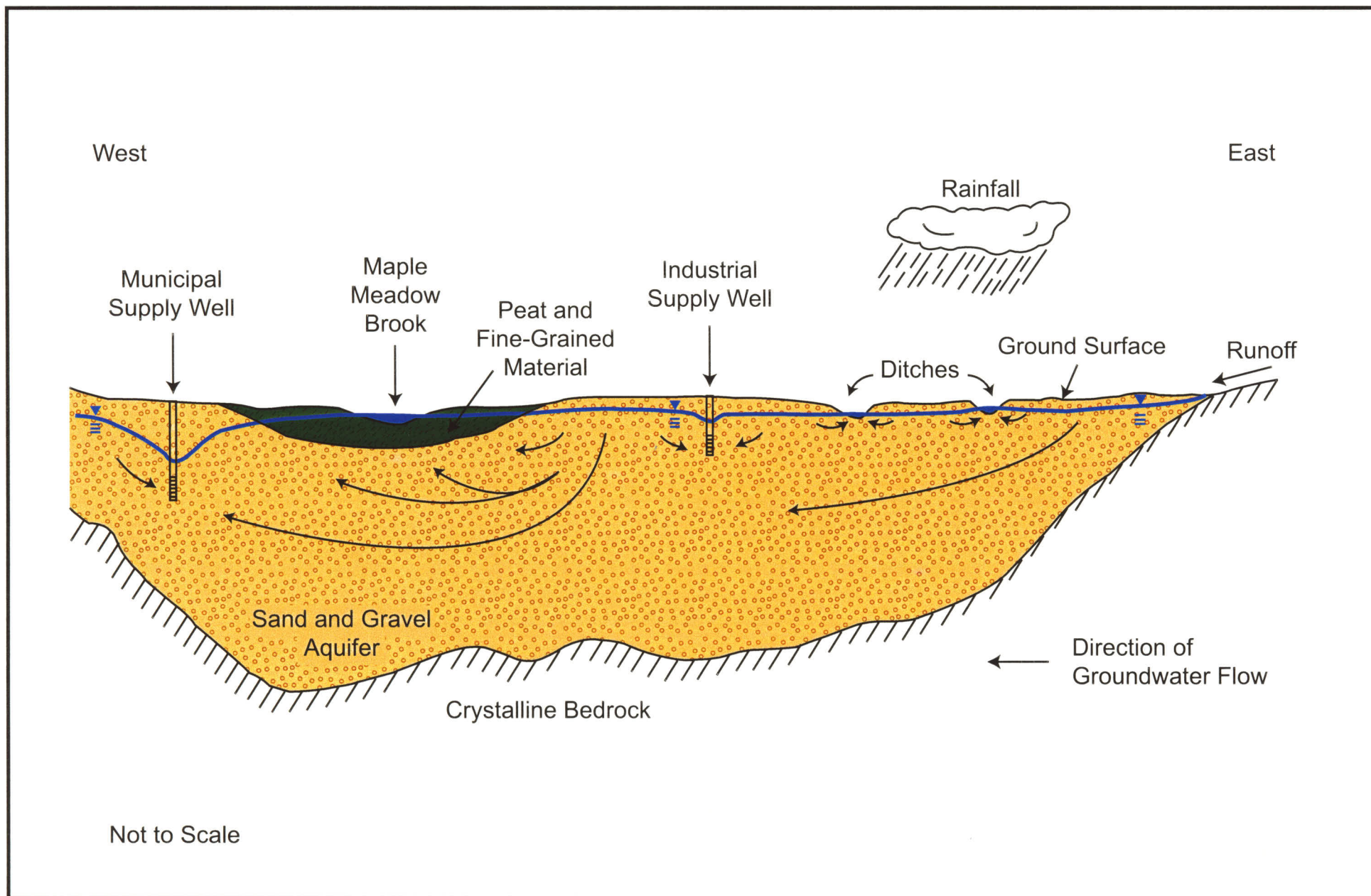
4/27/01

Figure 6. Potentiometric surface map based on deep wells, April 1998.



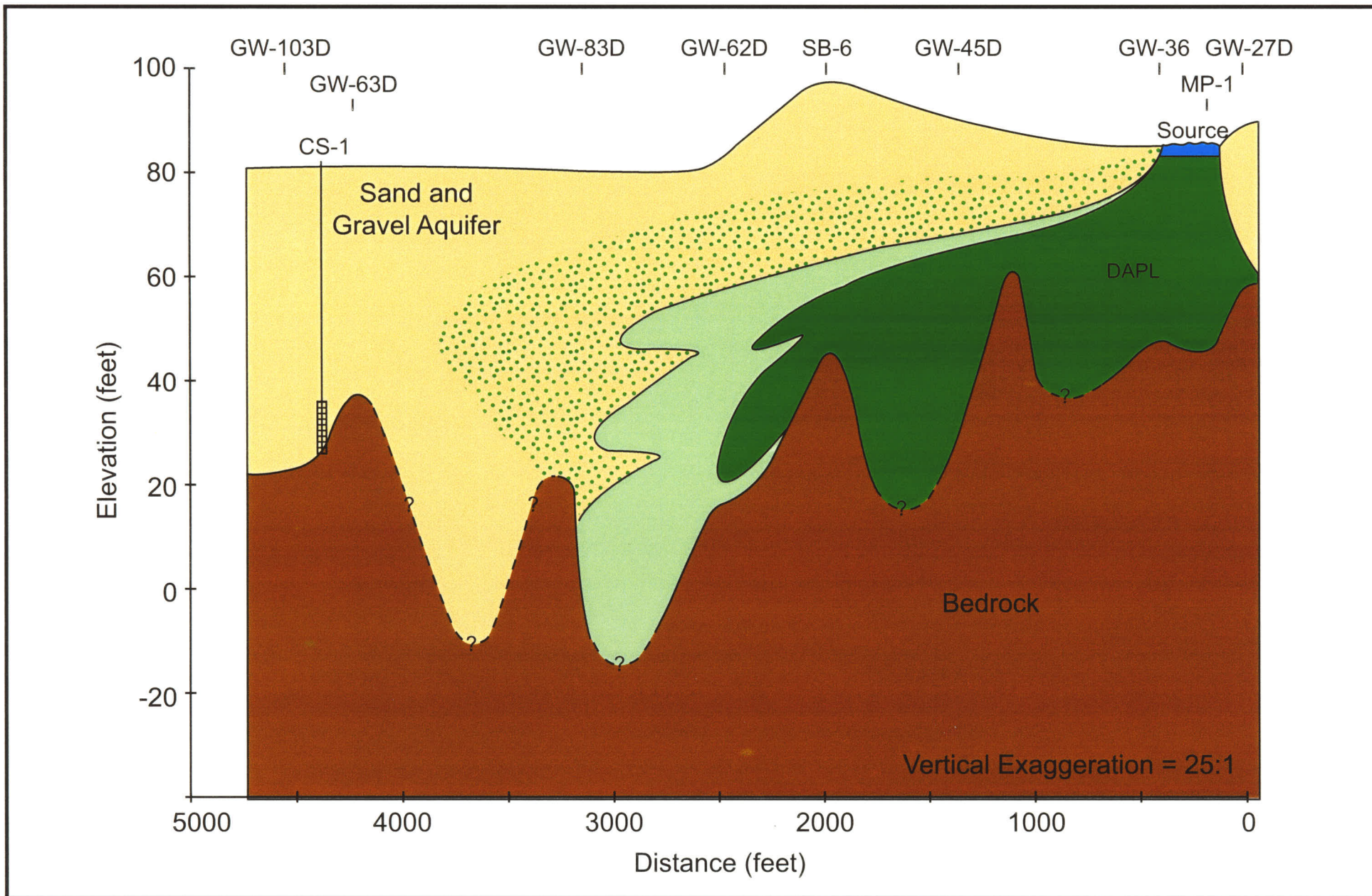
Generation  
Date:  
4/17/01

Figure 7. Thickness and extent of DAPL in 2000.



Generation  
Date:  
4/18/01

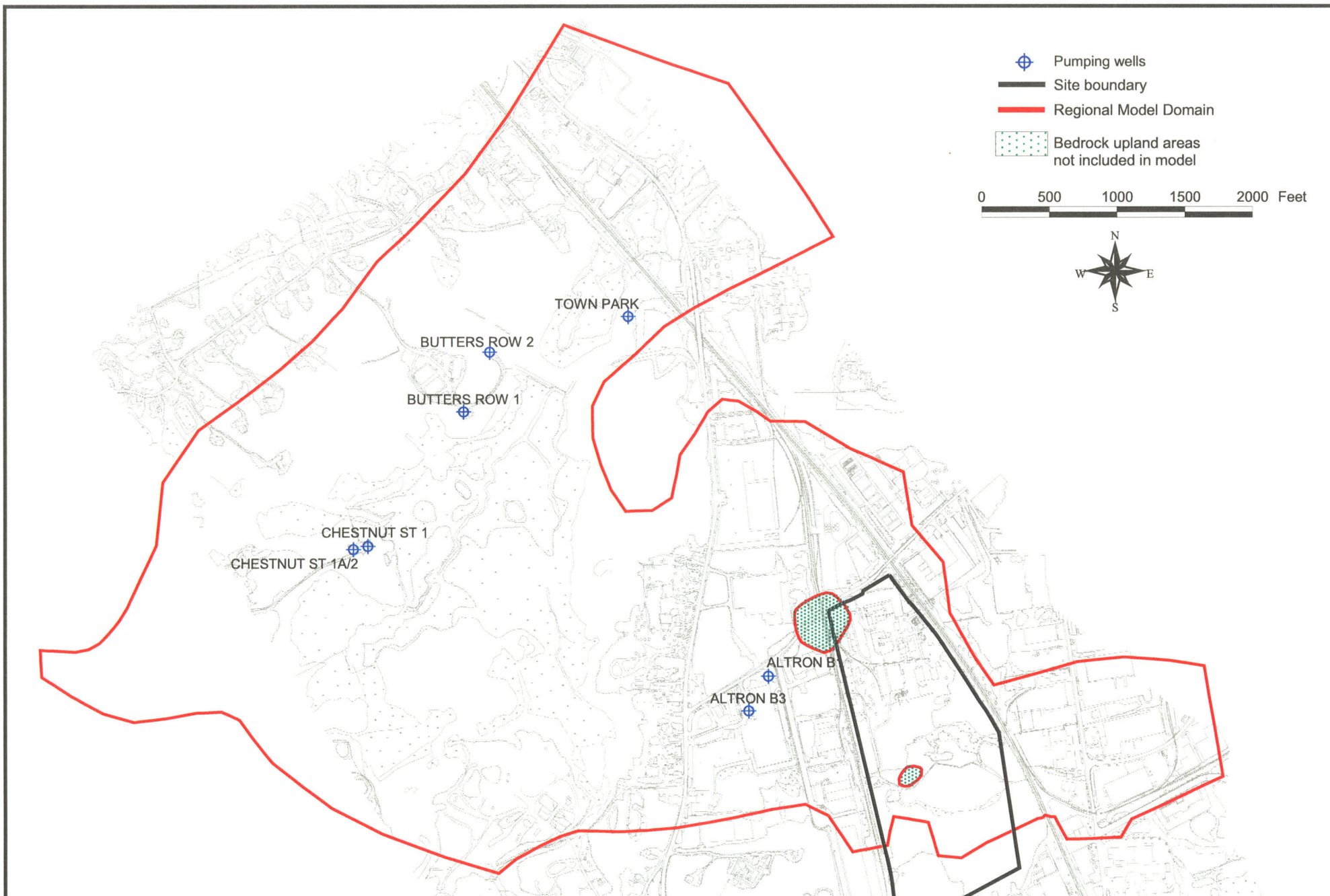
Figure 8. Schematic showing hydrological system.



Generation  
Date:  
4/18/01

Figure 9. Historical flooding of liquid waste.

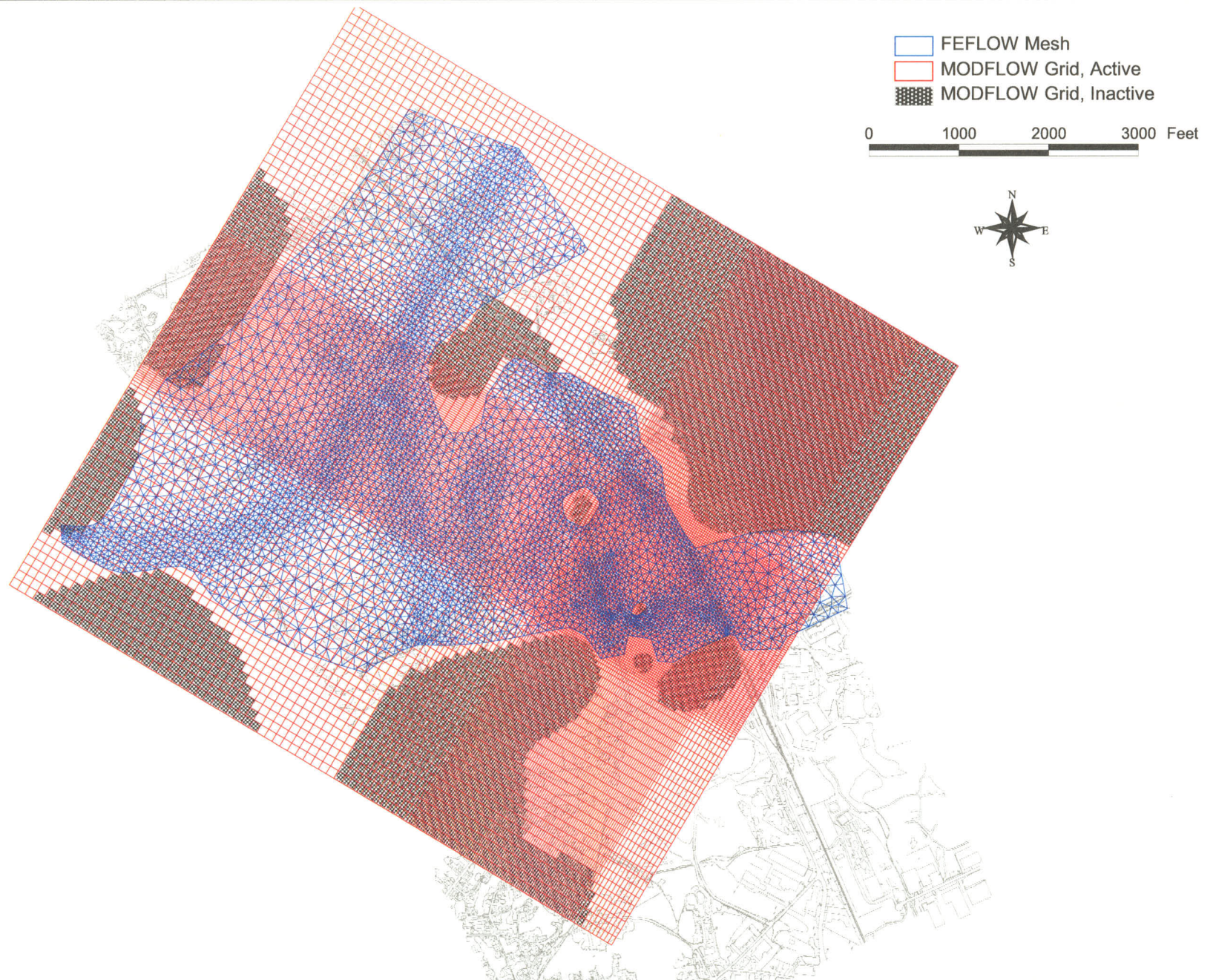




Generation  
Date:  
4/27/01

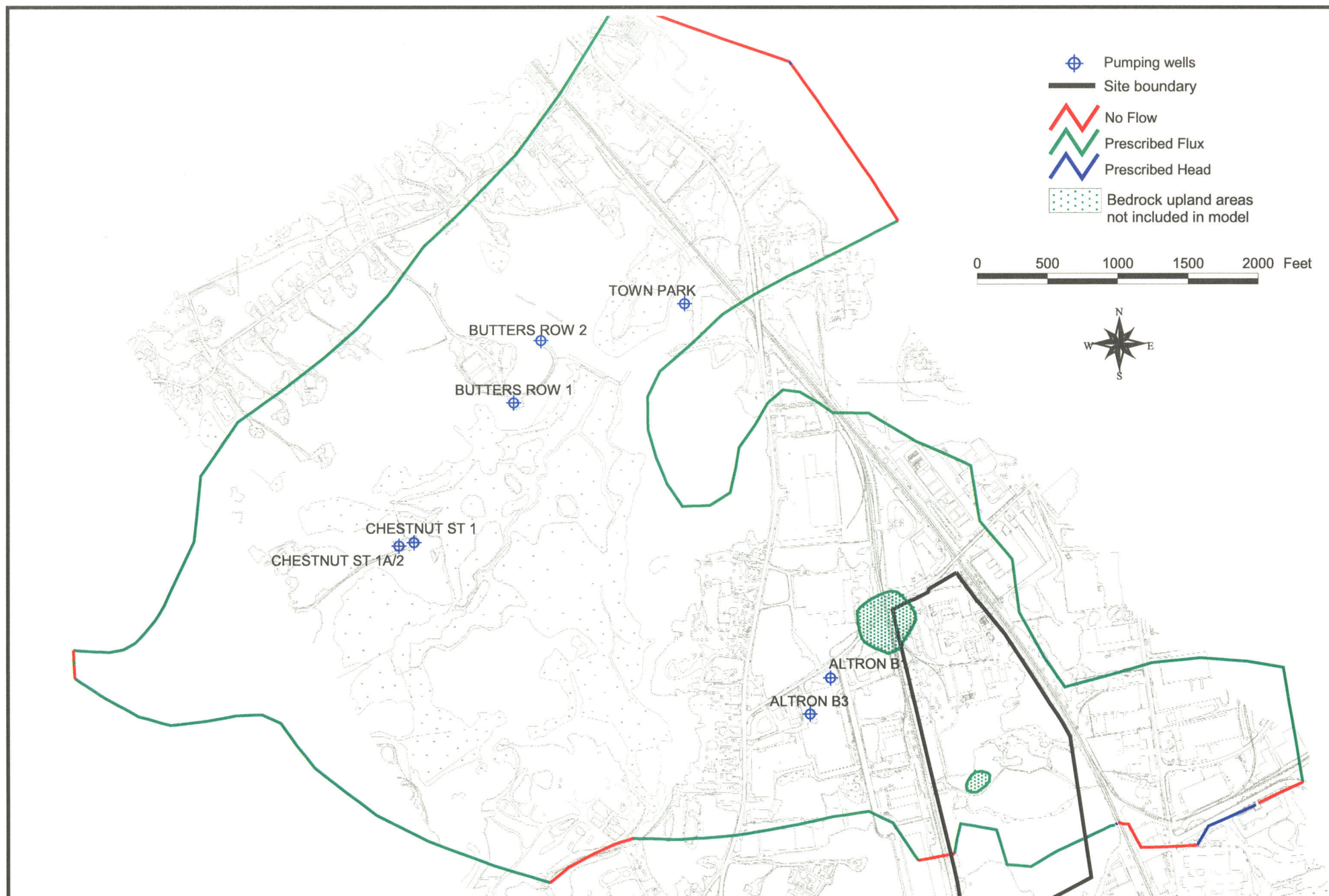
Figure 10. Regional model domain





Generation  
Date:  
4/27/01

Figure 11. Regional FEFLOW model mesh and MODFLOW model grid.



Generation  
Date:  
4/27/01

Figure 12. Regional model boundary conditions.

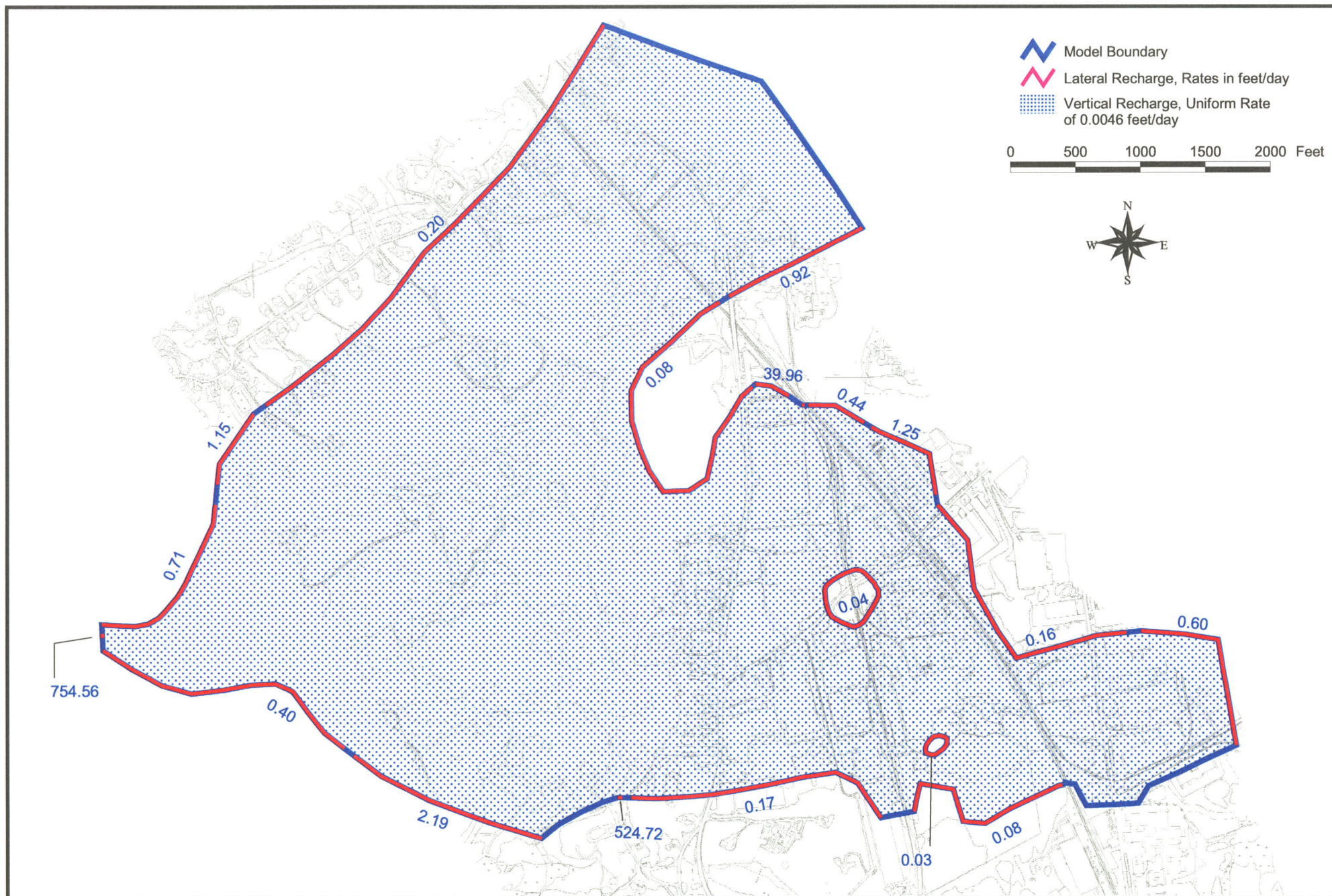




Generation  
Date:  
4/27/01

Figure 13. Bottom slice topographic elevations in regional model.

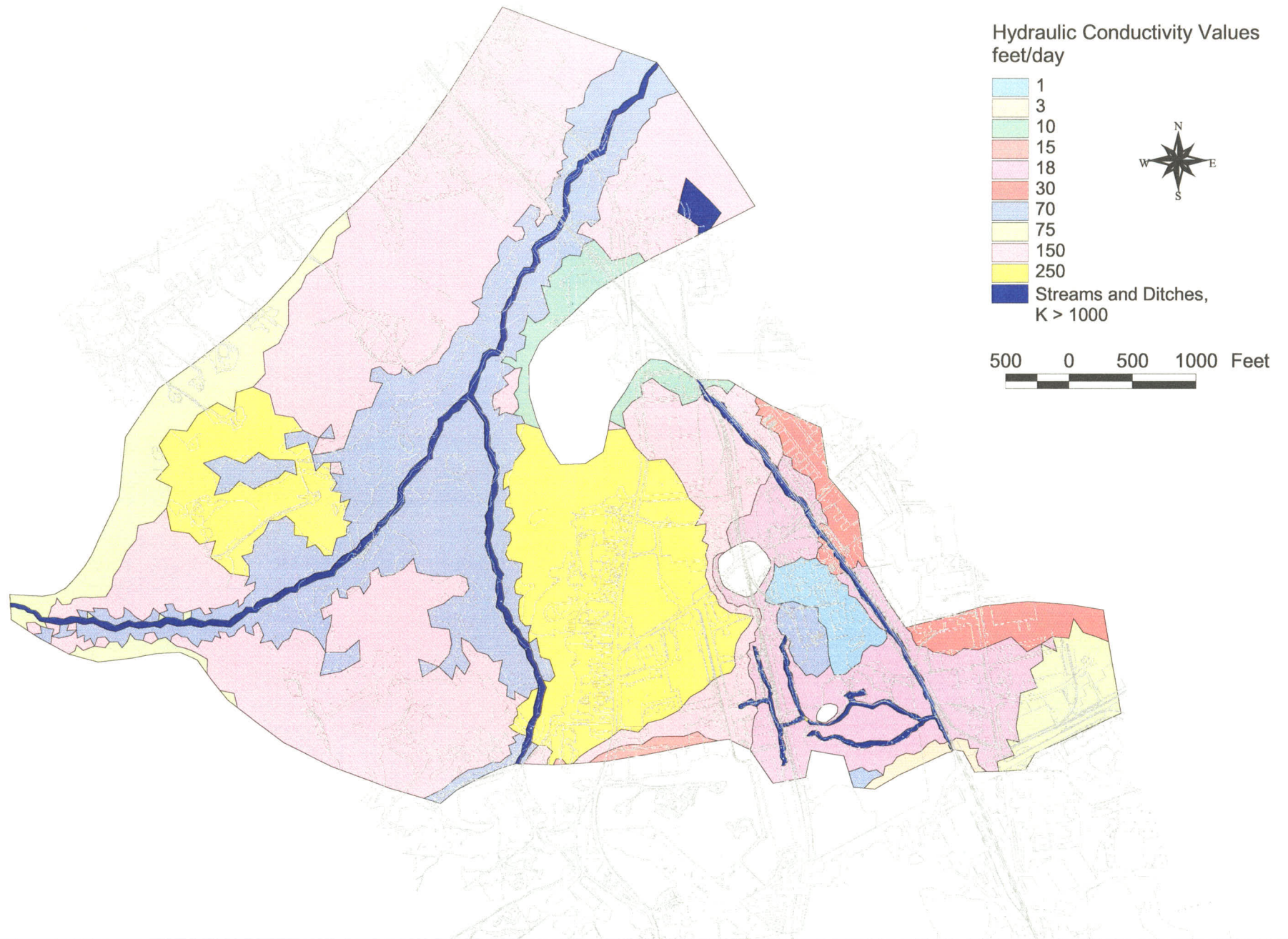




Generation  
Date:  
4/27/01

Figure 14. Regional model recharge distribution.

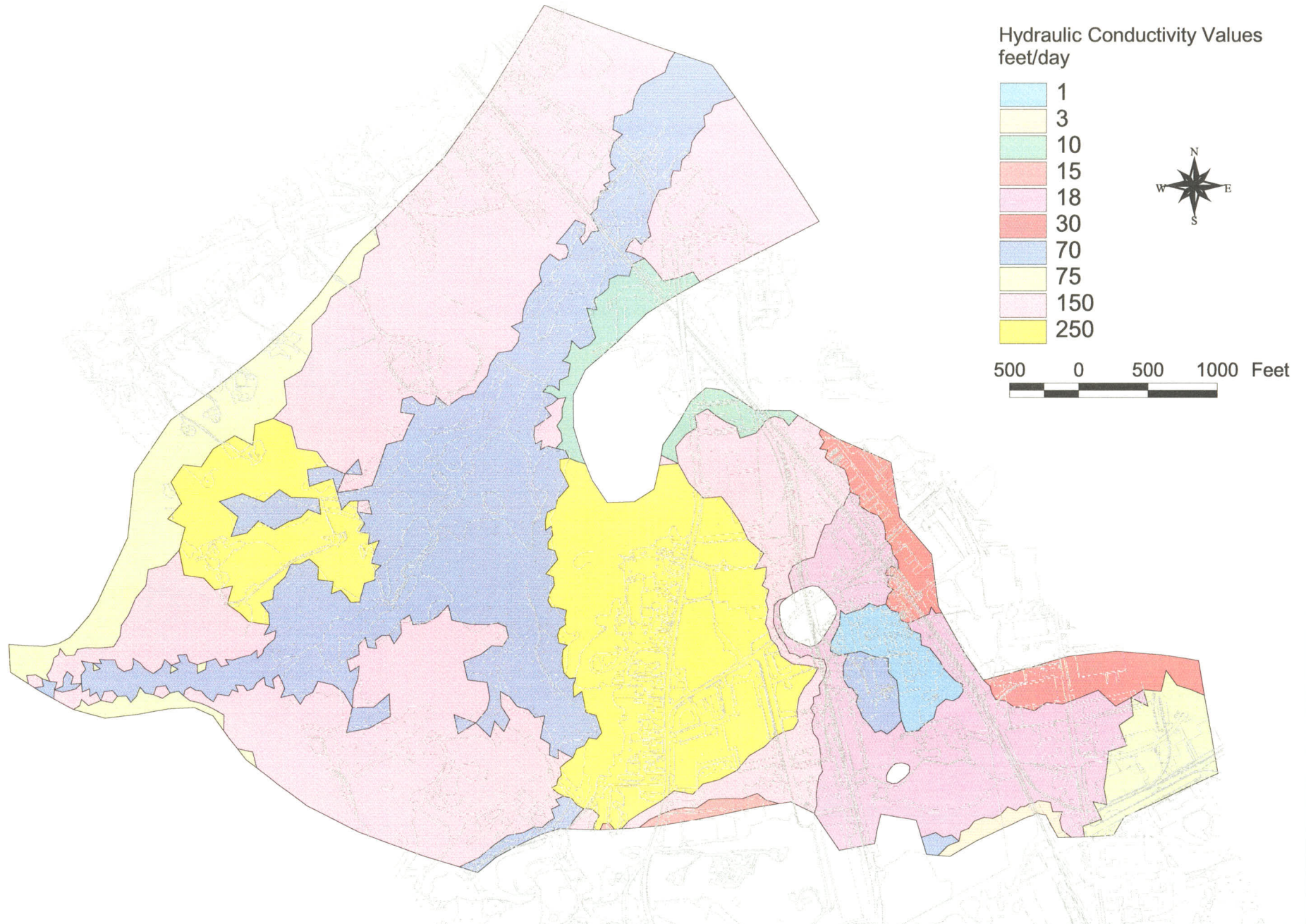




Generation  
Date:  
4/27/01

Figure 15. Hydraulic conductivity in layer 1.

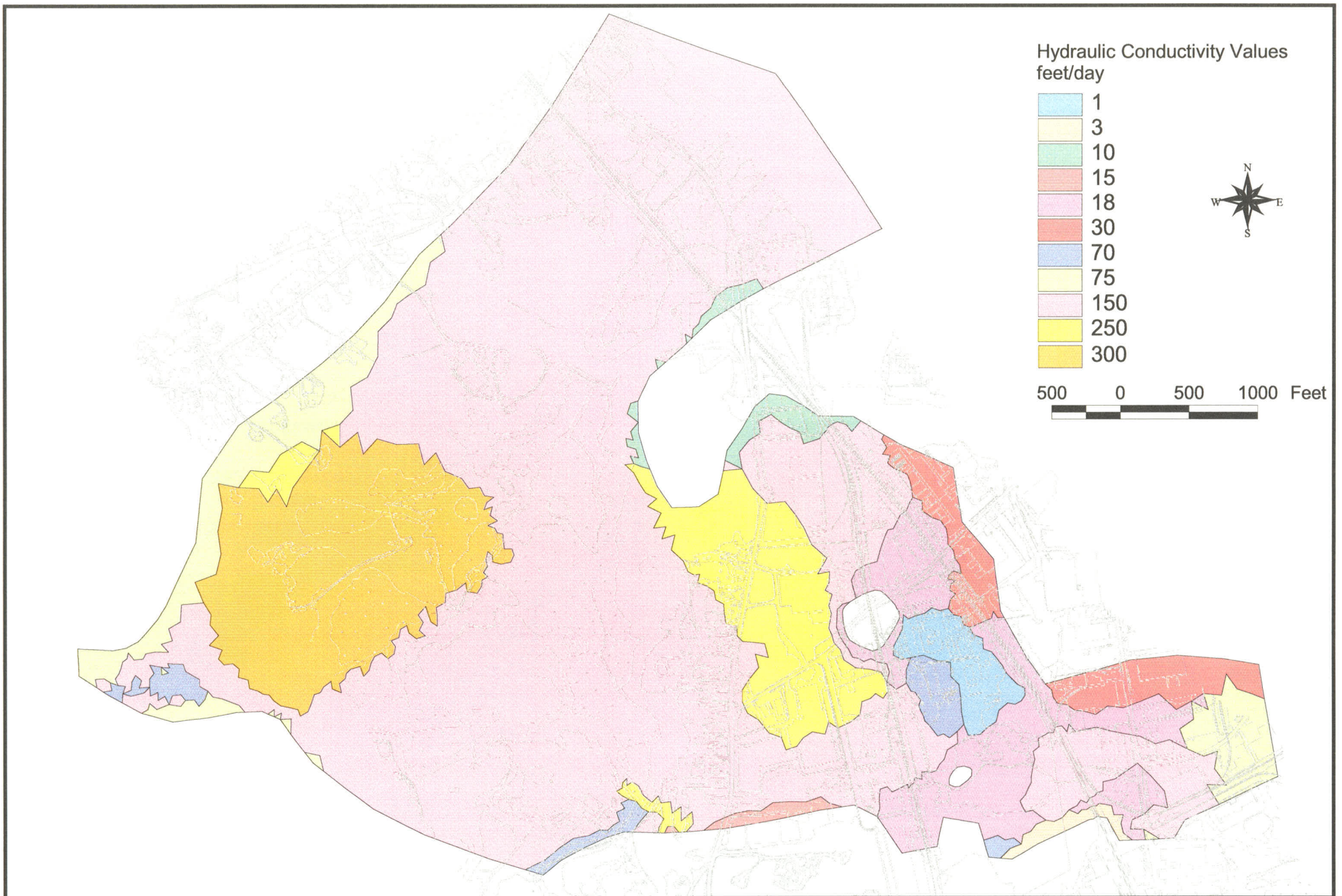




Generation  
Date:  
4/27/01

Figure 16. Hydraulic conductivity in layer 2.

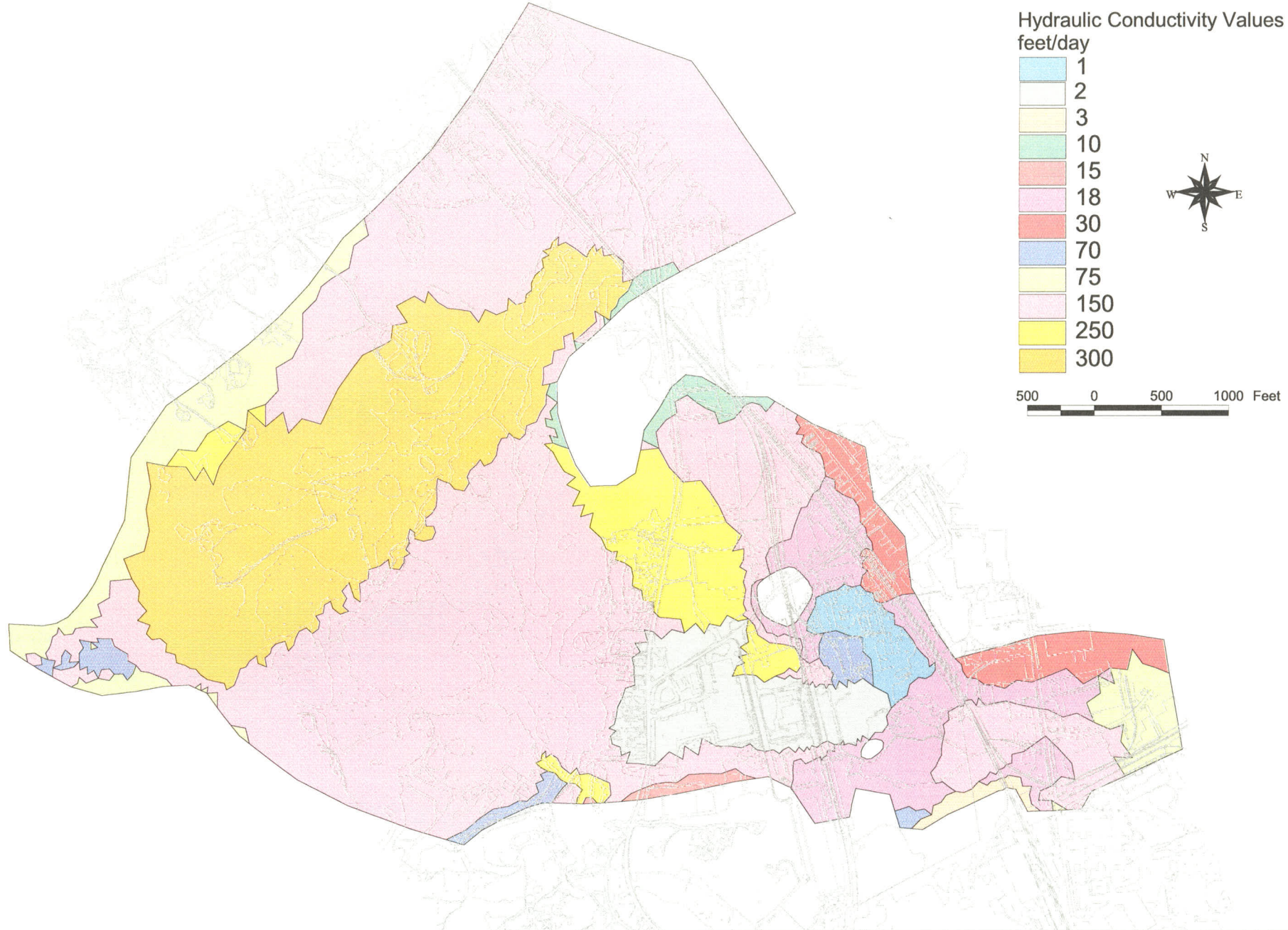




Generation  
Date:  
4/27/01

Figure 17. Hydraulic conductivity in layer 3.

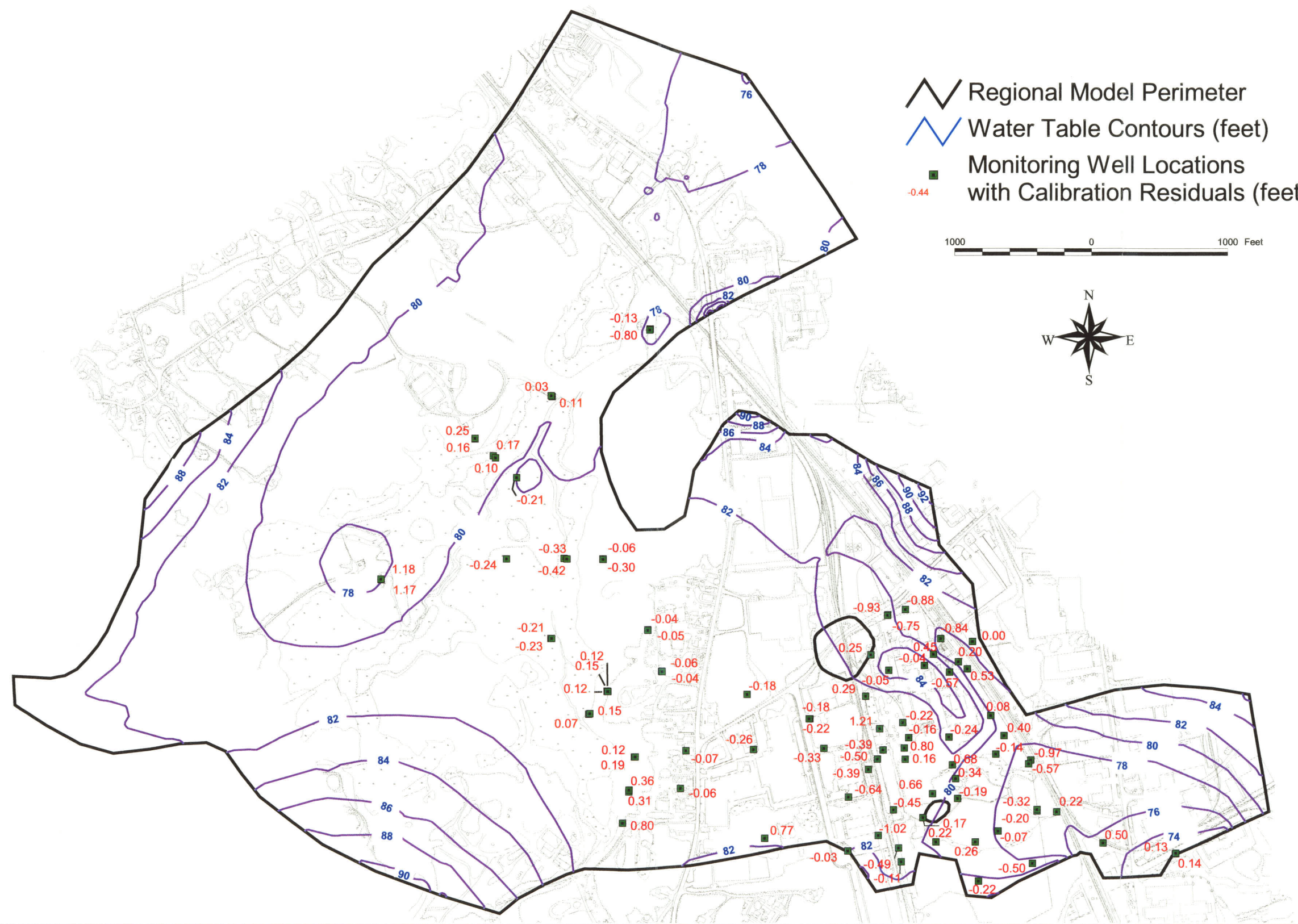




Generation  
Date:  
4/27/01

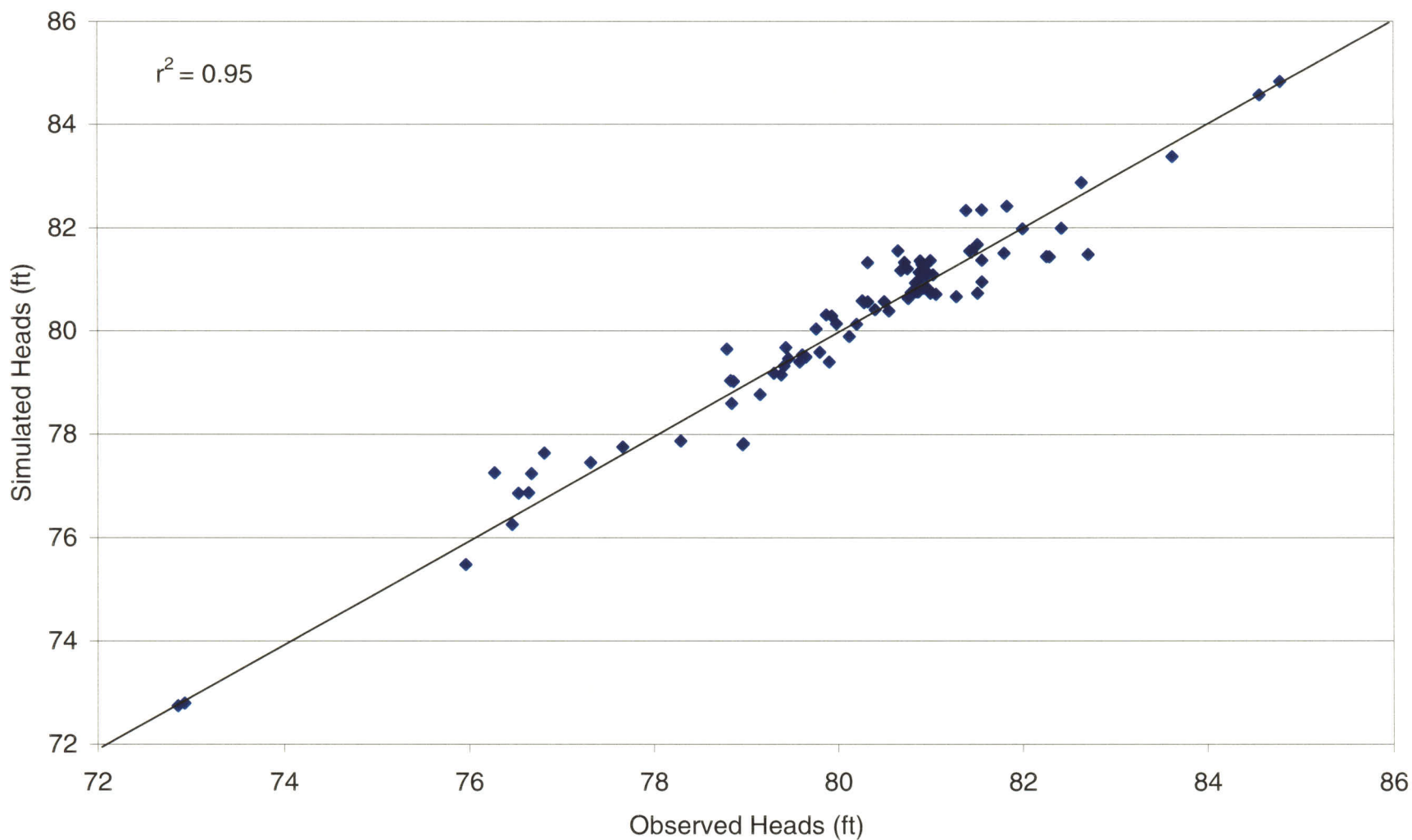
Figure 18. Hydraulic conductivity in layer 4.





Generation  
Date:  
4/27/01

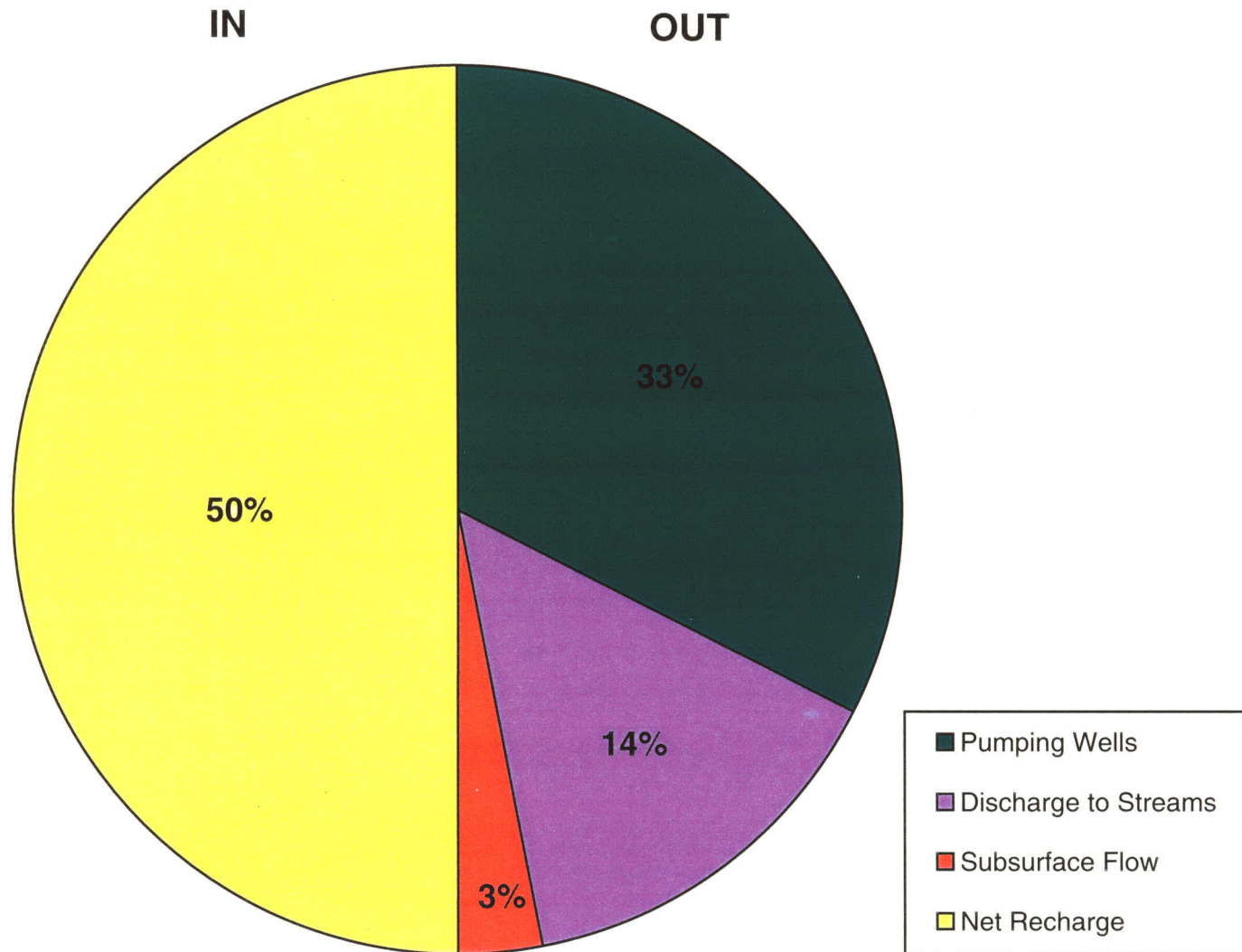
Figure 19. Contour map of simulated water table surface and calibration residuals.



Generation  
Date:  
4/18/01

Figure 20. Simulated vs. observed heads ( $r^2 = 0.95$ ).

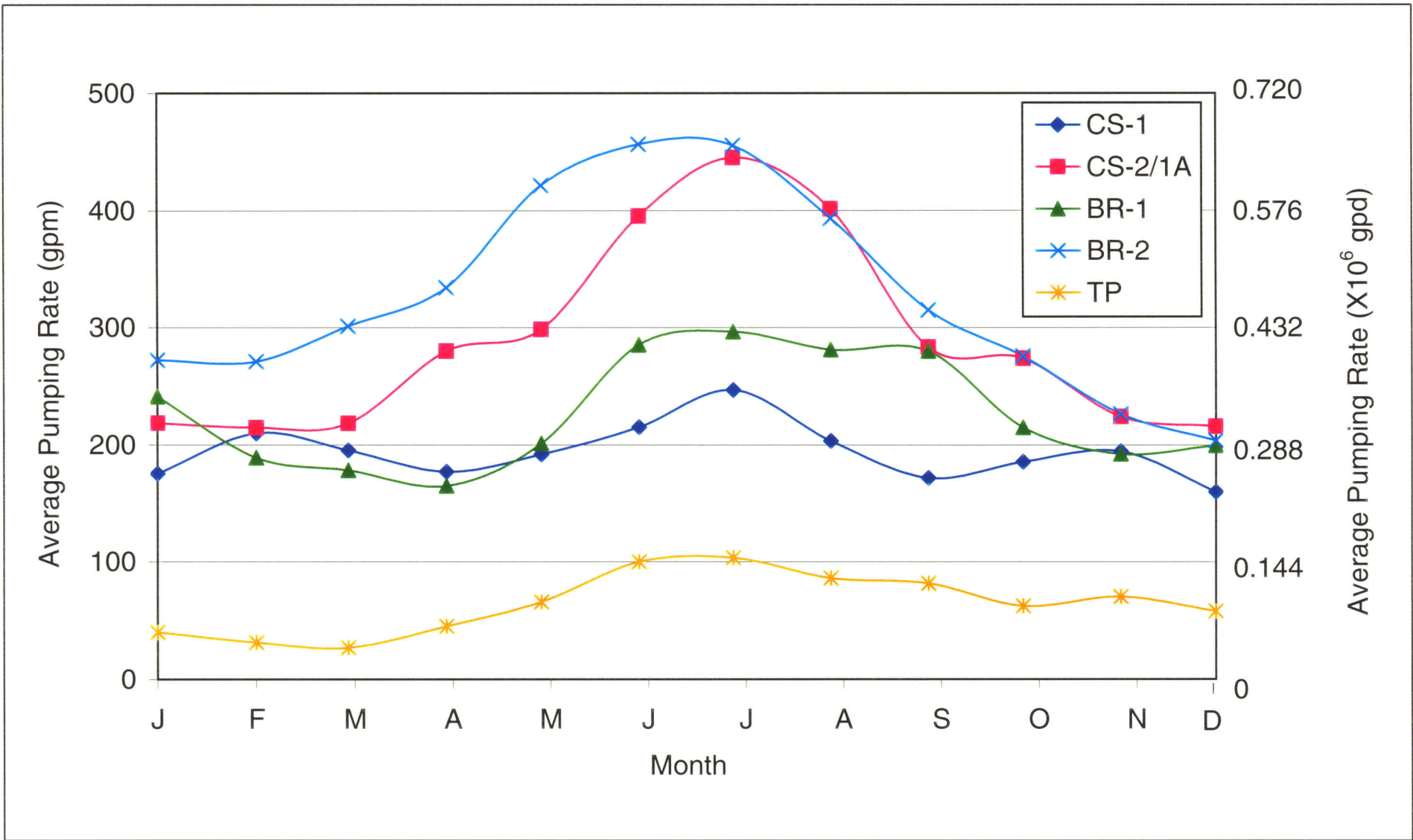




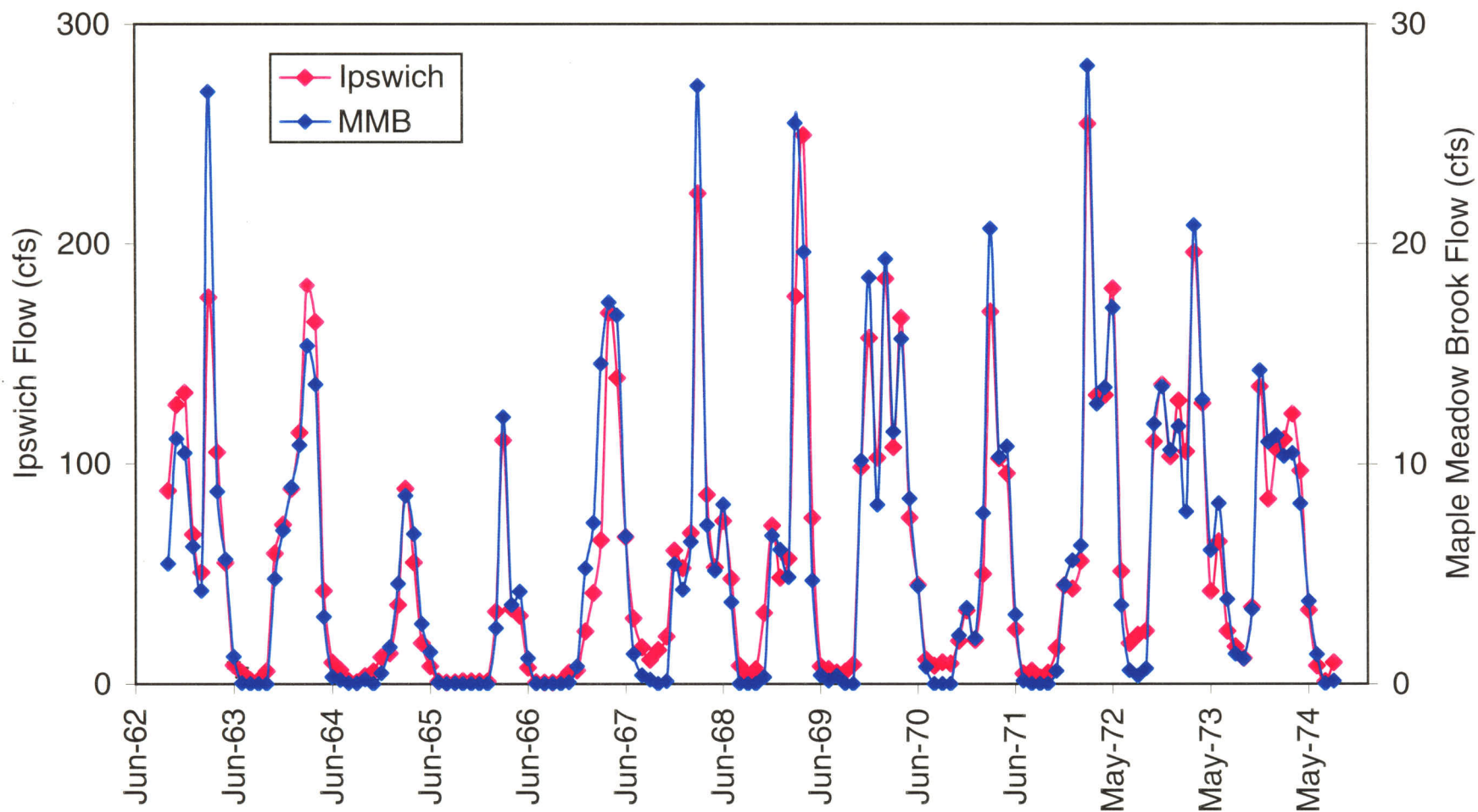
Generation  
Date:  
4/18/01

Figure 21. Generalized water budget for FEFLOW model domain.





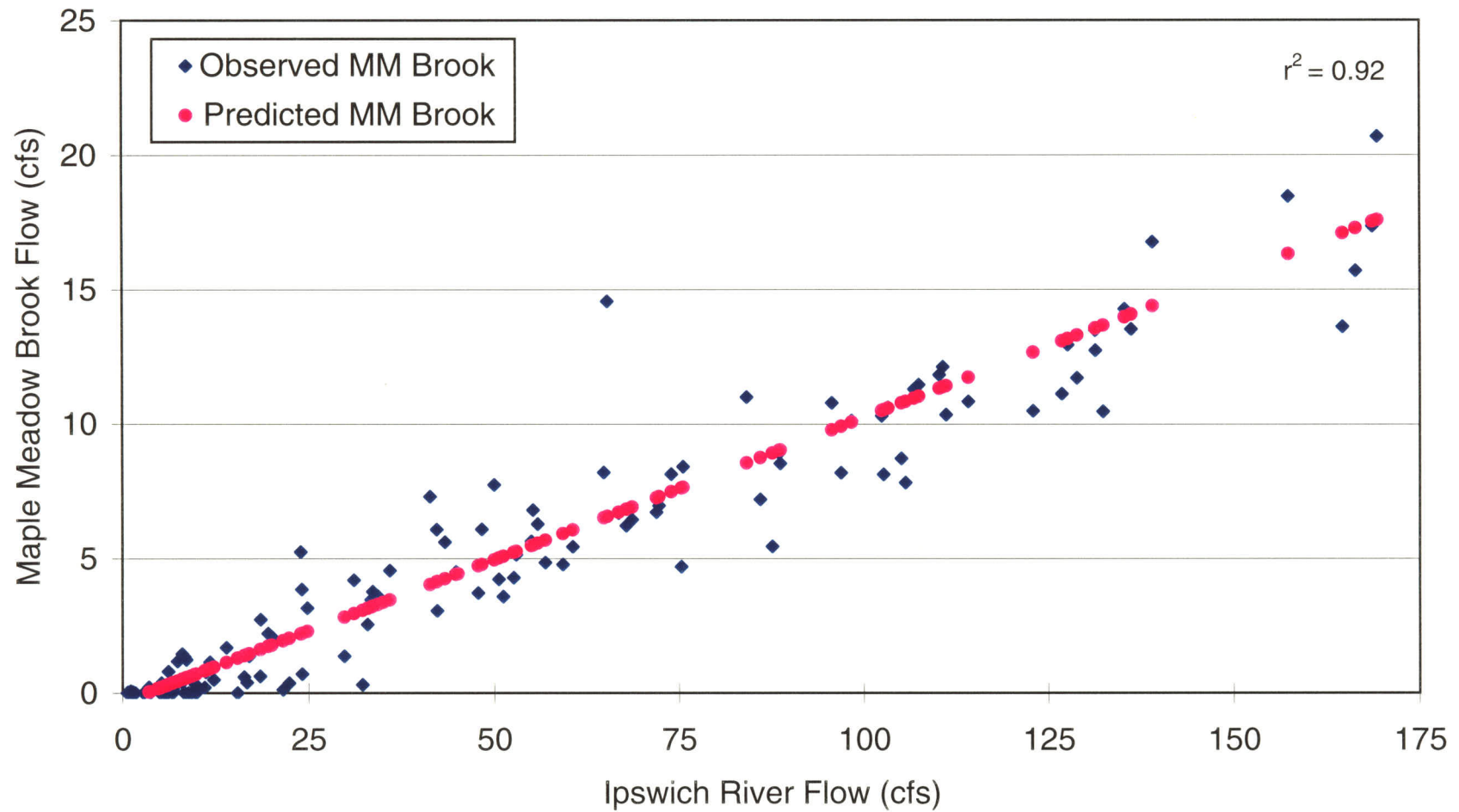
<p>Generation Date: 4/18/01</p>	<p>Figure 22. Average monthly pumping rates at Town Wells, 1989-99.</p>	
---------------------------------	---	--



Generation  
Date:  
4/18/01

Figure 23. Average monthly stream flows, 1962-74.

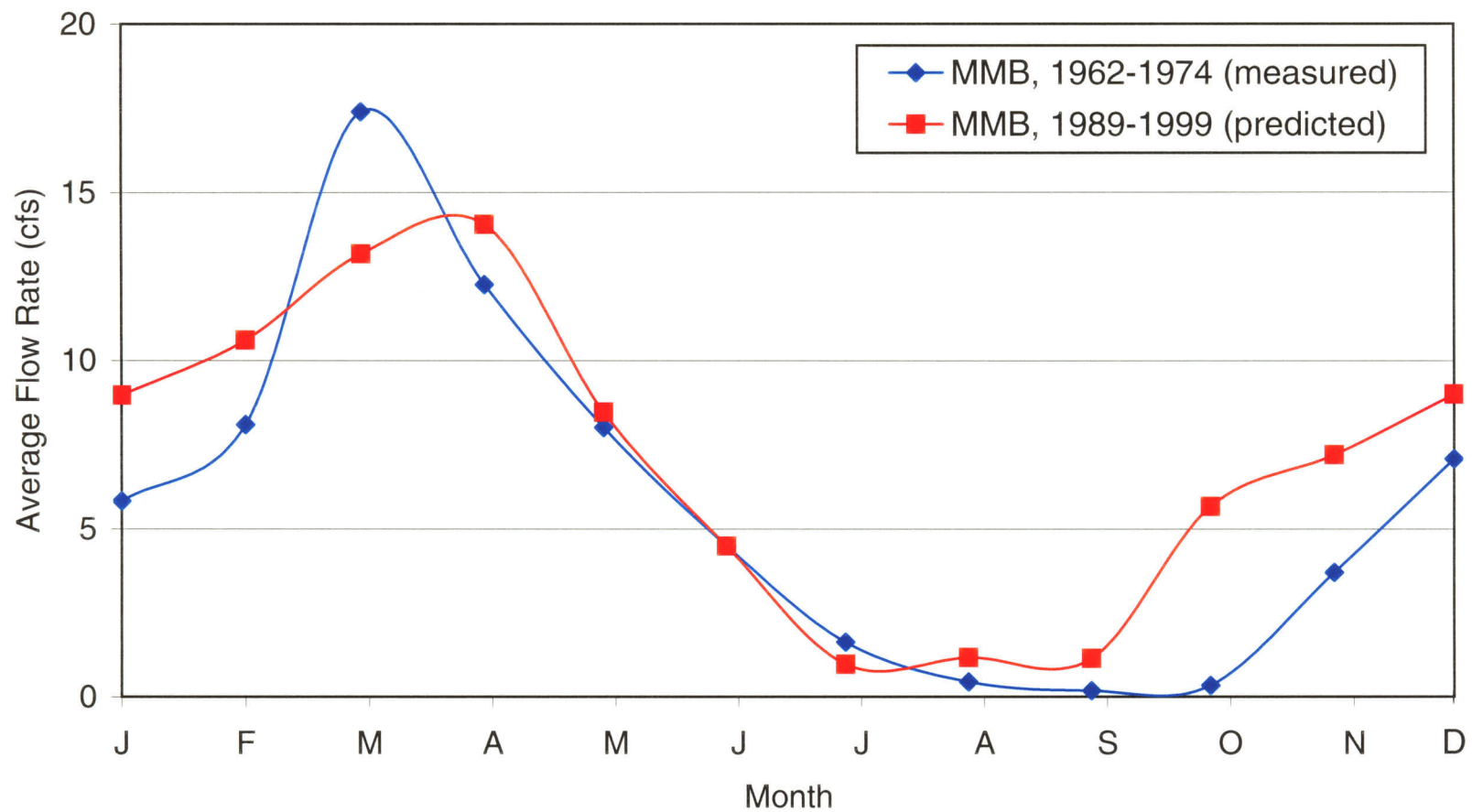




Generation  
Date:  
4/18/01

Figure 24. Maple Meadow Brook - Ipswich River regression results.

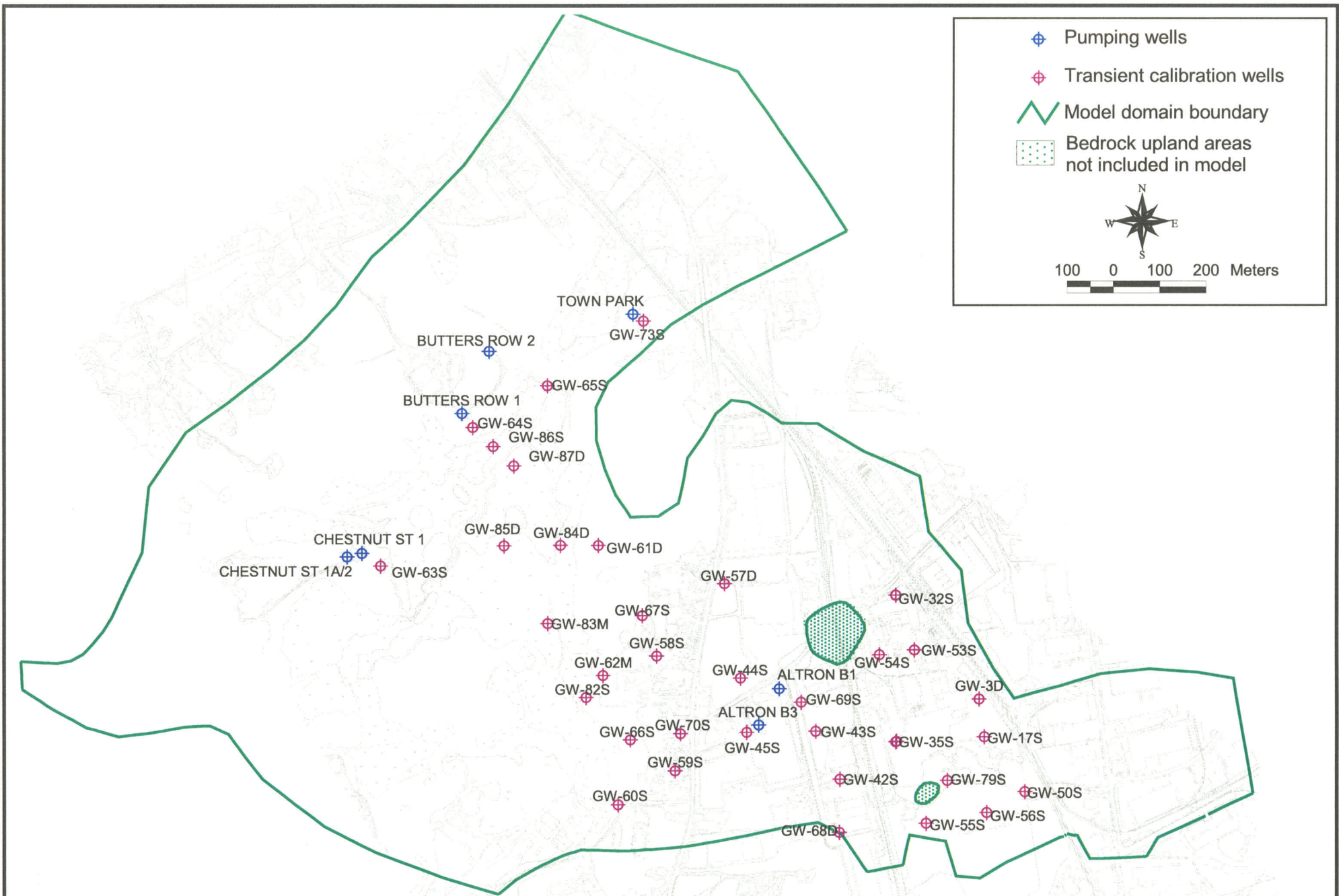




Generation  
Date:  
4/18/01

Figure 25. Average monthly stream flow in Maple Meadow Brook.



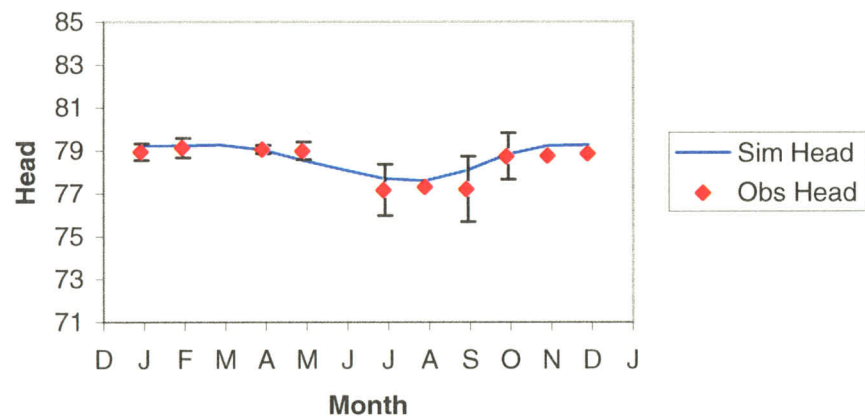


Generation  
Date:  
4/27/01

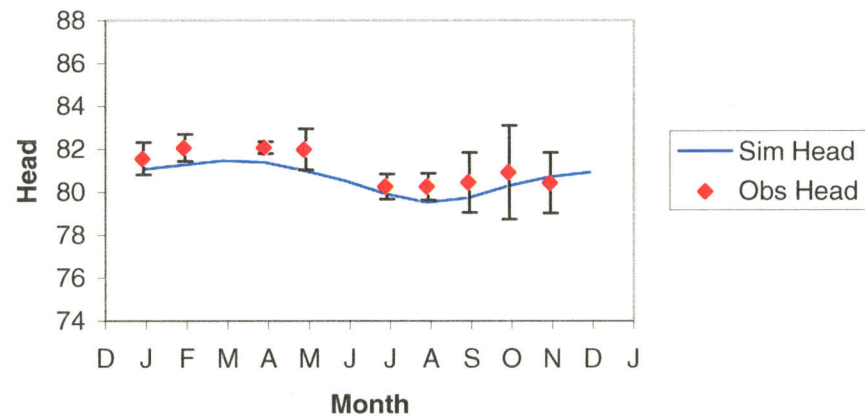
Figure 26. Locations of Monitoring Wells Used in Transient Model Calibration



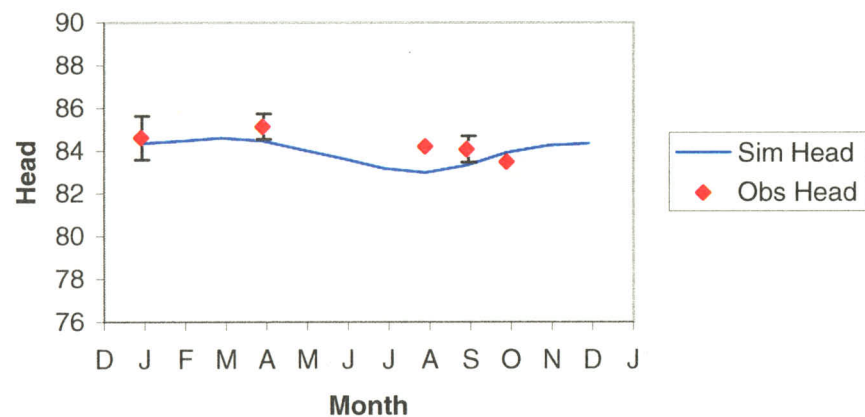
GW-17S



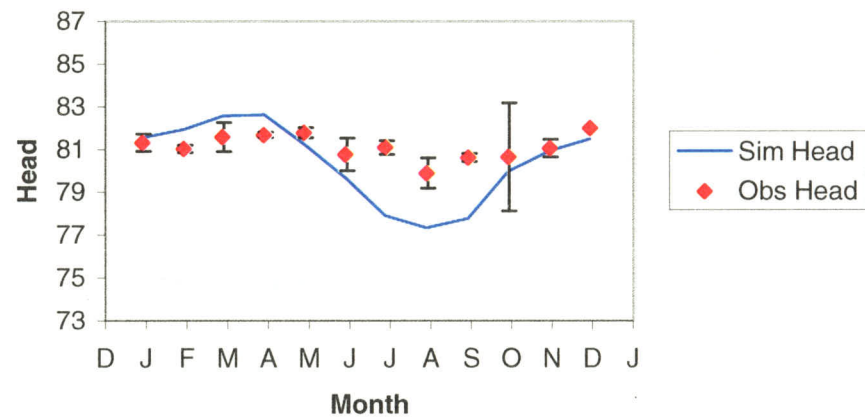
GW-35S



GW-54S



GW-60S

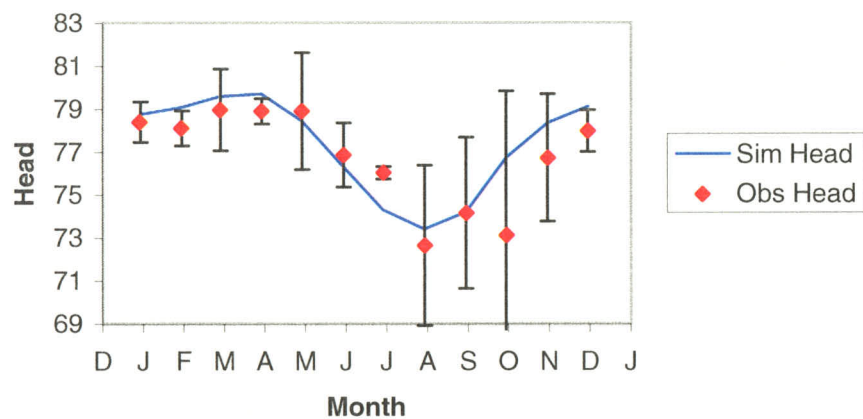


Generation  
Date:  
10/18/00

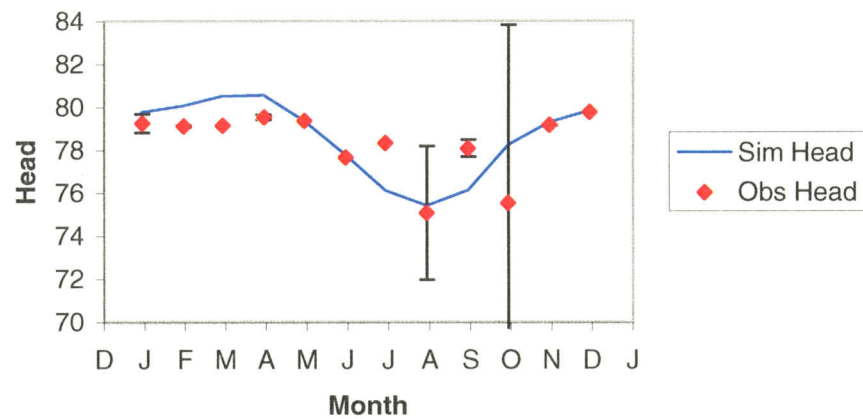
Figure 27a. Comparison of simulated and observed average monthly heads in transient calibration target wells.



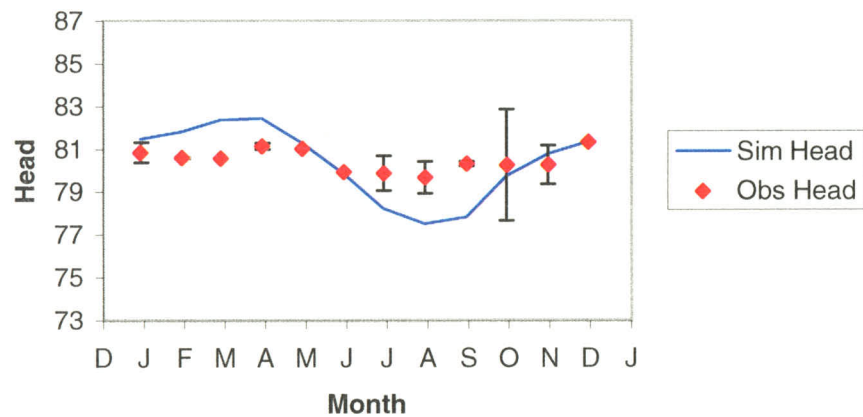
GW-64S



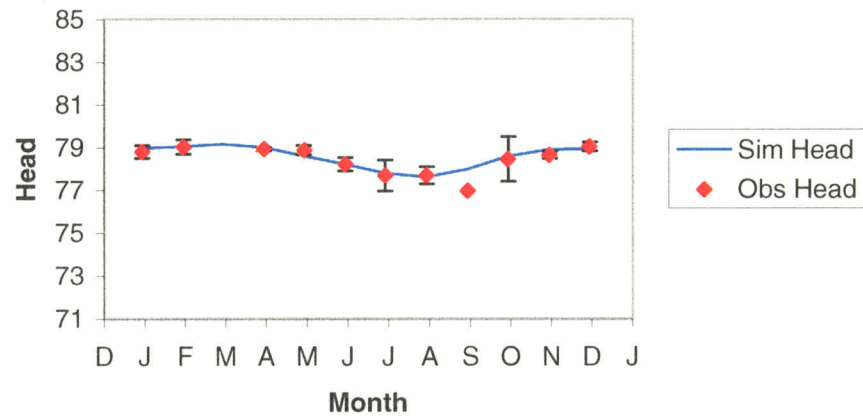
GW-65S



GW-66S



GW-79S

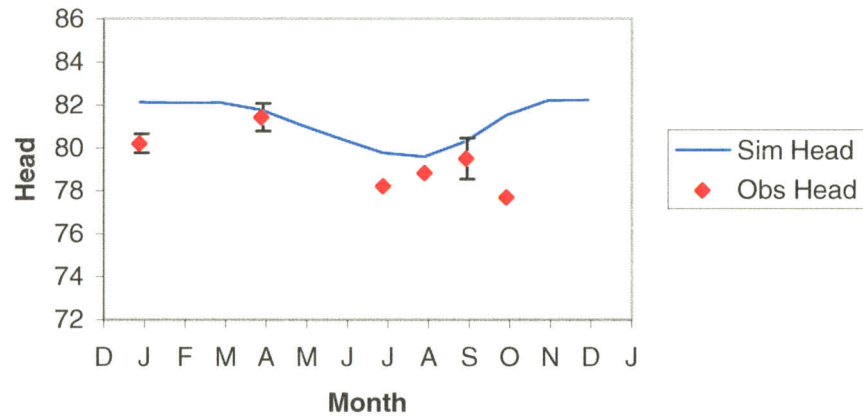


Generation  
Date:  
10/18/00

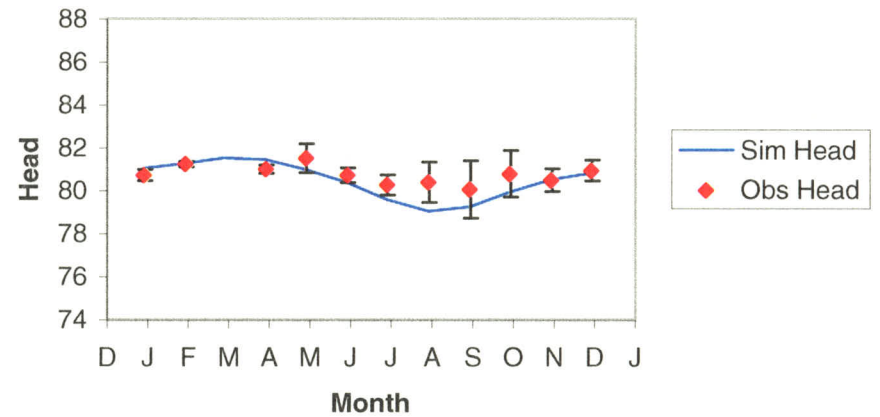
Figure 27b. Comparison of simulated and observed average monthly heads in transient calibration target wells.



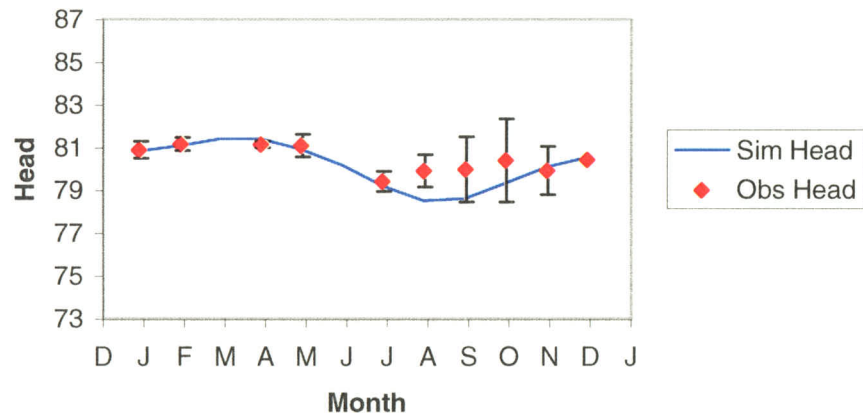
GW-32S



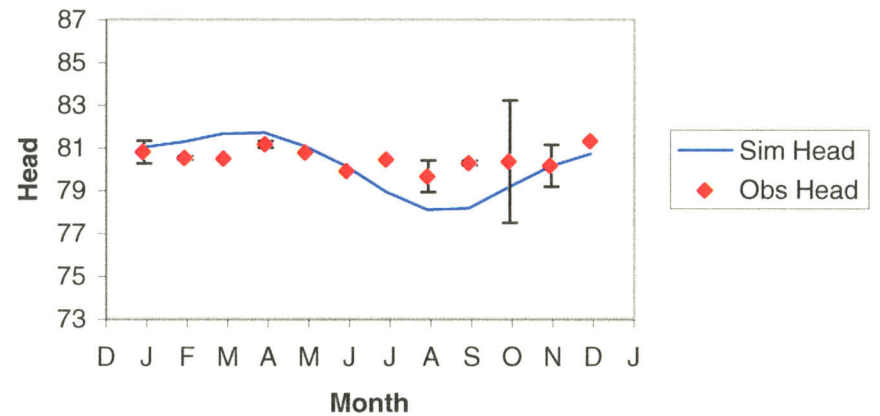
GW-42S



GW-43S



GW-44S

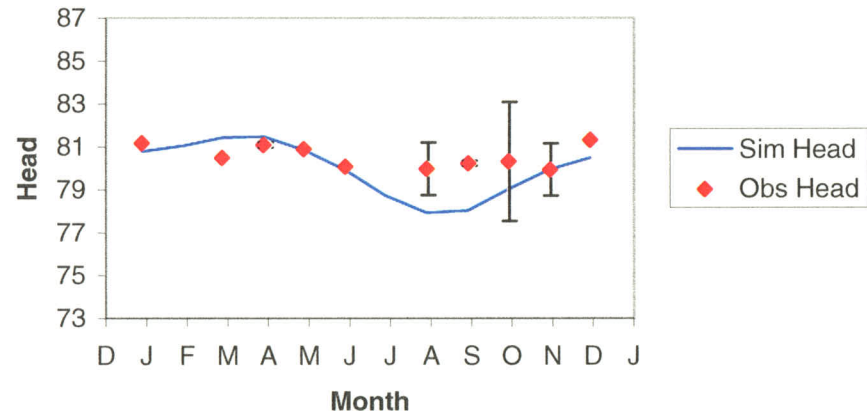


Generation  
Date:  
10/18/00

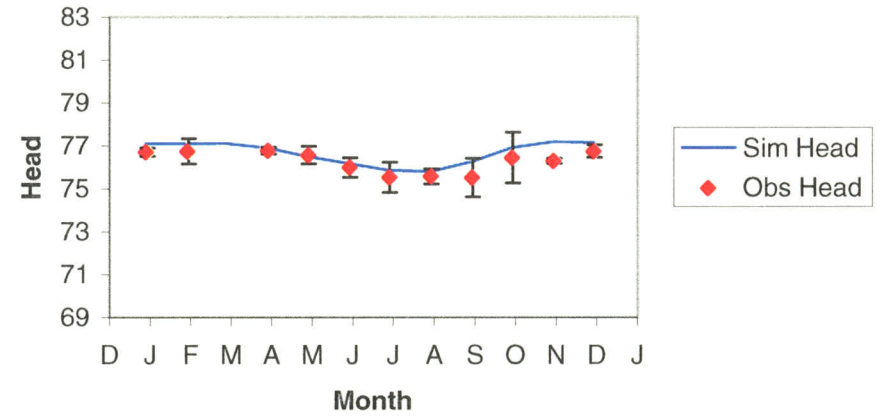
Figure 27c. Comparison of simulated and observed average monthly heads in transient calibration target wells.



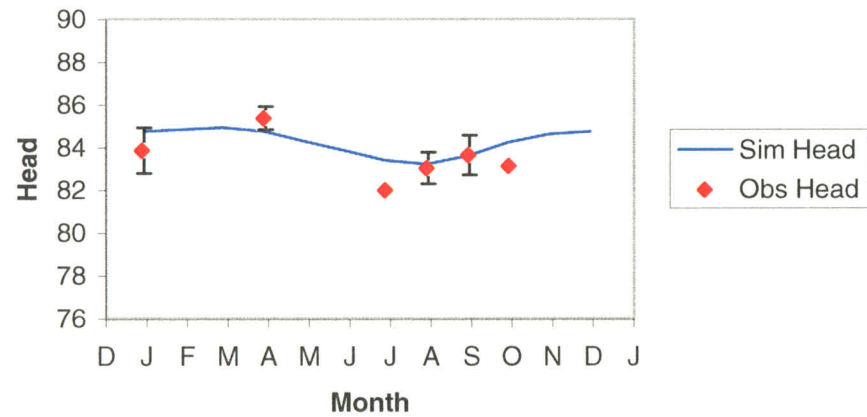
GW-45S



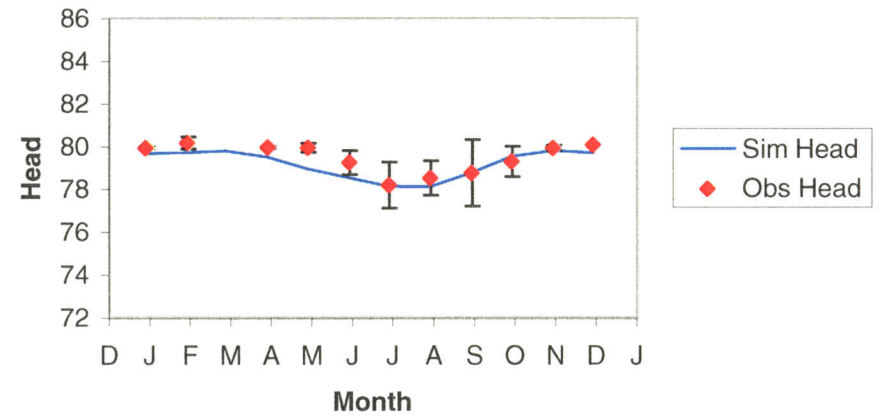
GW-50S



GW-53S



GW-55S

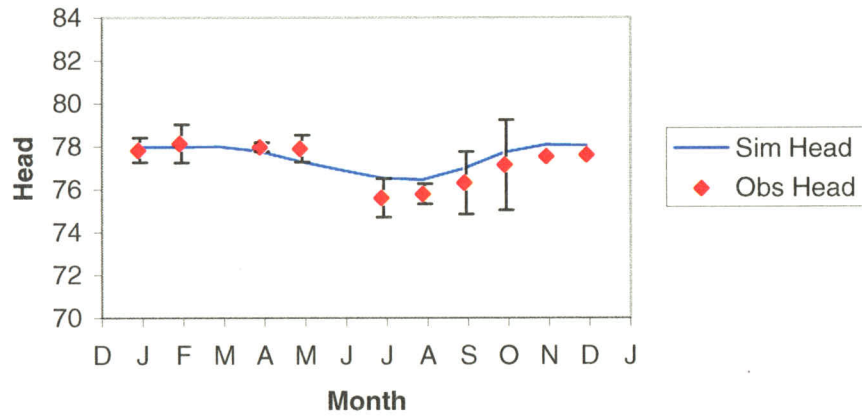


Generation  
Date:  
10/18/00

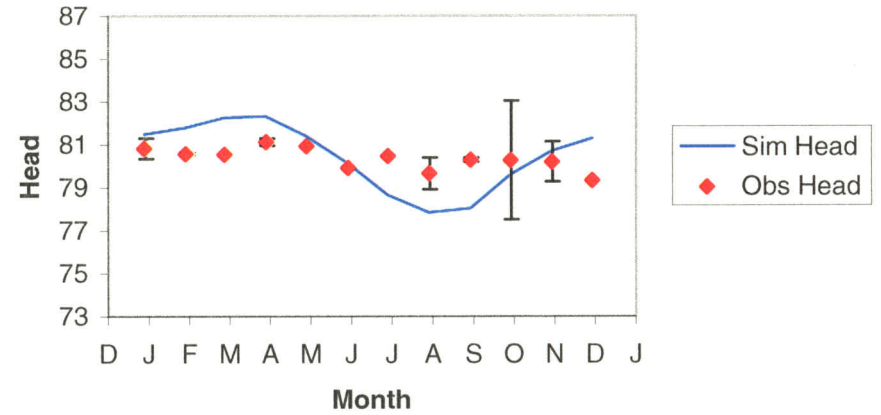
Figure 27d. Comparison of simulated and observed average monthly heads in transient calibration target wells.



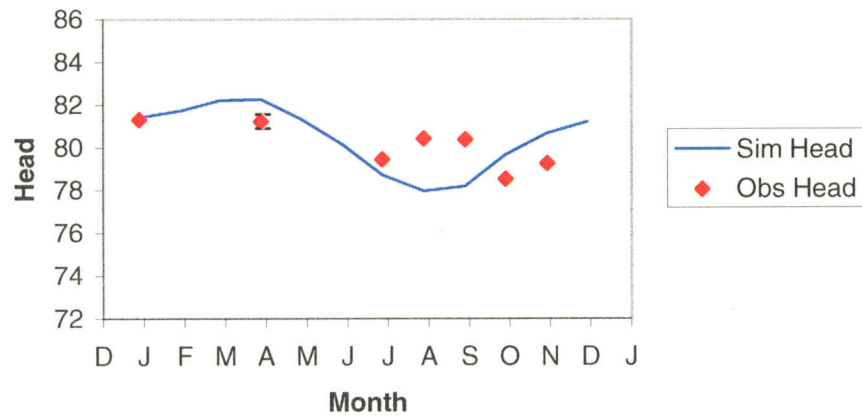
GW-56S



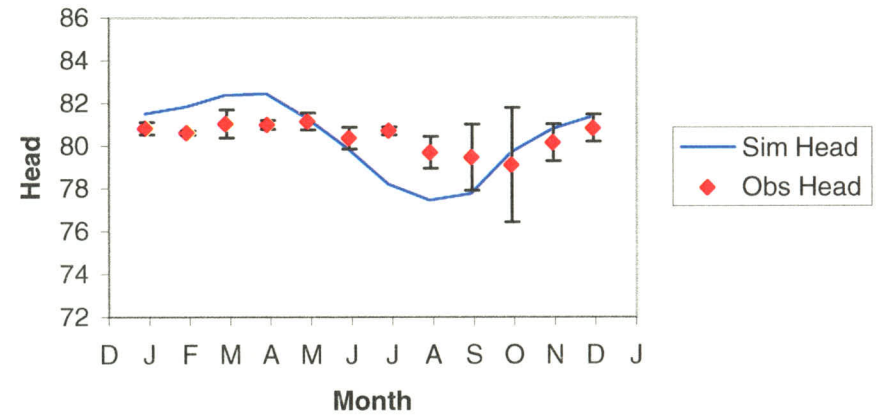
GW-58S



GW-59S



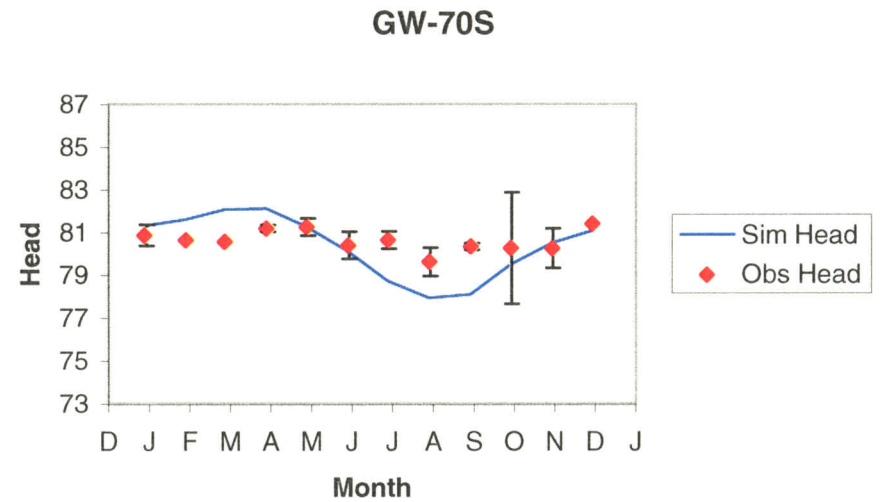
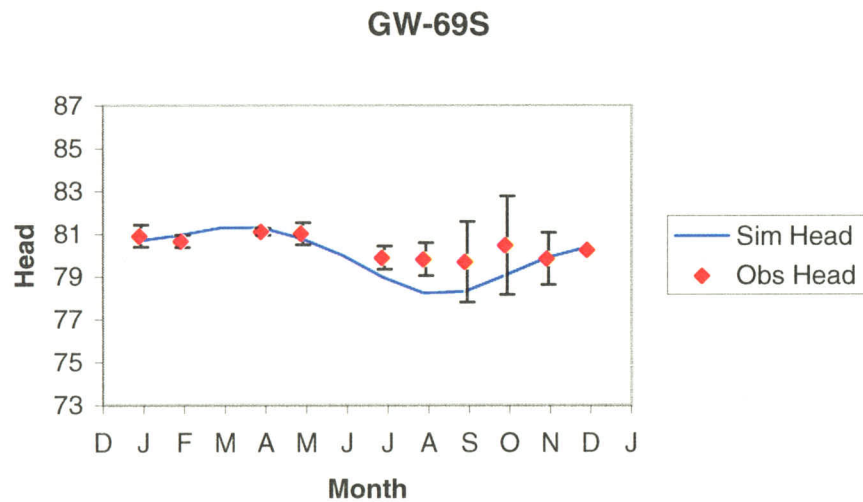
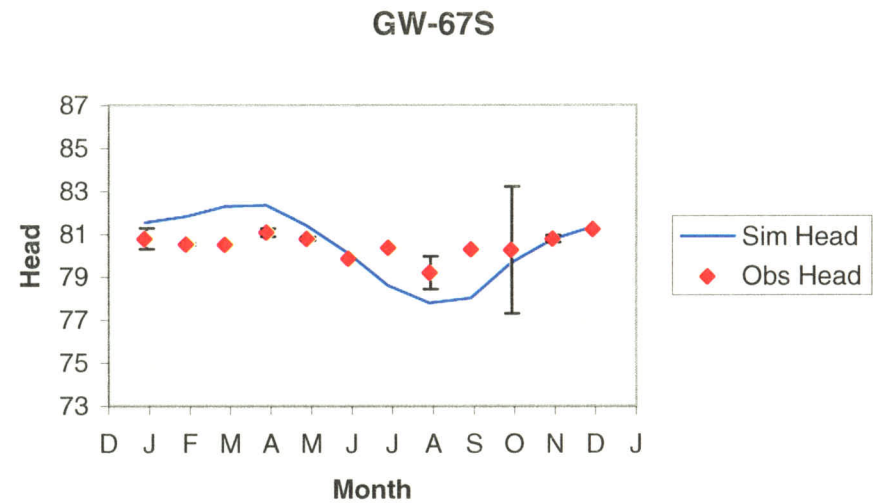
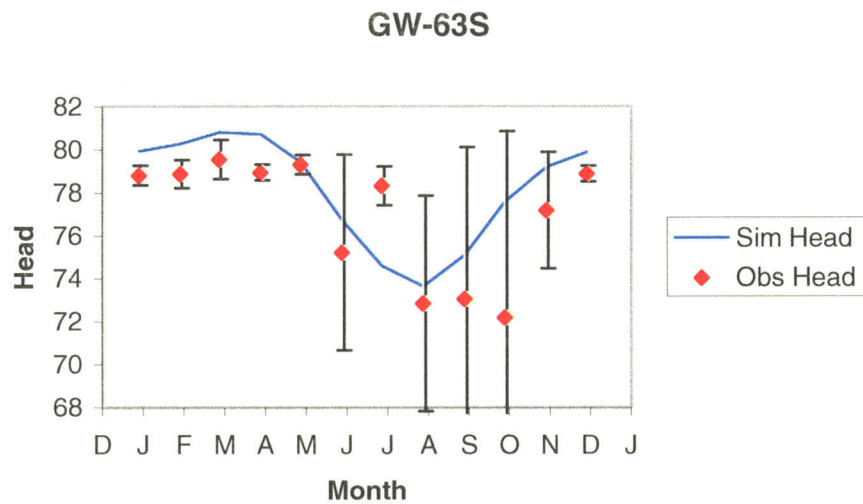
GW-62M



Generation  
Date:  
10/18/00

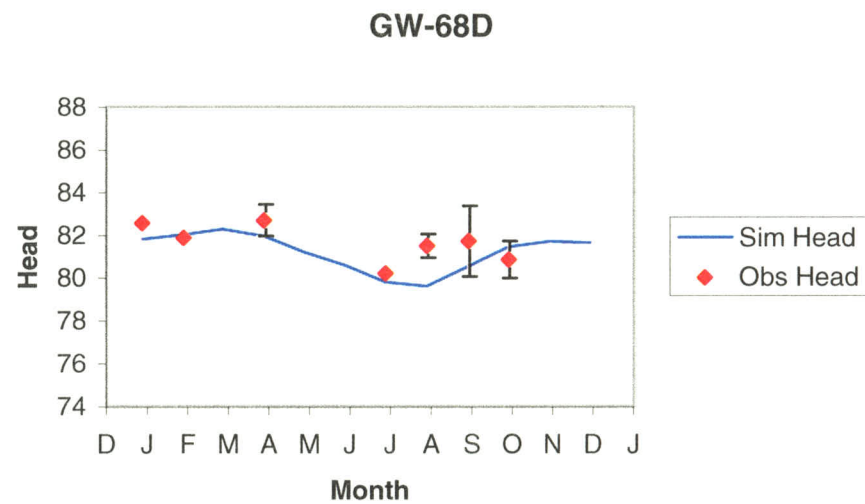
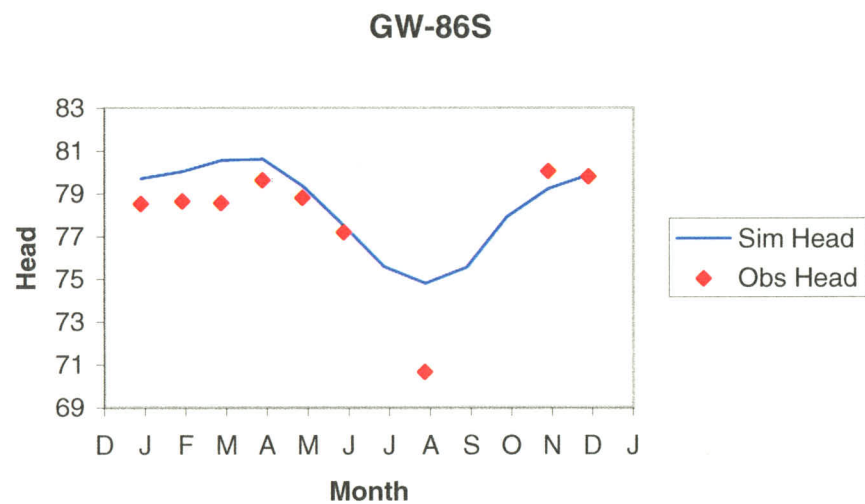
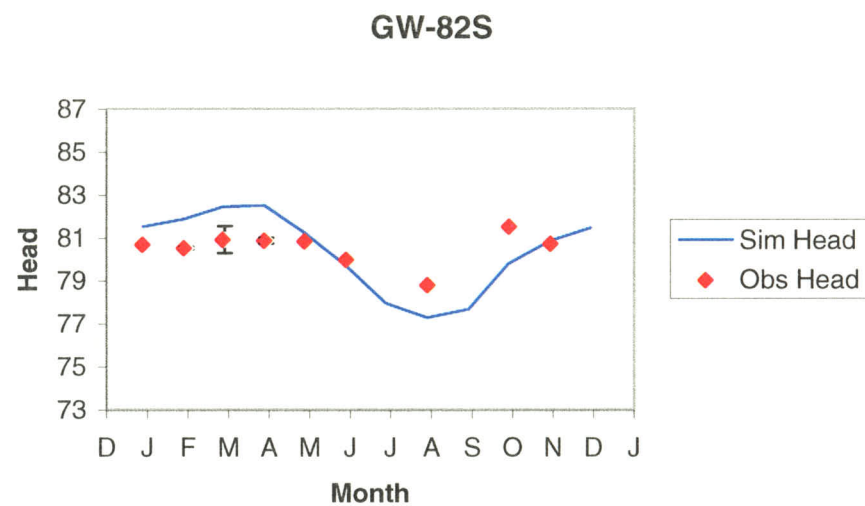
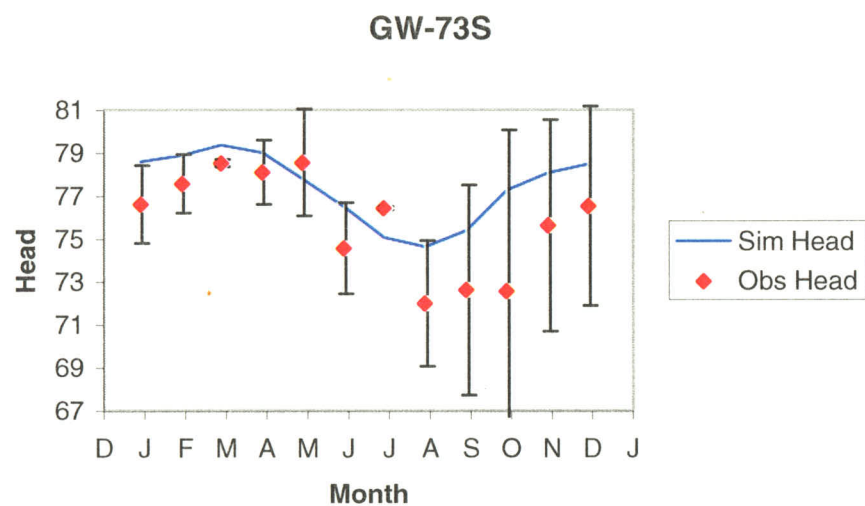
Figure 27e. Comparison of simulated and observed average monthly heads  
in transient calibration target wells.





Generation  
Date:  
10/18/00

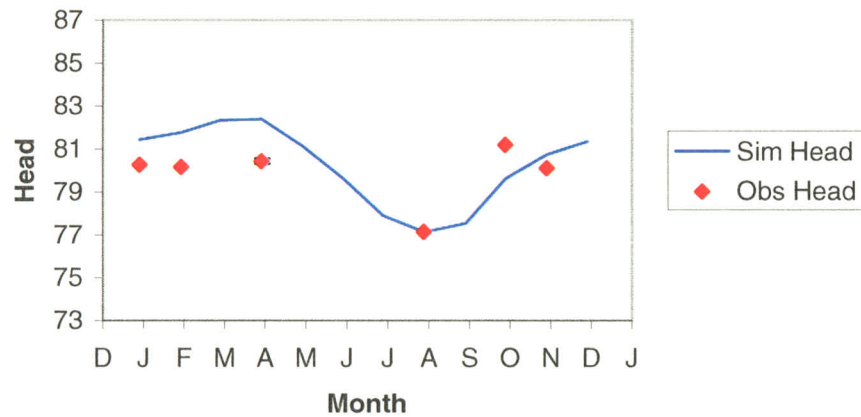
Figure 27f. Comparison of simulated and observed average monthly heads in transient calibration target wells.



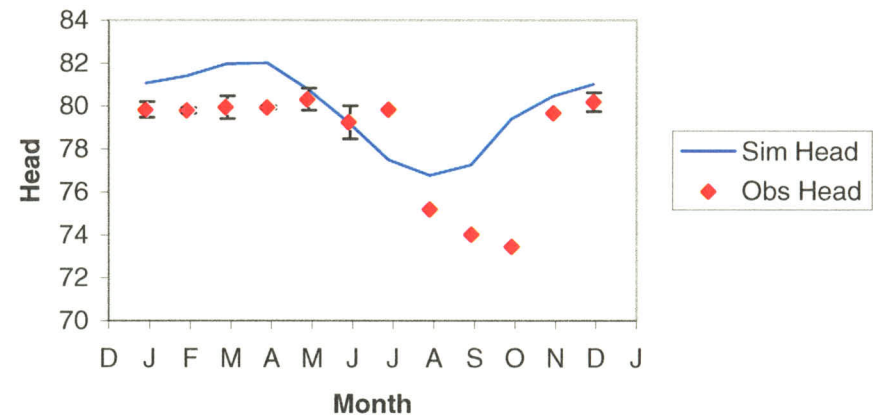
Generation  
Date:  
10/18/00

Figure 27g. Comparison of simulated and observed average monthly heads in transient calibration target wells.

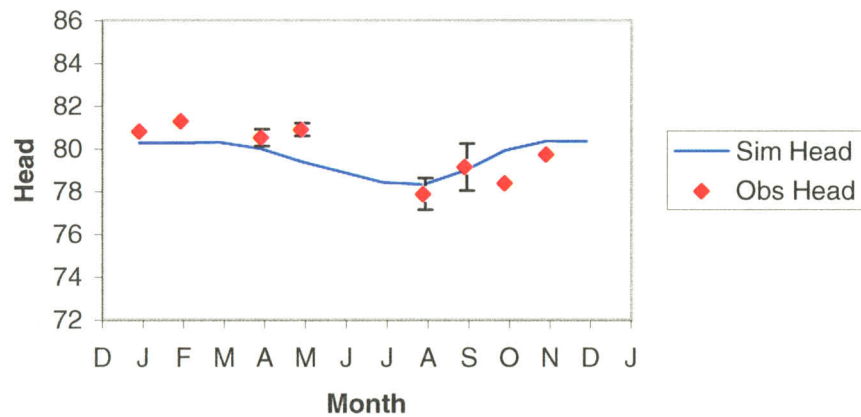
GW-83M



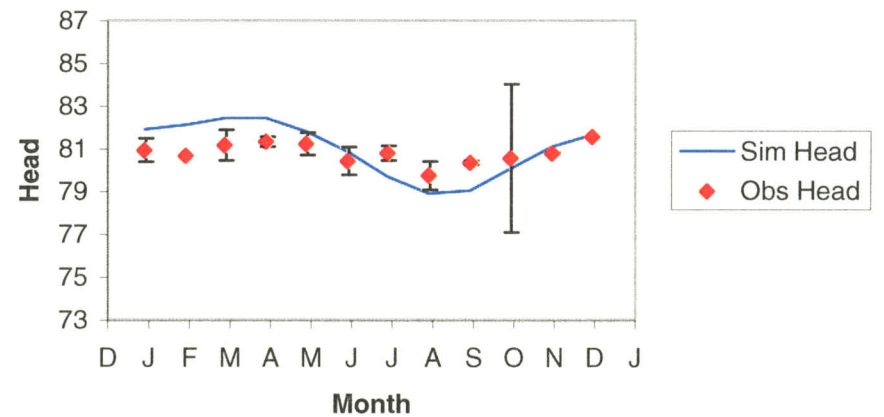
GW-84D



GW-3D



GW-57D

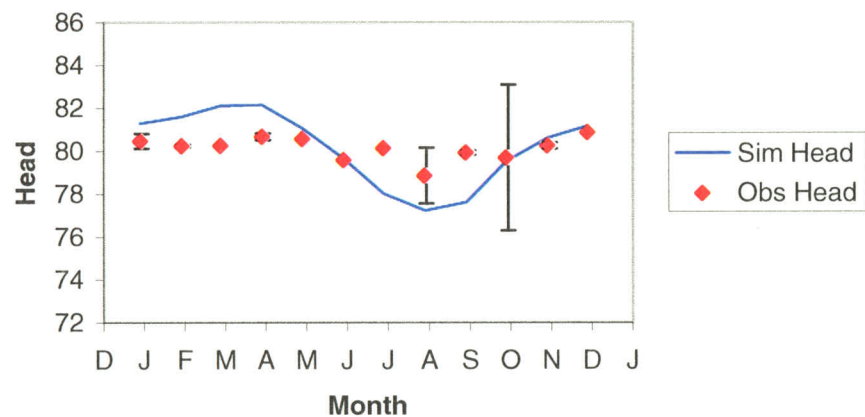


Generation  
Date:  
10/18/00

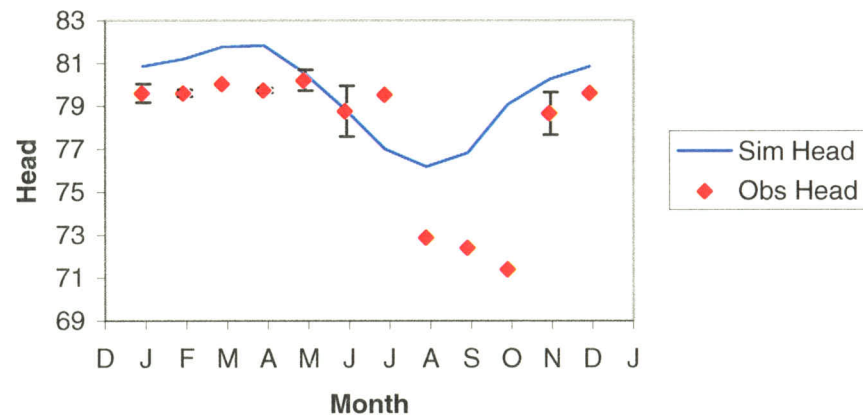
Figure 27h. Comparison of simulated and observed average monthly heads  
in transient calibration target wells.



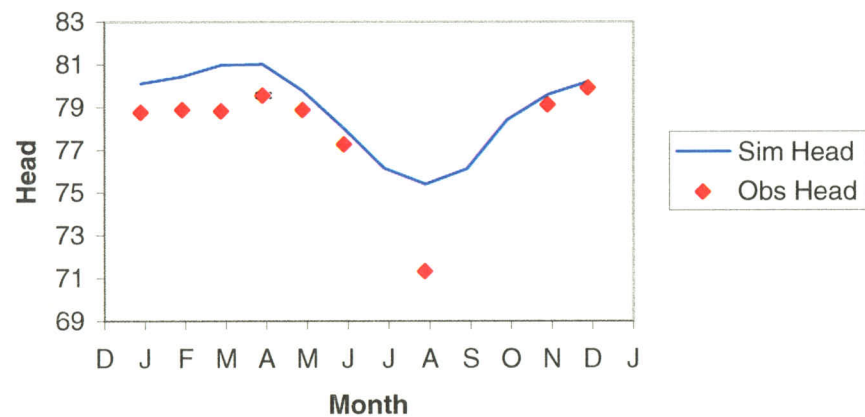
GW-61D



GW-85D



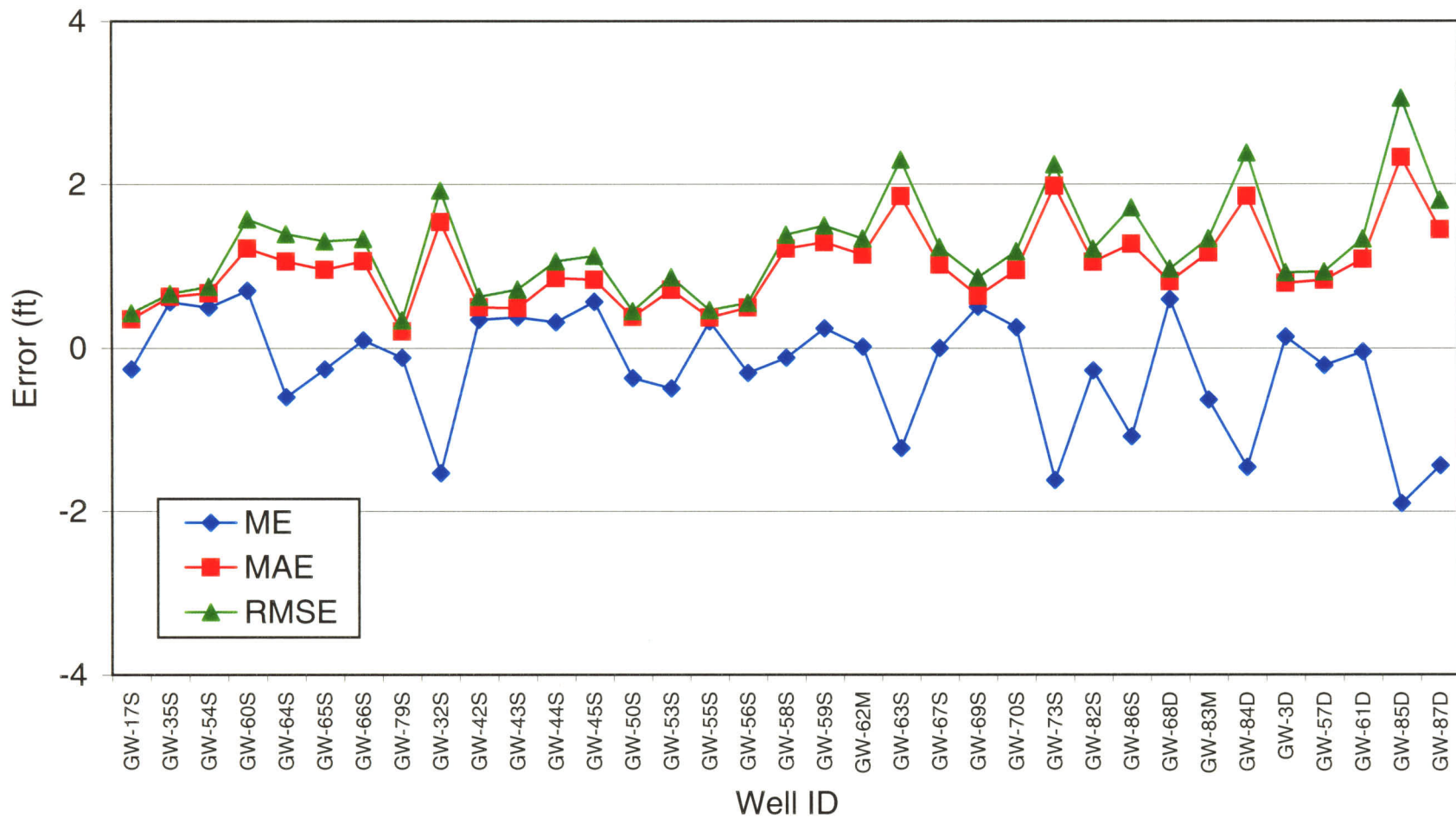
GW-87D



Generation  
Date:  
10/18/00

Figure 27i. Comparison of simulated and observed average monthly heads in transient calibration target wells.

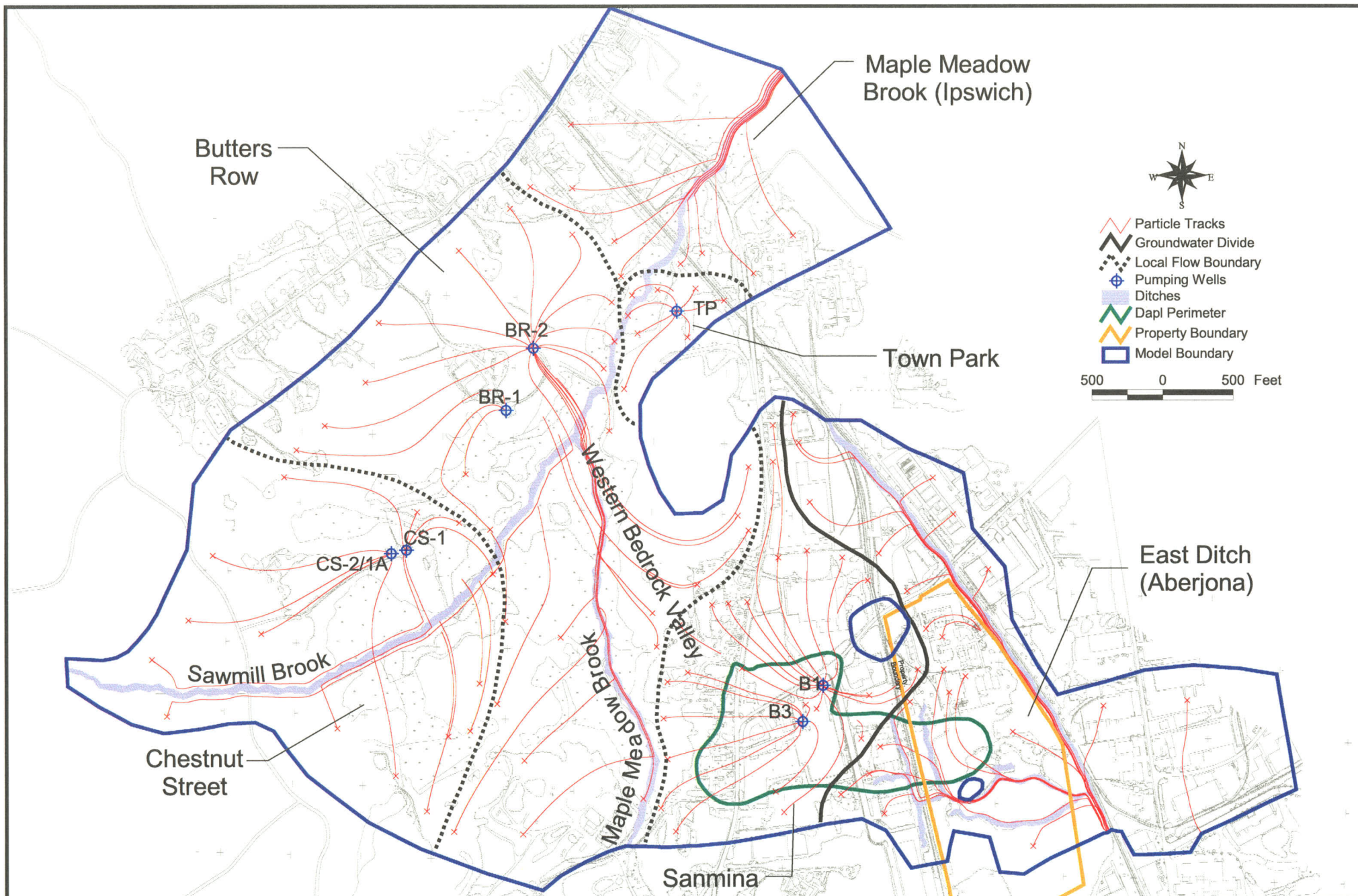




Generation  
Date:  
4/18/01

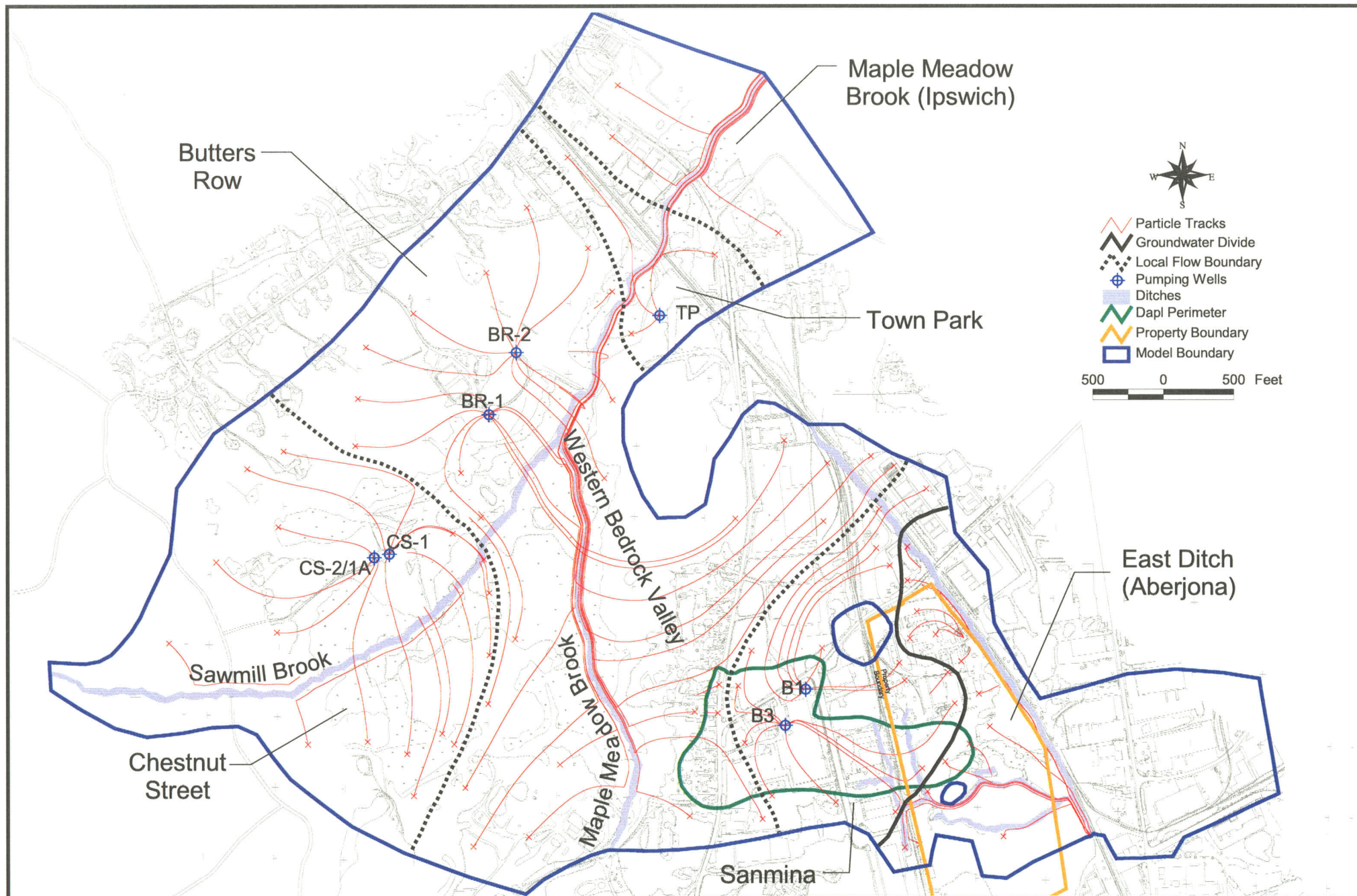
Figure 28. Transient calibration statistics by well.





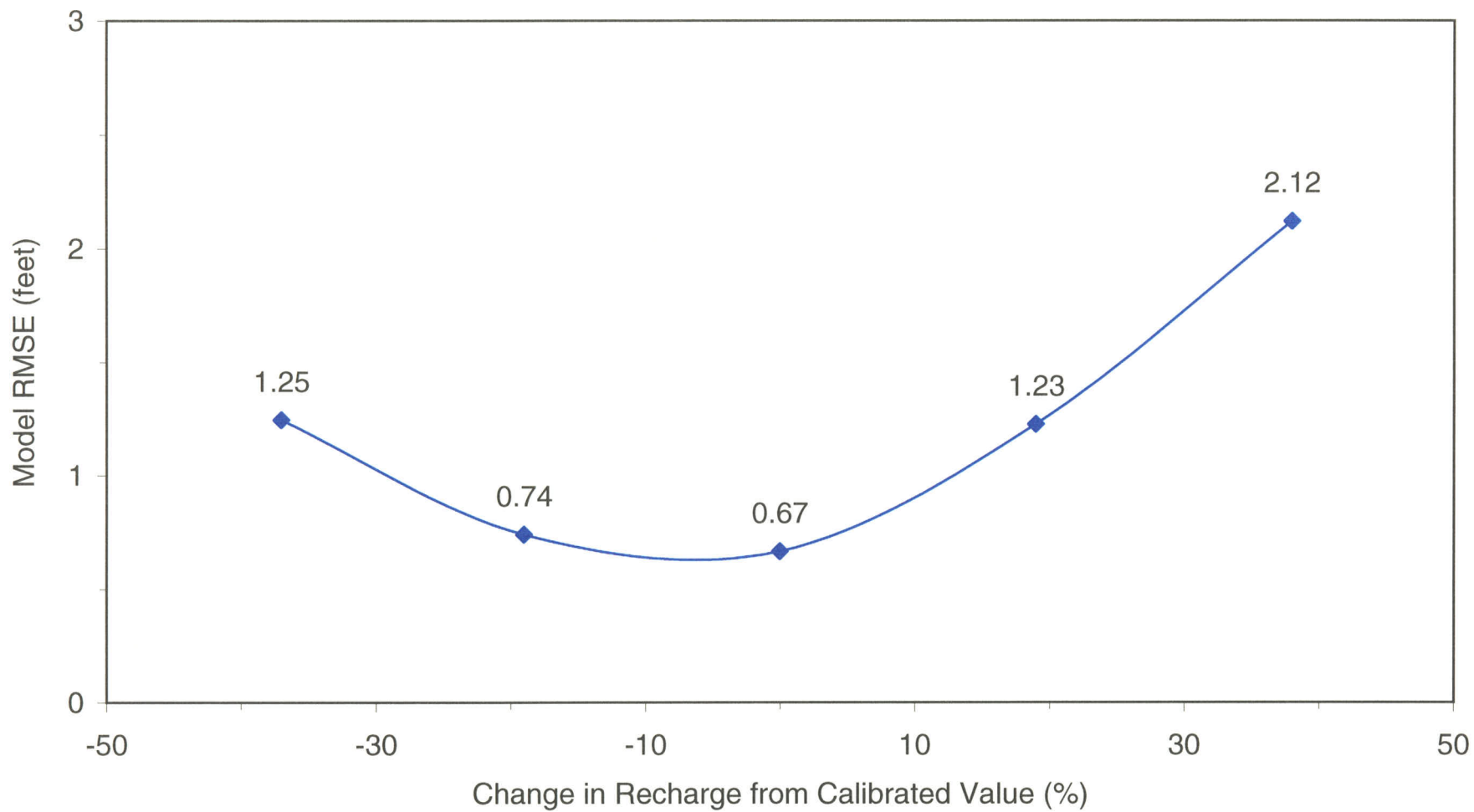
Generation  
Date:  
4/27/01

Figure 29. Particle tracks showing capture areas and flow zones for average wet conditions, (April)



Generation  
Date:  
4/27/01

Figure 30. Particle tracks showing capture areas and flow zones for average dry conditions (October)



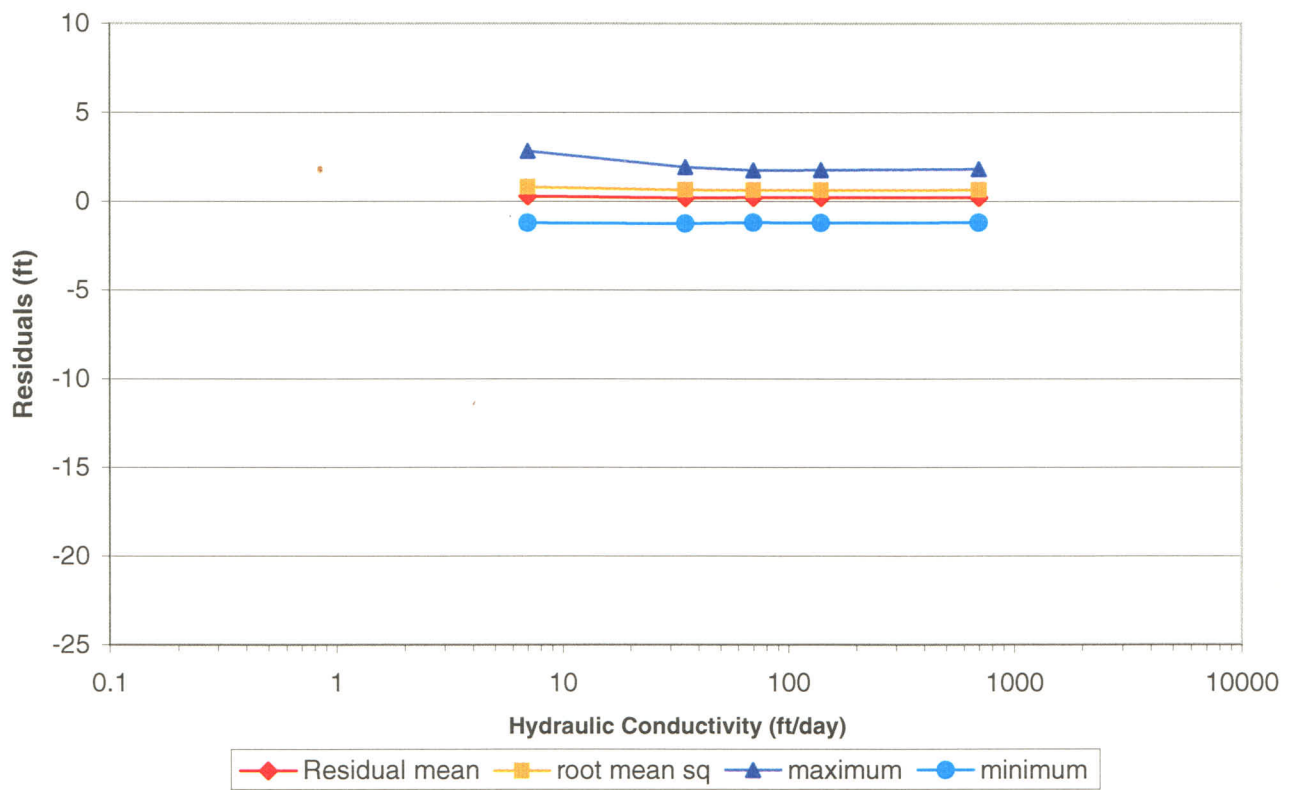
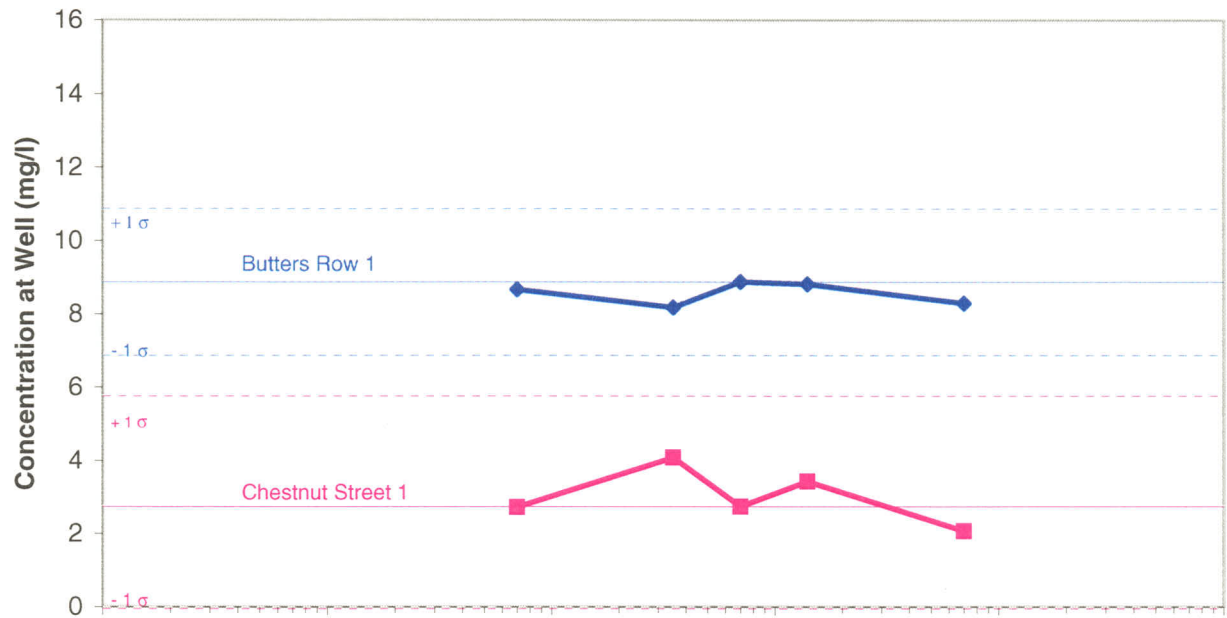
Generation  
Date:  
4/24/01

Figure 31. Groundwater model RMSE response curve.

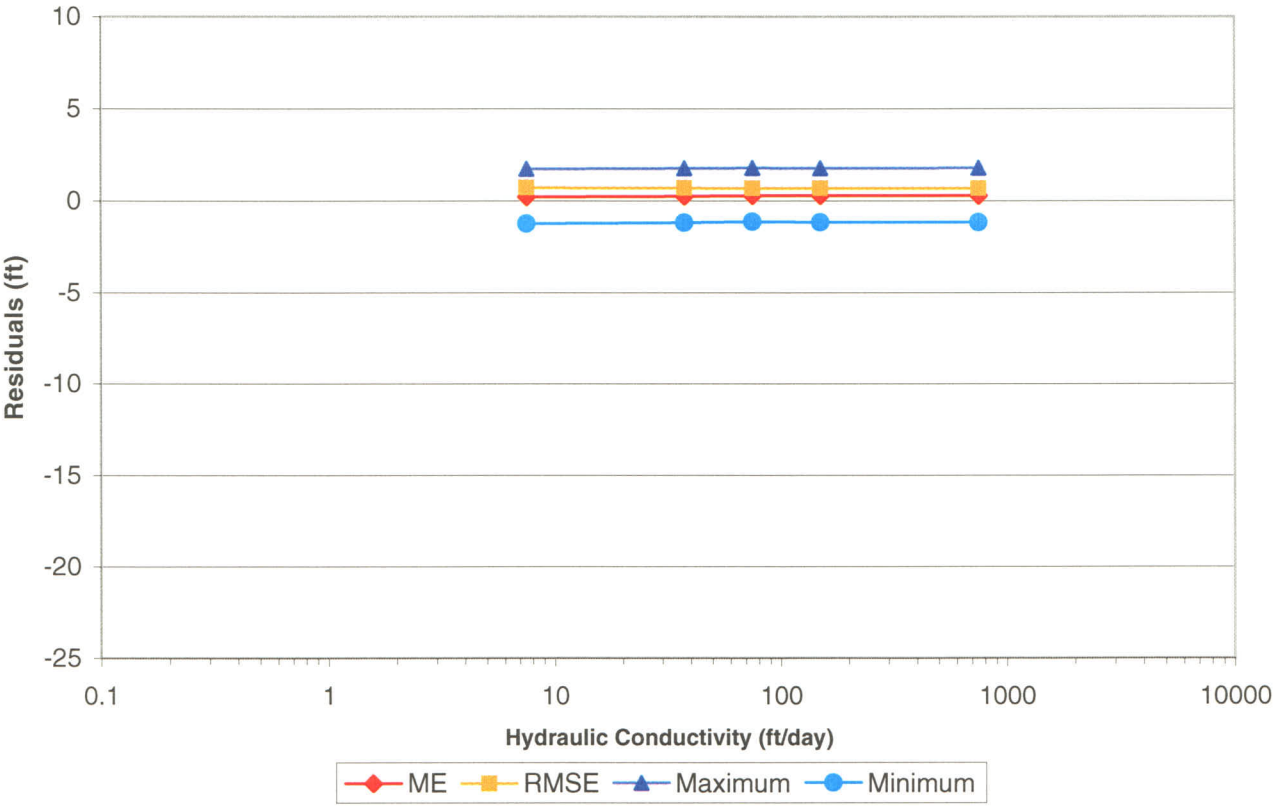




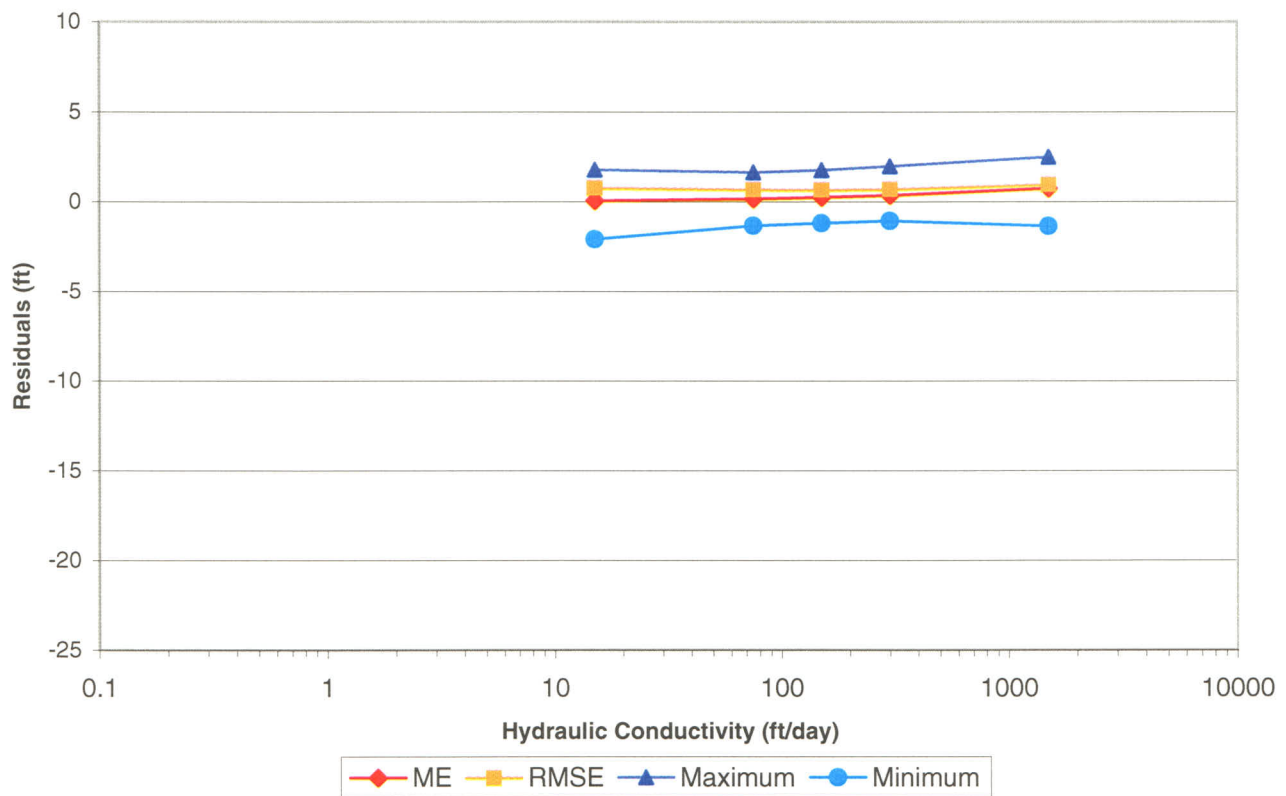
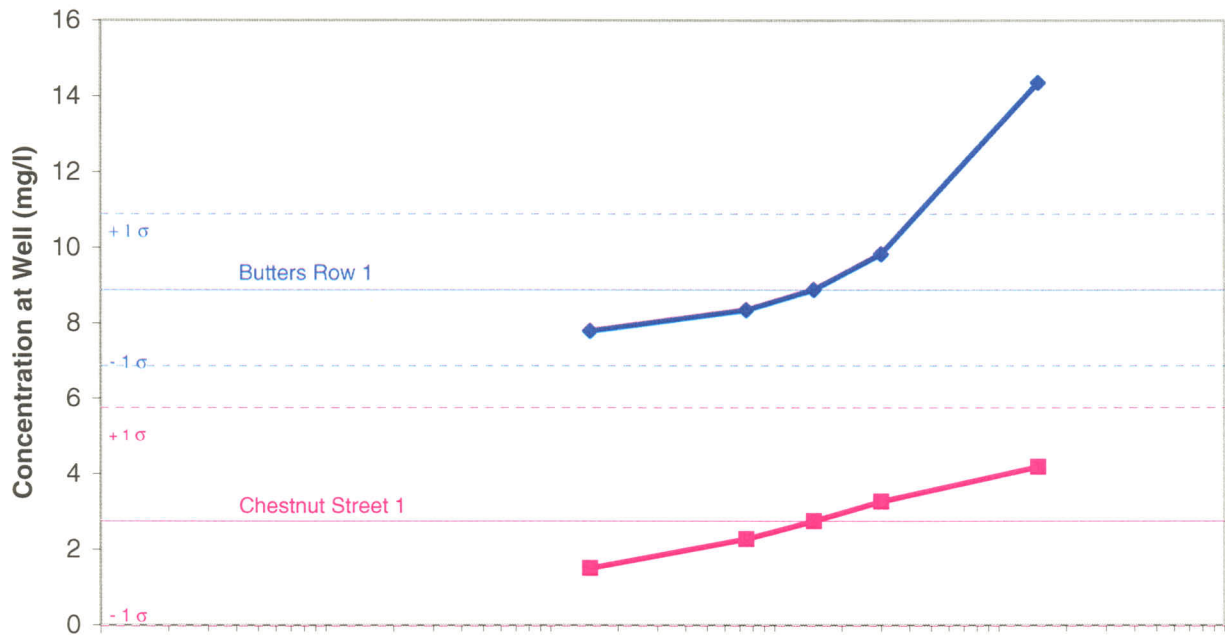
$K_h = 70 \text{ ft/day}$



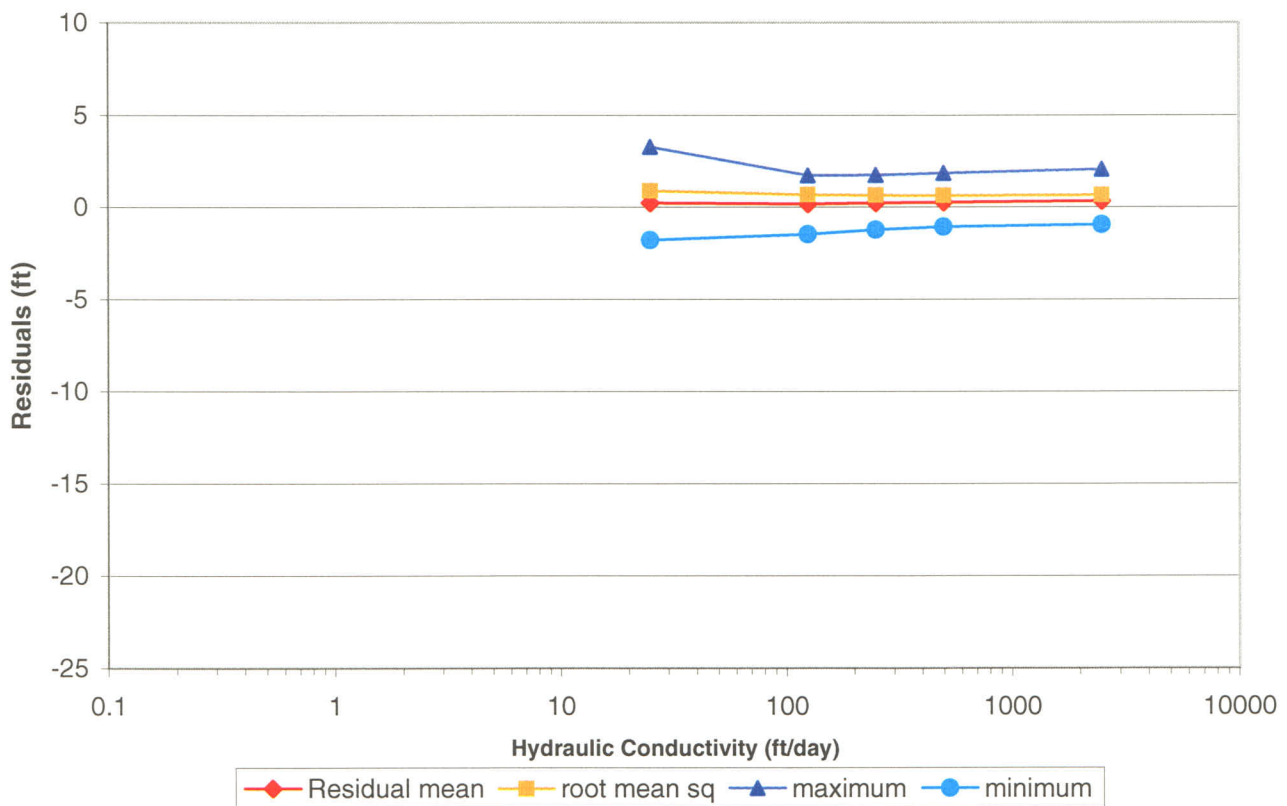
$K_h = 75 \text{ ft/day}$



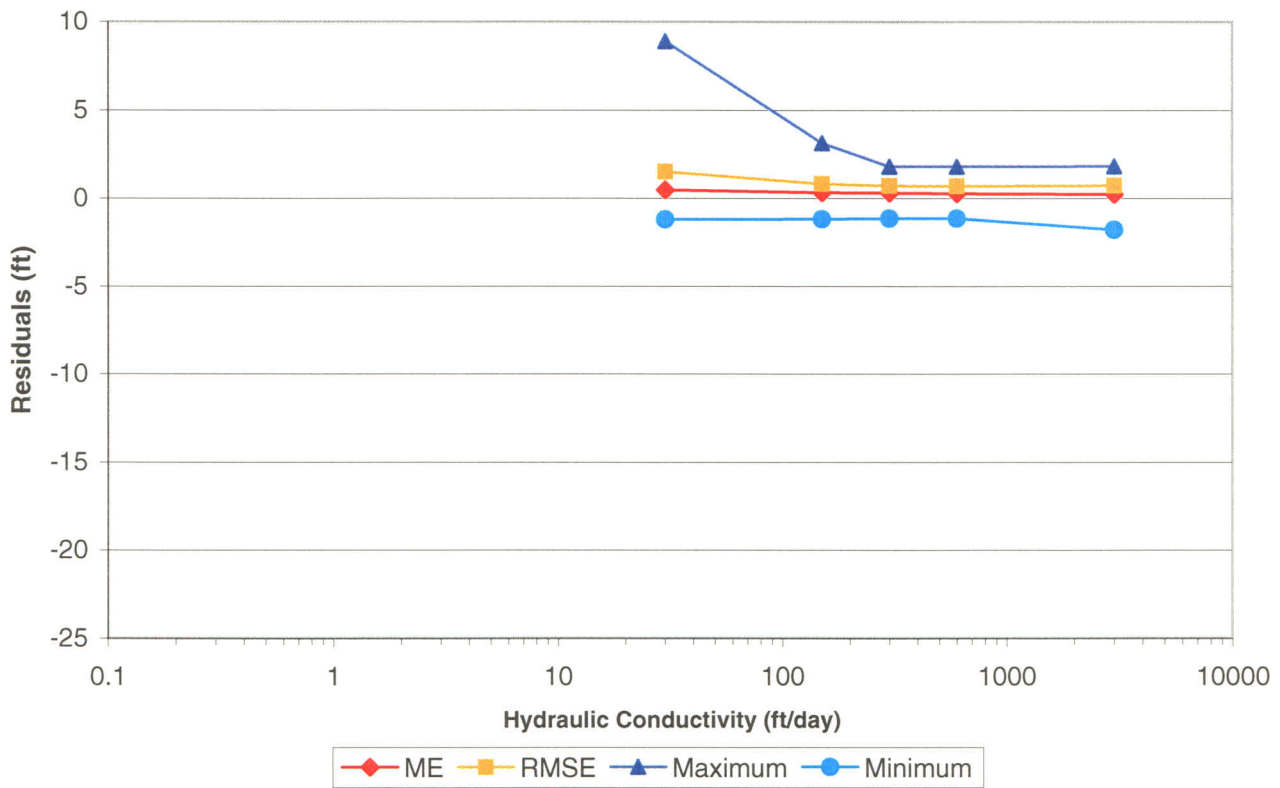
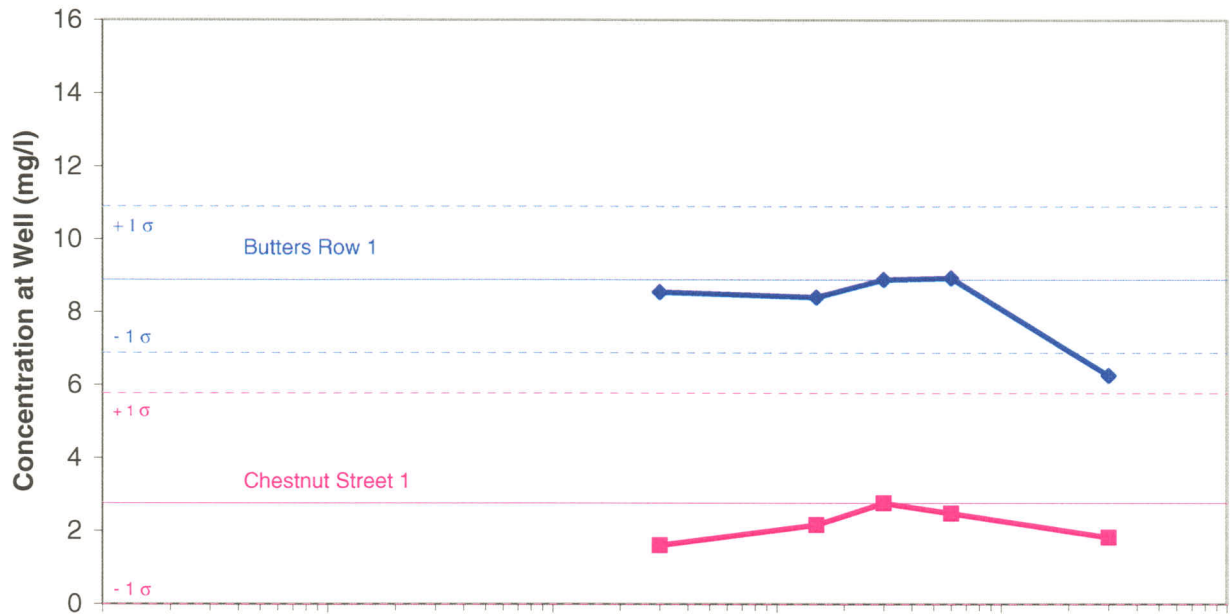
$K_h = 150$  ft/day



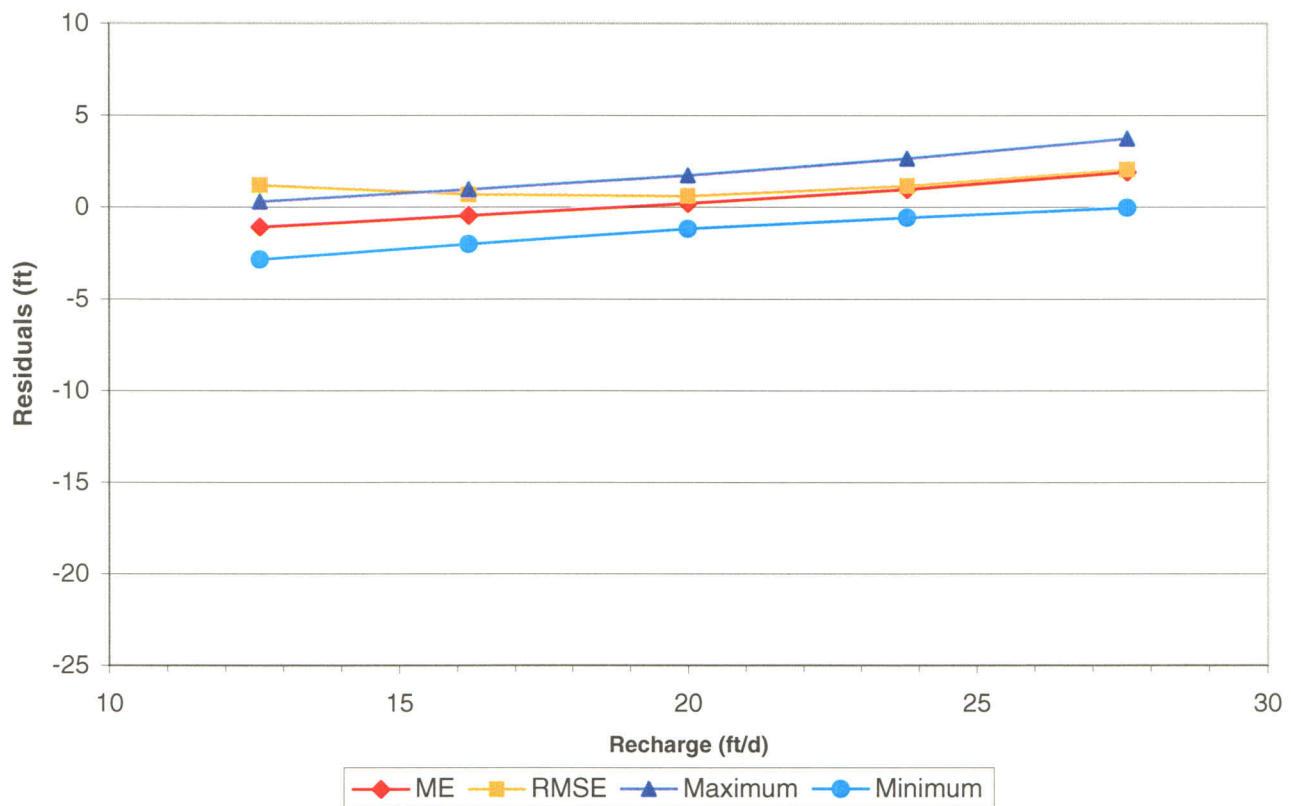
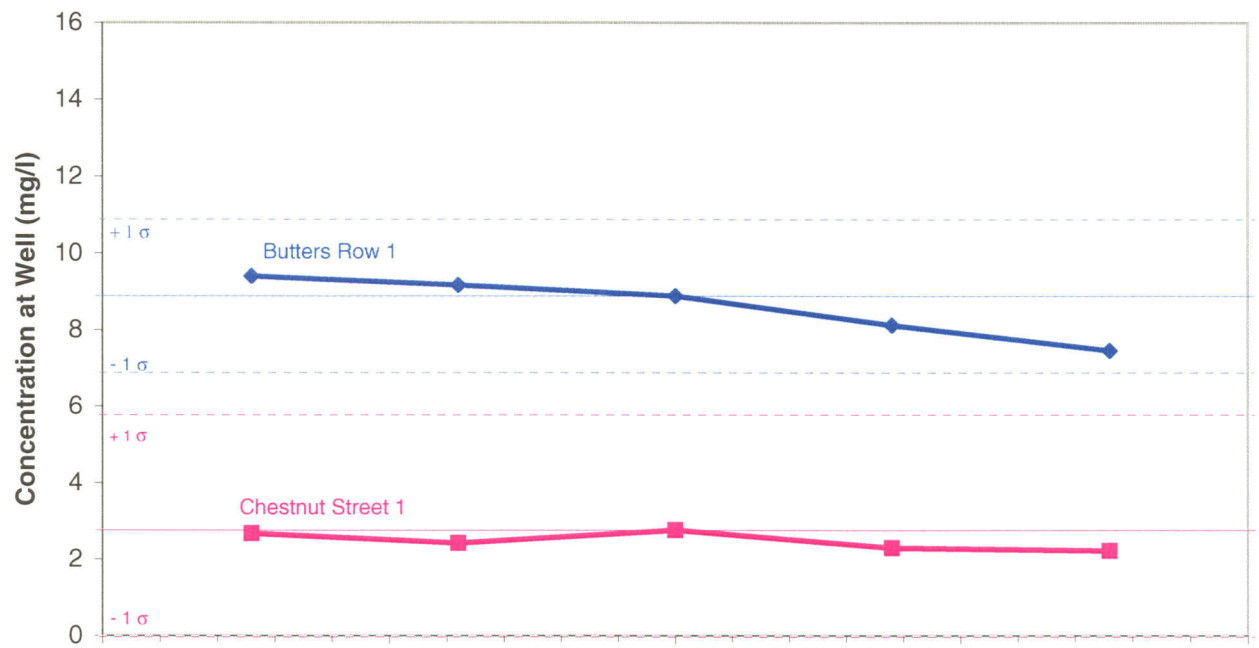
$K_h = 250 \text{ ft/day}$



$K_h = 300$  ft/day



## Recharge



## Specific Yield

